

# POLITECNICO DI MILANO



Facolta di Ingegneria dei Processi Industriali

Dipartimento di Chimica, Materiali e Ingegneria Chimica “Giulio Natta”

## Corrosion of Steel in Concrete: Effectiveness of Polymer modified Cementitious Coatings

Relatore: Prof. Fabio Bolzoni

Correlatore: Ing. Andrea Brenna

Student:

Doumingou Toussamba, Odilon Aymar

Mat no.755877

**A.A. 2011/2012**

## **Acknowledgement**

I would like to thank the Almighty God for his protection throughout my life and especially in my master studies and this work. Also, my sincere thanks go to my supervisor Prof. Fabio Bolzoni, Ing. Andrea Brenna and all the members of the Corrosion laboratory. To my friends and colleagues who helped me in this work I say thank you. Last and not the least to my family for the love and support (financially and morally) you showed to me and continue to do, I say may the Lord bless you.

# Table of Contents

Acknowledgement .....	2
Table of Contents .....	3
List of Figures .....	5
List of Tables .....	7
1.0 Introduction .....	8
2.0 Literature review .....	9
2.1 Concrete [2].....	9
2.1.1 Structure and Characteristics of cement [3] .....	10
2.1.2 Steel reinforcement bars.....	10
2.3 Hydration of Cement [3] .....	12
2.3 Porosity in reinforced concrete [3].....	13
2.4 Transport Processes in Concrete [4].....	16
2.4.1 Permeability .....	16
2.4.2 Diffusion .....	17
2.5 Deterioration of Reinforced concrete [3] .....	21
2.5.2 Corrosion of steel in concrete [3, 12, 13, 14, 15].....	25
3.0 Surface coating of reinforced concrete .....	38
3.1 Classification of surface protection [26, 5, 6].....	38
3.2 Requirements of a Surface Coating .....	40
3.4 Water Absorption .....	40
3.5 Diffusion coefficient .....	44
3.8 Physical and mechanical resistance of coatings [6].....	46
4.0 Methodology .....	48
4.1 Concrete Specimens .....	49
4.1.1 Geometry.....	49
4.1.2 Mix Design.....	52
4.2 Properties and application of the coatings .....	54
The different coatings have been developed in different time, so it can be said that the coatings are RIV 1-2 is an updated or “modified” version of the coatings RIV 1-1.....	55
4.3 Preparation of support.....	56
4.5 Exposure.....	57
4.6 Experimental Measures.....	58
4.7 Corrosion Monitoring .....	58
4.7.1 Measuring the potential of steel .....	58
4.7.2 Measurement of the polarization resistance.....	60
4.7.3 Determination of the concentration profiles of chloride.....	61
5.0 Experimental Results .....	65
5.1 Corrosion Monitoring .....	65
5.1.1 Uncoated specimens.....	65
5.1.2 Specimens coated with Polymer modified cementitious RIV 1-2 .....	67
5.1.3 Specimens coated with Polymer modified cementitious “improved” .....	70
5.1.4 Coatings with different p/c ratios .....	73
5.2 Measure of Chloride concentration.....	75
5.2.1 Specimens Coated with RIV 1-2.....	76
5.2.2 Specimens Coated with polymer modified cementitious improved RIV 1-1 .....	77
5.3 Measurement of Coating Thickness.....	79
6.0 Discussion .....	81
6.1 Specimens coated with Polymer Modified Cementitious RIV1-2.....	83
6.1.1 Chloride profile and surface concentration RIV 1-2.....	83
6.1.2 Diffusion coefficient of Chloride $D_{cl+riv}$ .....	85

6.2 Specimens coated with Polymer Modified Cementitious “improved” RIV1-1 .....	86
6.2.1 Chloride profile and surface concentration RIV 1-1 .....	86
6.2.2 Diffusion coefficient .....	87
6.3.1 Resistance of the coating and diffusion coefficient of the coating .....	88
6.3.2 Initiation of corrosion of the rebar .....	89
6. 4 Comparison between RIV 1-1 and RIV 1-2.....	92
6.5 Different Cycling: 101 and 52.....	92
7.0 Conclusion .....	95
8.0 References.....	96

## List of Figures

Figure 2.1: A tied rebar beam cage. This will be embedded inside cast concrete to increase the tensile strength of the concrete.....	11
Figure 2.2: Feldman–Sereda model for C–S–H [3] .....	13
Figure 2.3: Dimensional range of solids and pores in hydrated cement paste [3] .....	14
Figure 2. 4: graph of penetration volume versus pore diameter for different water/cement ratios [3] .....	15
Figure 2.5: Principal factors involved in the transport processes in concrete, essential in the phenomenon of corrosion. [3] .....	17
Figure 2. 6: Chloride profiles of a quay wall on the Dutch North Sea coast after 8 years of splash zone exposure, blast furnace slag cement; average of measured profiles (thin line), individual results of four cores (only symbols) and best fitting profile. [10].....	21
Figure 2. 7: Example of degradation in concrete .....	22
Figure 2. 8: Electrochemical mechanism of corrosion of steel in concrete [3] .....	26
Figure 2. 9: The relative volumes of iron and its corrosion reaction products [13].....	28
Figure 2. 10: A graph of corrosion penetration depth versus service life time [3].....	28
Figure 2. 11: Schematic representation of the depth of carbonation of concrete as a function of the time [17].....	31
Figure 2.12: Relationship between chloride content found in bridge decks and percentage of reinforcement showing corrosion [21].....	32
.Figure 2. 13: Schematic representation of pitting corrosion of steel in concrete [3].....	33
Figure 2. 14: Example of relationship between the molar ratio of $Cl^-$ and $OH^-$ in the pore solution and the corrosion rate of steel [24, 25].....	34
Figure 2.15: Schematic representation of the corrosion conditions of passive steel in concrete, under different conditions of moisture content. ....	35
Figure 2.16: Schematic representation of the anodic polarization curve of steel in concrete with different chloride content [3]. ....	36
Figure 3. 1: Groups of surface treatments: (a) coating and sealers (b) pore blocker (c) pore liner (adapted from [30]) .....	39
Figure 3. 2: Water vapour permeability according to ASTM E96-80 standard. (10 mm thickness concrete covered on a side by 1,1-1,6 mm coating; 2,6-3 mm thick sheet of coating without any support) [29].....	42
Figure 3. 3: capillary water absorption of treated and untreated concrete surfaces [30] .....	43
Figure 3. 4: Sorptivity of treated and untreated concrete specimens [30] .....	44
Figure 3. 5: Chloride diffusion coefficients in treated and untreated concrete systems [30].....	45
Figure 3. 6: Compressive strength (28 days of curing) as a function of different ratios p/c [6].....	46
Figure 3. 7: Flexural strength (28 days of curing) as a function of different ratios p/c [6] .....	46
Figure 3. 8: Influence of polymers in the stress-strain curves of the coatings [6] .....	47
Figure 4. 1: Cross section and top view of a concrete specimen type 1. ....	50
Figure 4. 2: Filmstrip reinforced type 1: a) particular of the reinforcement, reference electrode and b) provided with sample tray fro containing the test solution.....	50
Figure 4. 3: cross section and top view of concrete specimen type 2 .....	51
Figure 4. 4: Reinforced specimen of type 2 .....	51
Figure 4.5: Specimen of type 3 without rebar a) specimen for immersion and b) specimen for ponding.....	52
Figure 4. 6: Condition of exposure of the samples (ponding) .....	57
Figure 4. 7: Tools for measuring the corrosion potential .....	59
Figure 4. 8: Measurement of polarization resists .....	60

Figure 4. 9: Tools used for the determination of chloride concentration profiles: a) coring in column b) fitted with a circular saw cutting (diameter 25 mm, thickness 1 mm) .....	62
Figure 4. 10: Examples of measurement of coating thickness using stereoscope .....	62
Figure 4. 11: Instruments used for the determination of the concentration profiles of the chlorides: a) mill jaws for crushing the concrete, b) oven for drying of the powders .....	63
Figure 4.12: Automatic titrator to determine the profile of chlorides .....	64
Figure 5. 1: A graph of corrosion potential vs. time in days for the uncoated specimen .....	66
Figure 5. 2: Polarization resistance of the reinforced concrete of uncoated samples. ....	66
Figure 5. 3: A graph of potential vs. time for uncoated specimen C2.....	67
Figure 5. 4: Polarization resistance of the reinforced concrete of uncoated samples. ....	67
Figure 5. 5: A graph of potential vs. time for RIV 1-2.....	68
Figure 5. 6: Potential and polarization resistance of the rebar specimens C24 A1 and C24 A2 coated with RIV 1-2 (Measurement taken from 97 cycles to 101 cycles) .....	69
Figure 5. 7: Potentials vs. time for RIV 1-2 C25 w/c = 0.55 .....	69
Figure 5. 8: Polarization resistance of the rebar specimens C25 A1 and C25 A2 coated with RIV 1-2 (Measurement taken from 97 cycles to 101 cycles).....	70
Figure 5. 9: Potential resistance of the rebar specimens C23 A1 and C23 A2 coated with Map elastic smart (Measurement taken from 97 cycles to 101 cycles).....	71
Figure 5. 10: polarization resistance of the rebar specimens C23 A1 and C23 A2 coated with polymer modified cementitious (Measurement taken from 97 cycles to 101 cycles) .....	71
Figure 5. 11: Potential resistance of the rebar specimens C26 A1 and C26 A2 coated with polymer modified cementitious (Measurement taken from 97 cycles to 101 cycles).....	72
Figure 5. 12: Potential and polarization resistance of the rebar specimens C26 A1 and C26 A2 coated with polymer modified cementitious (Measurement taken from 97 cycles to 101 cycles)....	73
Figure 5. 13: Potential of reinforcement of reinforced specimen subjected to ponding.....	74
Figure 5. 14: Polarization resistance of reinforcement in concrete specimen subjected to ponding .	74
Figure 5. 15: shows the profiles of chloride penetration of the coated specimens of reinforced concrete with RIV 1-2 coating exposed to ponding.....	77
Figure 5. 16: Profiles of chloride penetration of the coated specimens of reinforced concrete with RIV 1-1 coating exposed to ponding. ....	78
Figure 5. 17: Examples of measurement of the coating thickness made with the stereoscope .....	79
Figure 6. 1: Example of Chloride concentration profile of coated specimen .....	82
Figure 6. 2: Chloride surface concentration for uncoated specimens at 40 cycles .....	83
Figure 6. 3: Surface Chloride concentration of RIV 1-2 coated specimens.....	84
Figure 6. 4: Diffusion coefficients of RIV 1-2 coated specimens.....	86
Figure 6. 5: Surface concentration RIV 1-1 coated and uncoated specimens with different w/c ratios. ....	87
Figure 6. 6: Diffusion coefficient for RIV1-1 coated specimens.....	88
Figure 6. 7: Coating resistances of all specimens .....	89
Figure 6. 8: Number of rebars corroding after various cycles for coated and uncoated specimens with w/c = 0.55 .....	90
Figure 6. 9: Cumulative corrosion of rebar for w/c = 0.55 specimens .....	90
Figure 6. 10: Number of rebars corroding after various cycles for coated and uncoated specimens with w/c = 0.65 .....	91
Figure 6. 11: Cumulative corrosion of rebar for w/c = 0.65 specimens.....	92
Figure 6. 12: Diffusion coefficient for all specimens at different cycling times (52 and 101).....	93
Figure 6. 13: Surface concentration for all specimens at different cycling times (52 and 101) .....	94

## List of Tables

Table 2. 1: components of cements [3] .....	10
Table 2. 2: Design problems and results for concrete degradation [11].....	22
Table 2. 3: Degradation caused by workmanship [11].....	23
Table 2. 4: Degradation caused materials [11].....	24
Table 2. 5: Degradation caused by environmental factors [11].....	24
Table 4. 1: Mix – design of specimen type 1 .....	53
Table 4. 2 Mix design of the specimens of type 2.....	54
Table 4. 3: coating properties .....	56
Table 4. 4: Coatings used .....	56
Table 4. 5: Experimental measurements .....	58
Table 4. 6: Criteria for corrosion as stated by ASTM C876-91 [34] .....	59
Table 5. 1: Coating thickness of reinforced specimen .....	80

## **1.0 Introduction**

At the present time, concrete is being used in every aspect of human civilization. Initially, the use of concrete was limited only to building construction, but nowadays concrete applications are quite common in various sectors. For example, highways, bridges and also facilities in industrial plants (fertilizer, petrochemical, refinery, water and waste water treatment facilities, heavy chemical industries...etc).

Rebar in alkaline concrete are protected by a thin oxide layer, called passive film.

In presence of CO<sub>2</sub> and chlorides this passive film can be broken giving rise to carbonation or chloride induced corrosion, respectively.

Most of the cases of reinforcement corrosion in concrete could be prevented applying the relevant standards and an adequate quality control in the design and construction stage.

Nevertheless, there are some cases in which, due to high aggressiveness of the environment or long design service life or in the repair of already damaged structures is necessary to adopt the so called “additional preventative measurement” to reach the target service life.

Among these preventative measurements, concrete coatings are widely used to improve durability of new, not yet damaged structures as a preventative measure, as well as in rehabilitation interventions. Nowadays various coatings systems are available, suitable for maintaining their protectiveness for long-time and for a good service life, providing that a proper application and an adequate maintenance of the coating are assured. However, the correct use of this technique in order to prevent the rebar corrosion requires knowledge of the protective mechanisms influencing the corrosion phenomena.

In this thesis the behaviour of two commercial polymer modified cementitious coatings has been studied: the experimental tests have been focused on the effect of these types of coatings on the rebar corrosion provoked by chlorides.



## **2.0 Literature review**

Reinforced concrete is concrete in which the undesirably low tensile strength of the concrete component is averted by including reinforcing structures of high tensile strength in the mass of the concrete. Reinforced concrete is a very versatile construction material. Properly designed concrete structures are both strong and durable. However, concrete structures are vulnerable to a number of factors that can cause deterioration. Deterioration can result in loss of strength and unsafe conditions. Therefore it is important to have an understanding of the vulnerabilities of concrete structures in order to help minimize long-term repair and maintenance cost [1].

### **2.1 Concrete [2]**

Concrete is a composite construction material composed primarily of aggregate, cement, and water. There are many formulations that have varied properties. The aggregate is generally coarse gravel or crushed rocks such as limestone, or granite, along with a fine such as sand. The cement, commonly Portland cement, and other cementitious materials such as fly ash and slag cement, serve as a binder for the aggregate. Various chemical admixtures are also added to achieve varied properties. Water is then mixed with this dry composite which enables it to be shaped (typically poured) and then solidified and hardened into rock-hard strength through a chemical process known as hydration. The water reacts with the cement which bonds the other components together, eventually creating a robust stone-like material. Concrete has relatively high compressive strength, but much lower tensile strength (Concrete tensile strength is about 10% of its compressive strength). For this reason is usually reinforced with materials that are strong in tension (often steel). Concrete is also highly alkaline. This property provides an environment that limits the corrosion of any embedded steel and helps to assure the durability of the reinforced concrete member. For this reason reinforcing bars are embedded well below the concrete surface. Concrete is a relatively durable and robust building material, but it can be severely weakened by poor manufacture or a

very aggressive environment. Concrete degradation can be a cause for concern on its own, or in reinforced structures it may lead to decreased protection to the steel. This in turn encourages corrosion of the steel, often followed by cracking and spalling of the concrete

### 2.1.1 Structure and Characteristics of cement [3]

Reinforced concrete is a material formed with cement as a matrix obtained from hydration of different aggregates. The most used cement is Portland cement. It is produced by grinding clinker, which is obtained by burning a suitable mixture of limestone and clay raw materials. Its main components are:

- tricalcium and dicalcium silicates ( $C_3S$  and  $C_2S$ ),
- the aluminate and ferroaluminate of calcium ( $C_3A$  and  $C_4AF$ )

(In the chemistry of cement, the following abbreviations are used:  $CaO = C$ ;  $SiO_2 = S$ ;  $Al_2O_3 = A$ ;  $Fe_2O_3 = F$ ;  $H_2O = H$ ;  $SO_3 = S$ .) Gypsum ( $CS$ ) is also added to clinker before grinding, to control the rate of hydration of aluminates.

Tricalcium silicate	$3CaO.SiO_2$	$C_3S$	45-60%
Dicalcium silicate	$2CaO.SiO_2$	$C_2S$	5-30%
Tricalcium aluminates	$3CaO.Al_2O_3$	$C_3A$	6-15%
Tetracalcium ferroaluminate	$4CaO.Al_2O_3 Fe_2O_3$	$C_4AF$	6-8%
Gypsum	$CaSO_4.2H_2O$	$CS$	3-5%

Table 2. 1: components of cements [3]

### 2.1.2 Steel reinforcement bars

A rebar, also known as reinforcing steel, reinforcement steel, or a deformed bar, is a common steel

bar, and is commonly used as a tensioning device in reinforced concrete and reinforced masonry structures holding the concrete in compression. It is usually formed from carbon steel, and is given ridges for better mechanical anchoring into the concrete.

Steel has an expansion coefficient nearly equal to that of modern concrete. If this were not so, it would cause problems through additional longitudinal and perpendicular stresses at temperatures different than the temperature of the setting.

The advantages these improved properties would provide in concrete reinforcement were recognized and steel in the form of reinforcing bars (rebars) became an effective method of providing ductility and tensile strength to concrete. Modern steel rebar typically has a Young's modulus of  $29 \times 10^6$  psi and behaves in an elastic-plastic manner. PSI is short for Pounds per Square Inch which is a unit measure of pressure.  $1 \text{ psi} = 6894.75729 \text{ Pascal}$ .



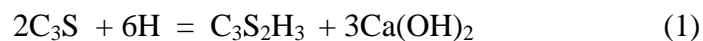
Figure 2.1: A tied rebar beam cage. This will be embedded inside cast concrete to increase the tensile strength of the concrete.

## 2.3 Hydration of Cement [3]

The hydration of compounds of Portland cement form colloidal hydrated products of very low solubility. Aluminates react first, and are mainly responsible for setting, that's to say solidification of the cement paste. The hydration of  $C_3A$  and  $C_4AF$ , in the presence of gypsum, mainly gives rise to hydrated sulfoaluminates of calcium. The hydration of silicate is the main effect of solidification and Hardening of cement paste. The hydration of  $C_3S$  and  $C_2S$  gives rise to calcium silicate hydrates forming a rigid gel indicated as C–S–H [3].

It is composed of extremely small particles with a layer structure that tend to aggregate in formations a few  $\mu\text{m}$  in dimension, characterized by interlayer spaces of small dimensions (1–2 nm) and by a large surface area (100–700  $\text{m}^2/\text{g}$ ). Hydration of calcium silicates also produces hexagonal crystals of calcium hydroxide ( $\text{Ca}(\text{OH})_2$ , Portlandite). These have dimensions of the order of a few  $\mu\text{m}$  and occupy 20 to 25 % of the volume of solids. They do not contribute to the strength of cement paste. However,  $\text{Ca}(\text{OH})_2$ , as well as  $\text{NaOH}$  and  $\text{KOH}$  that are present in small amounts, are very important with regard to protecting the reinforcement, because they cause an alkaline pH up to 13.5 in the pore liquid.

The hydration reactions of tricalcium and dicalcium silicates can be illustrated as follows:



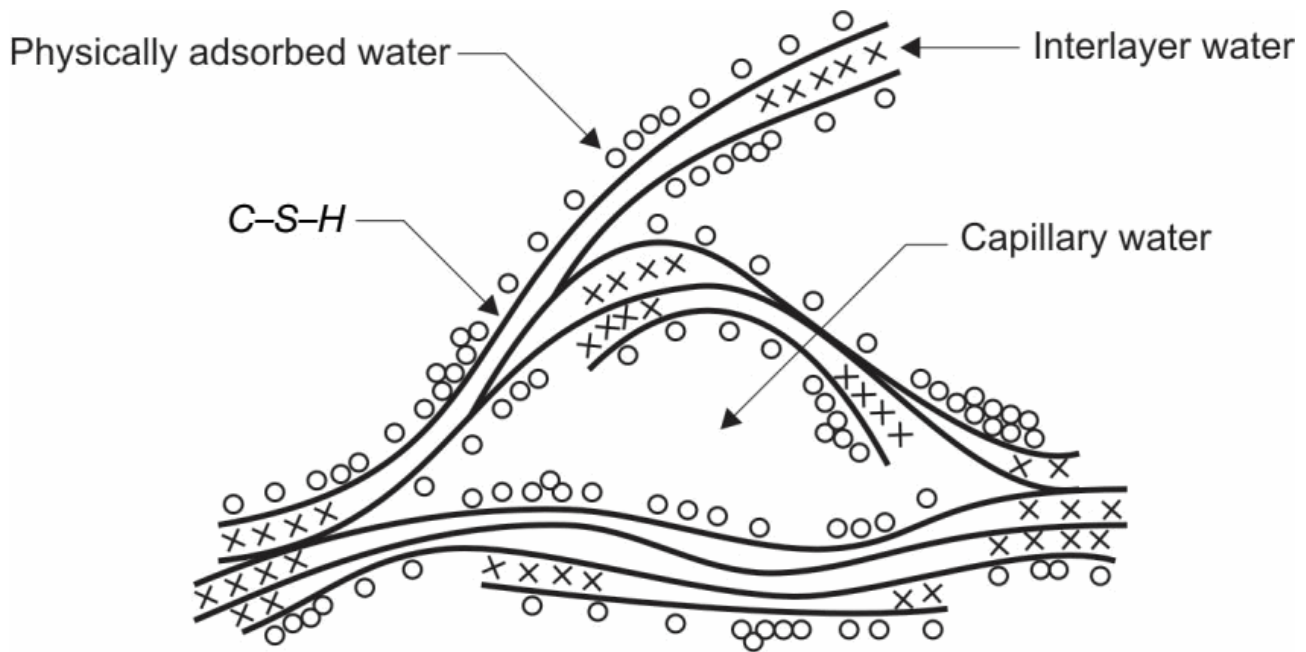


Figure 2.2: Feldman-Sereda model for C-S-H [3]

### 2.3 Porosity in reinforced concrete [3]

After the hydration of the reinforced concrete, we'll have the presence of several types of different sizes of pores. The pores can be divided into 3 types:

- Gel pores C-S-H have a volume equal to about 28 % of the gel and dimensions ranging from a few fractions of a nm to several nm .These do not affect the durability of concrete and its protection of the reinforcement because they are too small to allow significant transport of aggressive species.
- The capillary pores are the voids not filled by the solid products of hydration of hardened cement paste. They have dimensions of 10 to 50 nm if the cement paste is well hydrated and produced using low water/cement ratios (w/c), but can reach up to 3-5  $\mu\text{m}$  if the concrete is made using high w/c ratios or it is not well hydrated.
- Entrapped air voids are larger pores of dimensions of up to a few mm. They are not removed by compaction of fresh concrete.

- Air bubbles with diameters of about 0.05–0.2 mm may also be introduced in the cement paste intentionally by means of air-entraining admixtures, so as to produce resistance to freeze-thaw cycles

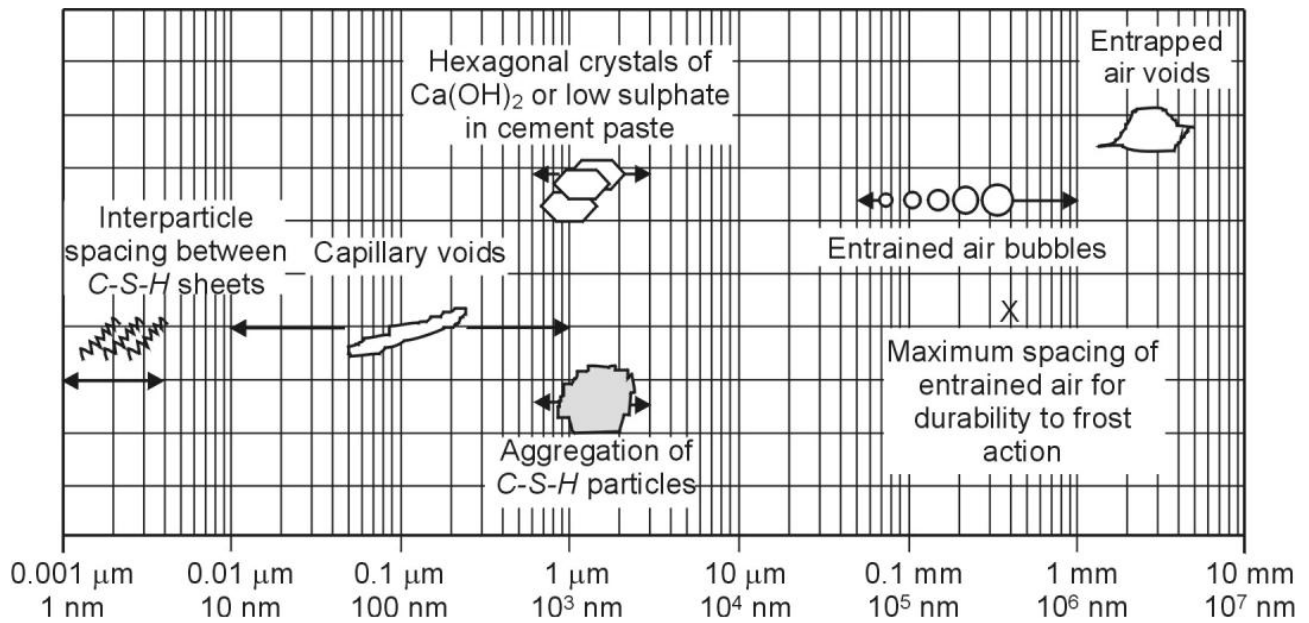


Figure 2.3: Dimensional range of solids and pores in hydrated cement paste [3]

When the cement paste is kept moist (curing), the hydration proceeds and the volume of the capillary pores decreases and will reach a minimum when the hydration of cement has completed.

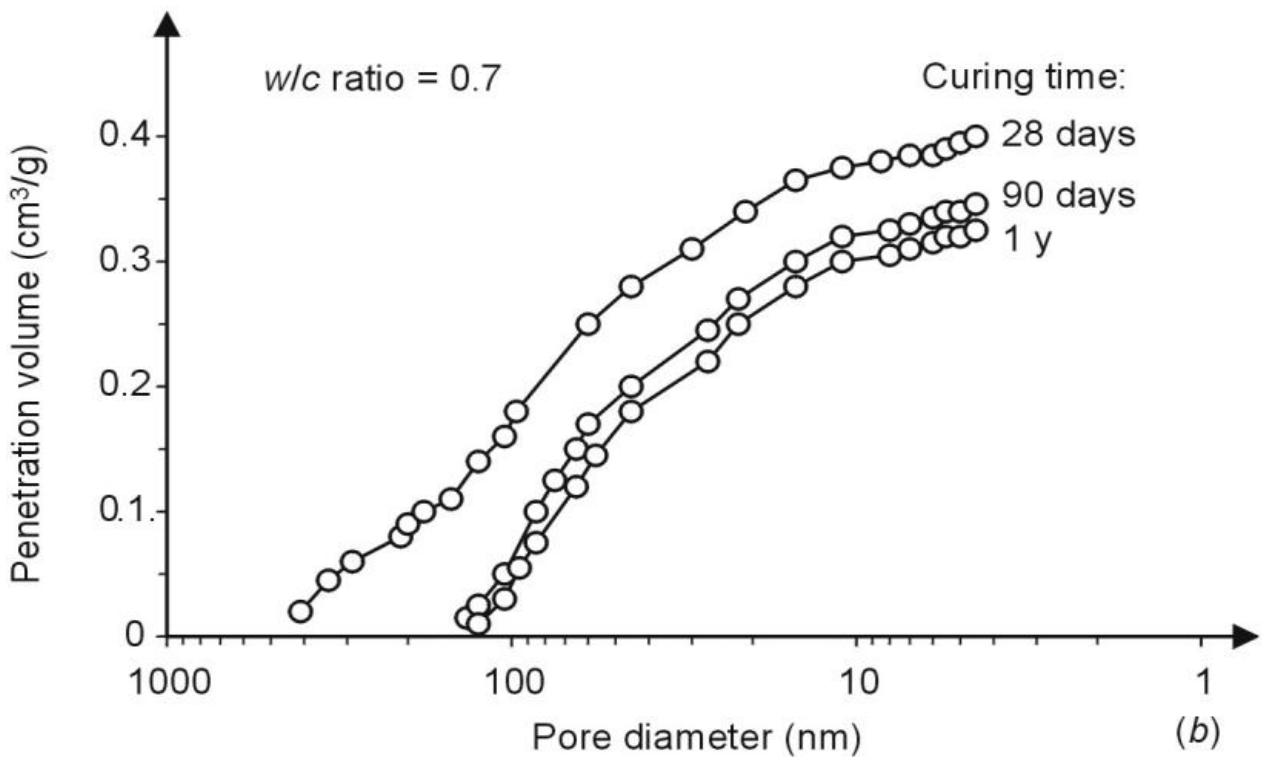
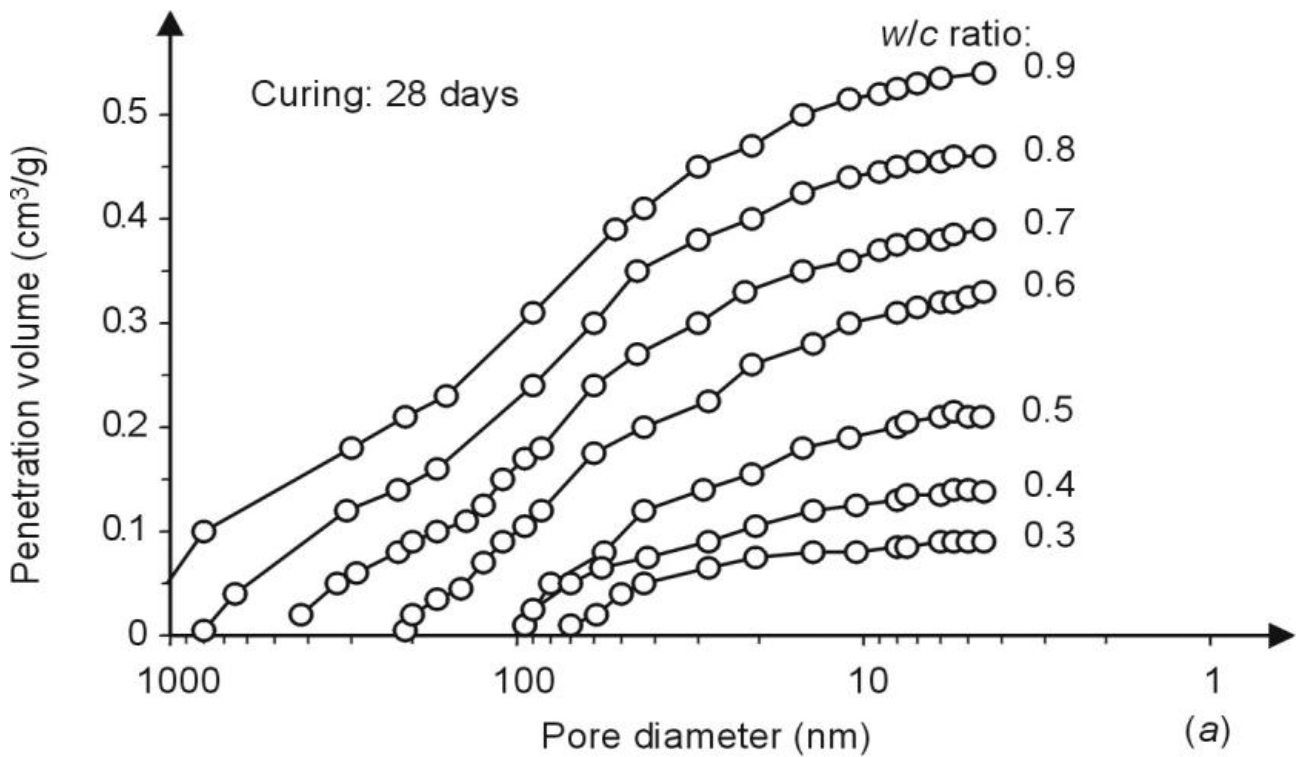


Figure 2. 4: graph of penetration volume versus pore diameter for different water/cement ratios [3]

Nevertheless, the value reached after complete hydration will be greater in proportion to the initial distance between the cement particles and thus to the amount of mixing water.

In reality, the permeability of a porous system is dependent not only on the porosity of the medium,

but also on the connectivity of the pores. Among the various types of pores in concrete, the air voids are usually isolated (only the air bubbles added for freeze-thaw! Except in honeycombs) while the capillary pores are generally interconnected in the form of capillaries; even at the same porosity, they contribute quite differently to the permeability of concrete.

## **2.4 Transport Processes in Concrete [4]**

Concrete can be penetrated, through its pores, by gases (e. g. nitrogen, oxygen and CO<sub>2</sub> present in the atmosphere) and liquid substances (e. g. water, in which various ions are dissolved

### **2.4.1 Permeability**

The term permeability indicates, in general, the property of concrete to allow the ingress of these substances. The permeability of concrete is not only important for water-retaining structures and elements (pipes, canals or tanks), but is a decisive factor in the durability of reinforced concrete. Phenomena that lead to degradation of reinforced concrete depend on the processes that allow transport of water, carbon dioxide, chloride ions, oxygen, sulphate ions and electrical current within the concrete.

The movement of fluids and ions through concrete can take place according to four basic mechanisms:

- a) Capillary suction, due to capillary action inside capillaries of cement paste,
- b) Permeation, due to pressure gradients,
- c) Diffusion, due to concentration gradients,
- d) Migration, due to electrical potential gradients



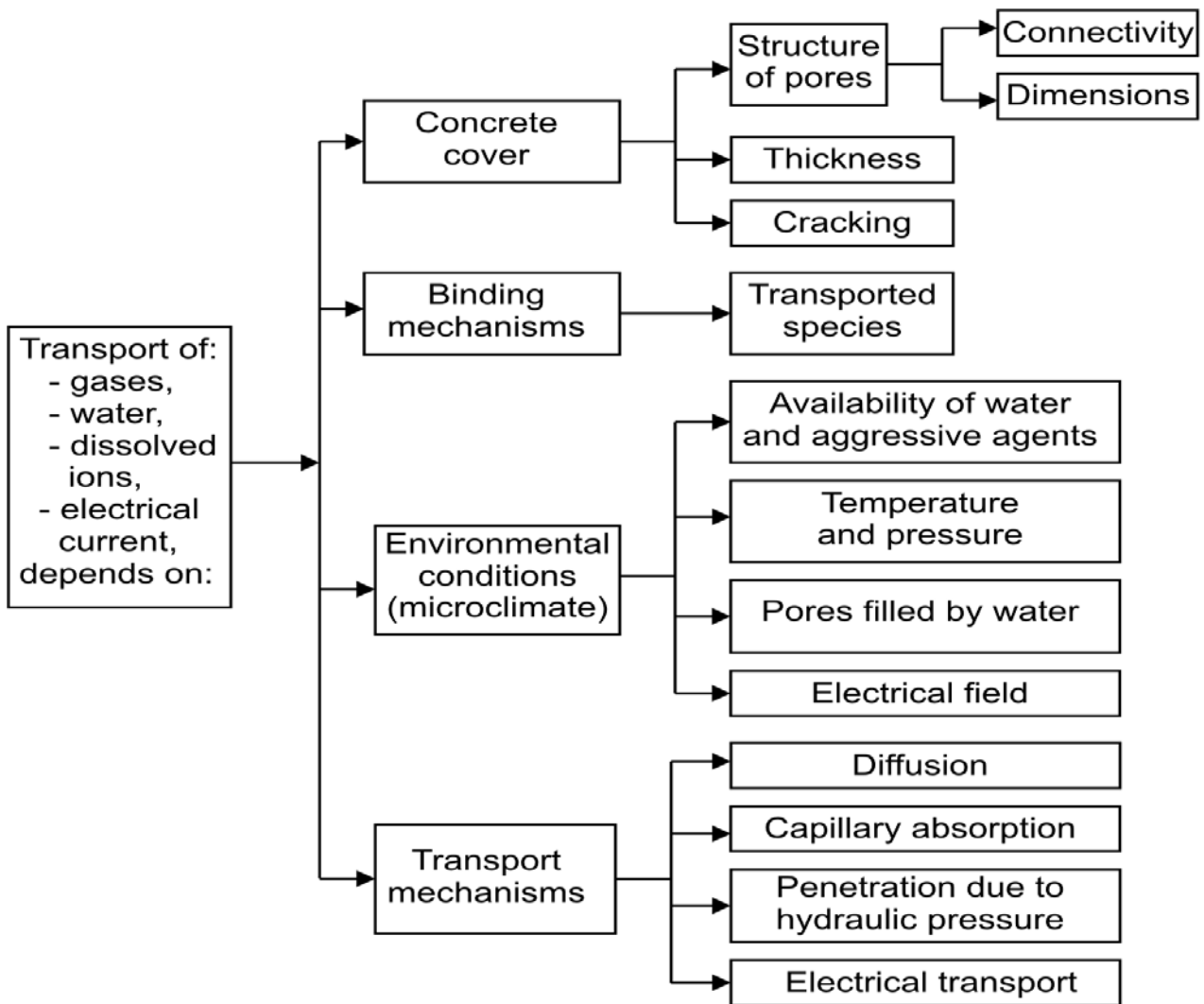


Figure 2.5: Principal factors involved in the transport processes in concrete, essential in the phenomenon of corrosion. [3]

## 2.4.2 Diffusion

The penetration of aggressive species within concrete often occurs by diffusion, that is, by the effect of a concentration gradient.  $O_2$ ,  $CO_2$ ,  $Cl^-$  or  $SO_4^-$  move through pores from the surface, where they are present in higher concentrations to internal zones where their concentration is lower. Gases diffuse much more rapidly through open pores than through water-saturated ones (diffusion of gases in water is 4-5 orders of magnitude slower than in air). On the other hand, chloride and sulphate ions diffuse only when dissolved in pore water; the diffusion is more effective in saturated than in partially saturated pores [4].

### 2.4.2.1 Stationary Diffusion

Under conditions of stationary (unidirectional and constant) mass transfer, Fick's first law describes the phenomenon of diffusion:

$$F = -D \cdot \frac{dC}{dx} \quad (3)$$

Where:  $F$  is the flux ( $\text{kg}/\text{m}^2 \cdot \text{s}$ ),  $C$  is the concentration of the diffusing species present at distance  $x$  from the surface.  $D$  is the diffusion coefficient, expressed in  $\text{m}^2/\text{s}$ , which depends on the diffusing species, on the characteristics of the concrete and on the environmental conditions. This coefficient can change as a function of position and time, following variations in the pore structure (i. e. due to hydration of the cement paste), or of the external humidity (thus the degree of saturation of pores) or the temperature.

### 2.4.2.2 Non-stationary Diffusion

Collepari et al [7] demonstrated that chloride diffusion into concrete can usefully be modelled by the error function solution to Fick's second law of diffusion by Crank [8]. Equation (1) mathematically expresses Fick's second law of diffusion for the non-steady state condition, where the concentration  $C$  of the medium is changing with time  $t$ .

$$\frac{\partial C}{\partial t} = D \cdot \frac{\partial^2 C}{\partial x^2} \quad (4)$$

It is only applicable to one-dimensional flow with the space co-ordinate  $x$ , measured normal to the section. The parameter  $D_{ca}$  is the apparent diffusion coefficient. The equation may be solved for a semi-infinite medium using the Laplace transformation, assuming that the surface concentration is constant ( $C_0$ ), the initial concentration in the concrete is zero and the infinite point condition  $C_{(x=\infty, t>0)}$  is also zero since it is far enough away from the surface,  $D_{ca}$  is constant in time and space. The error function solution as applied by Crank is based on these assumptions, and may be stated as

Equation 5.

$$C = C_0 [1 - \operatorname{erf}\left(\frac{x}{2\sqrt{(D_{ca}t)}}\right)] \quad (5)$$

where erf is the error function. The error function as defined in Equation 2.6 is a standard mathematical function, which occurs in statistics and various studies in physics and heat conduction equations to which Fick's laws of diffusion are closely related equation 6

$$\operatorname{erf}(x) = \frac{2}{\sqrt{\pi}} \int_0^x e^{-t^2} dt \quad (6)$$

It is accepted that diffusion theory alone may not fully describe the relevant transport mechanisms and therefore coefficients  $D_{ca}$  derived from Crank's application of the error function solution are best characterised as empirical values, and are sometimes referred to as 'apparent diffusion coefficients', based on a best fit curve between theoretical and actual performance. The concrete is sampled at various depth intervals and analysed for chloride content to establish a chloride profile. Samples may be obtained by the collection of dust drillings at specified depth intervals or by profile grinding of a concrete core. The established profile is then compared with a predetermined profile or analysed by producing a best-fit least squares curve using the error function solution to Fick's second law of diffusion. This will produce an apparent diffusion coefficient  $D_{ca}$  and a notional surface concentration  $C_{sn}$ . The surface chloride concentration cannot be determined accurately and so a notional surface concentration is estimated by continuing the determined concentration profile using the error function equation until it intersects the Y-axis. The point at which the profile intersects the Y-axis is then known as the notional surface concentration  $C_{sn}$  and Equation 2 become the modified form of the error function equation shown in Equation 7

$$C = C_{sn} [1 - \operatorname{erf}\left(\frac{x}{2\sqrt{(D_{ca}t)}}\right)] \quad (7)$$

The method used to produce the best fit least squares curve using the modified form of the error function equation is well suited to statistical based computer packages. One such statistical package is 'Microsoft Excel' which includes the 'Solver' analysis tool as part of its analysis tool pack. 'Microsoft Excel Solver' is based on well-established numerical analysis and is used for equation solving and optimisation by iterative procedure.

Bamforth [9] noted that there was very little time-dependent change in  $D_{ca}$  for Portland cement concrete but there were significant reductions for PFA and GGBS mixes over the period of exposure. Using both his work and other published results, Bamforth expressed the relationship between the decreasing apparent chloride diffusion coefficient  $D_{ca}$  value and the exposure time for PFA and GGBS concretes:

$$D_{ca} = a \cdot t^n \quad (8)$$

where

$t$  exposure time

$a$  value of  $D_{ca}$  at time  $t = 1$  year

$n$  slope of the line relating  $\log D_{ca}$  and  $\log t$

The coefficients  $a$  and  $n$  are derived from regression analysis of the data, which was collected by Bamforth. This further refinement has not been included in the judgements made in this paper, thus erring on the conservative side.

Figure 2.6 shows an example of the profile of chloride penetration through the concrete structure.

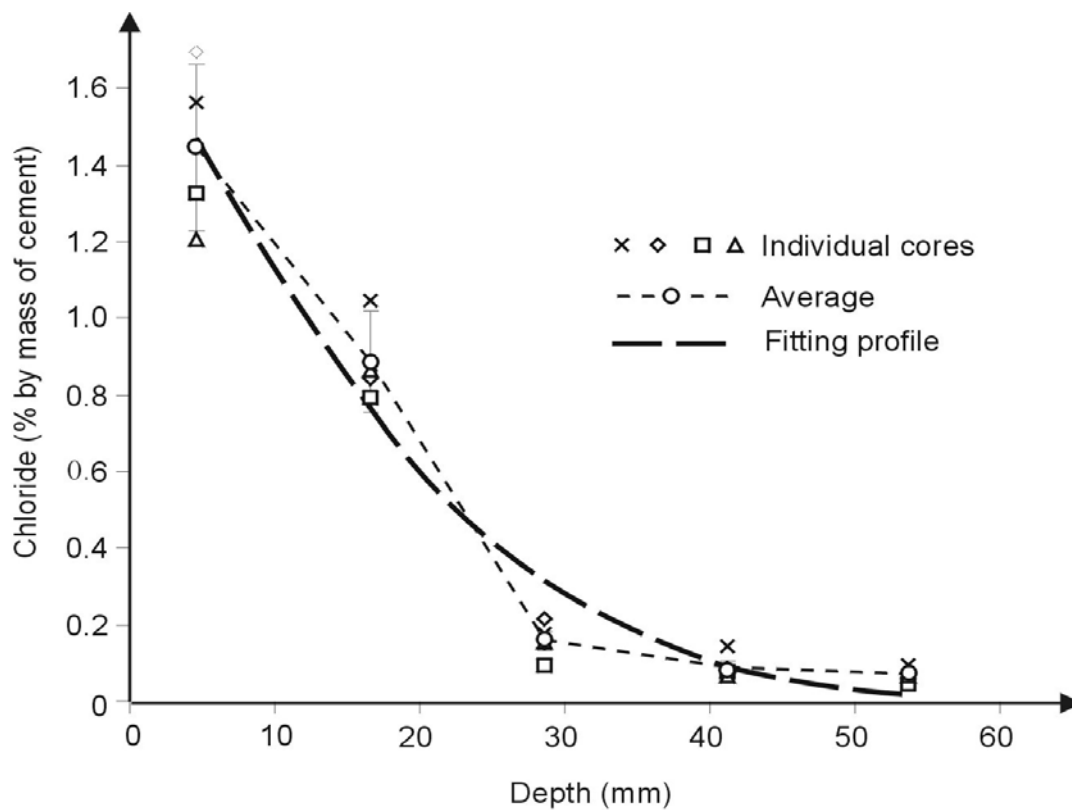


Figure 2. 6: Chloride profiles of a quay wall on the Dutch North Sea coast after 8 years of splash zone exposure, blast furnace slag cement; average of measured profiles (thin line), individual results of four cores (only symbols) and best fitting profile. [10]

## 2.5 Deterioration of Reinforced concrete [3]

Reinforced concrete structure may deteriorate because of deterioration of the concrete itself or because of corrosion of the steel reinforcing bars inside the concrete. Common causes of the deterioration of concrete include alkali-aggregate reaction, chemical attack, freezing and thawing action, abrasion and fire. There is often the misunderstanding that carbonation and chloride attack would cause deterioration of concrete. In actual fact, carbonation and chloride attack would not cause any harm to the concrete itself; they mainly cause depassivation of the steel in concrete, which then leads to steel corrosion. Deterioration of concrete is not a common problem. In most cases, if there is any problem with the durability of a concrete structure, it is the corrosion of the steel reinforcing bars that is most likely to be the major cause.

## 2.5.1 Deterioration of the concrete itself <sup>[11]</sup>



Figure 2. 7: Example of degradation in concrete

### 1. Design problems

There are a number of design and specification problems that can result in reinforced-concrete deterioration.

Cause of the problem	Results
Poor reinforcement details, for example congested or inadequate reinforcement, inadequate cover to reinforcement	Leads to cracking, poor compaction, loss of alkaline environment, and voids around the steel
Poor detailing of fixings, window frames, handrails, supports, and expansion joints	Water penetration, localised cracking, and balcony weakness
Long, slender components	Excessive flexing may lead to cracking
Inadequate design for creep	Deflection due to strain under continued stress that can result in cracking
Poor drainage	Leads to water ponding and localised corrosion/degradation
Incorrect concrete grade for purpose	Can produce concrete that is too weak/too strong
Mixes that result in high drying shrinkage	Can result in cracking
Mixes that are permeable to chloride ions	Chloride induced reinforcement corrosion

Table 2. 2: Design problems and results for concrete degradation [11]

## 2. Workmanship

Care and attention during construction is crucial to the long-term durability of reinforced concrete. Current building codes, including AS 3600 [11] give guidance appropriate to the exposure conditions, and on mix design (particularly the water/cement ratio and amount of cement binder), additives, compaction, detail, and thickness of cover. The type of cement binder is also now well defined. However, this has not always been the case and durability problems of earlier concrete are summarised in the following table 2.3.

<b>Causes of problems</b>	<b>Results</b>
Poor mixing	Leads to inhomogeneous concrete, localised weakness, and reinforcement corrosion
Incorrect water/cement ratios	Can lead to variable strength, inadequate durability, increased drying shrinkage, excessive permeability
Poor compaction/vibration	Results in honeycombing, voids, excessively permeable concrete, localised reinforcement corrosion
Varying and inadequate cover depths around the steel	Leads to localised reinforcement corrosion, penetration of damaging substances
Poor curing techniques	Results in shrinkage cracks, increased permeability, poor durability
Premature stripping of formwork	Can result in cracking

Table 2. 3: Degradation caused by workmanship [11]

## 3. Materials

Lack of knowledge about the importance of careful selection and specification of materials and the use of additives has created a number of durability problems for historic concrete structures. They can be the result of the use of the following.

<b>Causes of problems</b>	<b>Results</b>
Too low cement content	Results in weakened and poor durability concrete
Too high cement content	Can result in excessive shrinkage/poor workability and cracking
Additives, such as calcium chloride	Chloride ions destroy the protective passive-oxide layer on the steel
High alumina cement	Weakening concrete in wet environment
Too finely-ground cements	Causing excessive shrinkage and cracking that compromises the permeability of the concrete
Poor quality aggregates	Resulting in alkali-aggregate reaction, poor workability of the concrete, poor compaction, high drying shrinkage and weak concrete
Contaminated aggregates	Resulting in corrosion of steel and degradation of concrete in extreme cases
Poorly shaped and badly graded aggregates	Results in poor workability often necessitating extra water or vibration during forming which can lead to segregation, bleeding etc
Incorrect water/cement ratios	Giving rise to weak concrete, loss of durability, increased permeability to gases and chloride ions

Table 2. 4: Degradation caused materials [11]

#### 4. Environmental influences

These play an important part in reinforced-concrete deterioration and include the following.

<b>Environmental conditions</b>	<b>Result</b>
Carbon dioxide and acidic gases	Lower pH around the steel that enables corrosion to progress
Water	Can introduce depassivating chloride ions into concrete
Freeze thaw in colder zones	Breakdown of surface, progressive cracking, water penetration to reinforcement that enables corrosion to progress
Salt ingress	Marine salt introduces depassivating chloride ions into the surface of the concrete
Chemical attack	Chemical attack by chlorides can cause corrosion of steel or sulphates that can cause degradation of the cementitious matrix
Vibration	Causes cracking, spalling, and delamination
Impact damage	Causes physical weakening of structural components, exposure of steel reinforcement, cracking etc

Table 2. 5: Degradation caused by environmental factors [11]

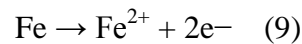


## 2.5.2 Corrosion of steel in concrete [3, 12, 13, 14, 15]

Corrosion of steel in concrete is an electrochemical process. The corroding system consists of an anode in which steel is corroded, a cathode, an electrical conductor, and an electrolyte (concrete pore solution). The potential difference between anode and cathode is the driving electrical force for steel corrosion. Usually, the process can be divided into primary electrochemical processes and secondary processes.

### Primary Electrochemical Processes

For steel in concrete, as the passive film is degraded by chloride ions or the pH reduced by carbonation, the metallic Fe at the anode is oxidized to form ferrous ions  $\text{Fe}^{2+}$ :

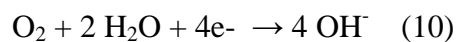


The electrons released at the anode flow through the steel to the cathodic areas, as illustrated in

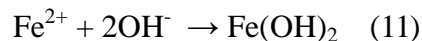
Figure 2.8 [12]

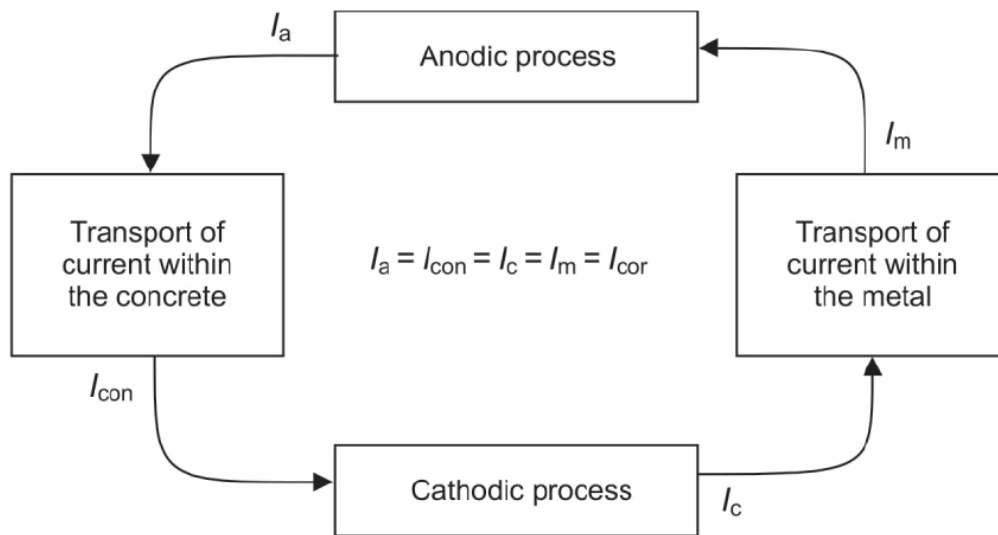
The above reaction is initially balanced by cathodic reaction of dissolved oxygen

( $\text{O}_2$ ) to hydroxyl ions ( $\text{OH}^-$ ):



The anodic product  $\text{Fe}^{2+}$  reacts with the cathodically formed hydroxyl ions to produce precipitate of ferrous hydroxide ( $\text{Fe}(\text{OH})_2$ ):





*Anodic process*

iron + water → corrosion products of iron + acidity + electrons (within the metal phase)

*Cathodic process*

oxygen + water + electrons (from the metal phase) → alkalinity

*Transport of current within concrete*

ion movement in the presence of water; enhanced by increase in pH and presence of chloride

*Transport of current in the metal*

electrons move from the anode, where they are produced, towards the cathode, where they are consumed

Figure 2. 8: Electrochemical mechanism of corrosion of steel in concrete [3]

$$I_a = I_c = I_m = I_{con} = I_{corr}$$

The common value of all these currents ( $I_{corr}$ ) is, in electrochemical units, the rate of the overall process of corrosion. The corrosion rate will thus be determined by the slowest of the four partial processes.

In reality, the electrical resistance of the reinforcement is always negligible with respect to that of the concrete. Therefore, the transport of current within the reinforcement is never a slow process and thus never contributes to reducing the rate of corrosion [3].

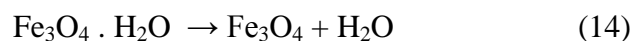
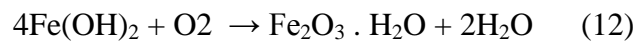
Instead, under particular conditions inside the concrete, each of the other three processes can take place at negligible rate and thus become the kinetically controlling one. More precisely, the corrosion rate is negligible when one of the following conditions exists:

- the anodic process is slow because the reinforcement is passive, as when the concrete is not carbonated and does not contain chlorides;
- the cathodic process is slow because the rate at which oxygen reaches the surface of the reinforcement is low, as in the case of water-saturated concrete;
- the electrical resistance of the concrete is high, as in the case of structures exposed to environments which are dry or low in relative humidity.

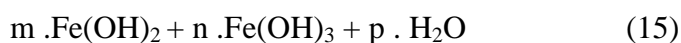
### Secondary Processes

The  $\text{Fe}(\text{OH})_2$  can be further converted to hydrated ferric oxide ( $\text{Fe}_2\text{O}_3 \times \text{H}_2\text{O}$ ), also known as ordinary red-brown rust, and black magnetite ( $\text{Fe}_3\text{O}_4$ ) preceded by the formation of green

hydrated magnetite ( $\text{Fe}_3\text{O}_4 \times \text{H}_2\text{O}$ ):



The composition of rust on iron may be expressed as a general formula:



Where the values of m, n and p vary considerably depending on conditions such as pH of the solution, the oxygen supply and moisture content

Since the volume of rust products is much higher (about 4 to 6 times) than that of the iron as shown in Figure 2.9 <sup>[13]</sup>, the formation of rust products will lead to cracking and spalling of the cover concrete when expansive stress exceeds the tensile strength of the concrete, and reduction of steel reinforcing cross section may lead to structure failure

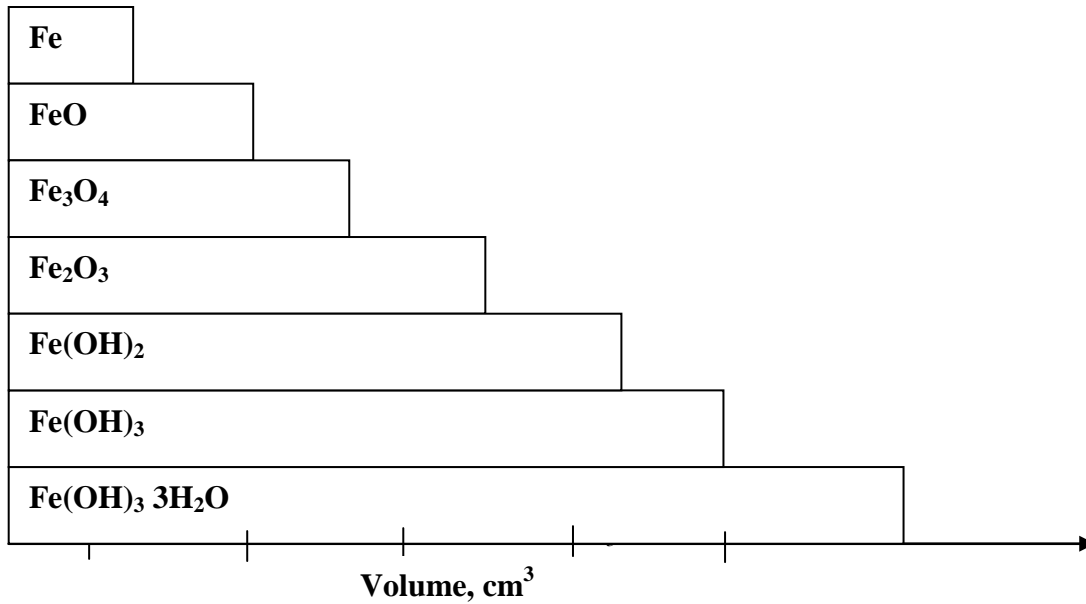


Figure 2. 9: The relative volumes of iron and its corrosion reaction products [13]

The model has three distinct phases: diffusion, corrosion and deterioration (see Figure 2.9). The first phase, initiation of corrosion, is defined as the time for chloride ions to penetrate the concrete cover and reach the corrosion threshold limit on steel surfaces (for example considering a cover depth equal to 2.5% of the cover depth distribution). The diffusion time usually can be determined empirically using Fick's second law [14].

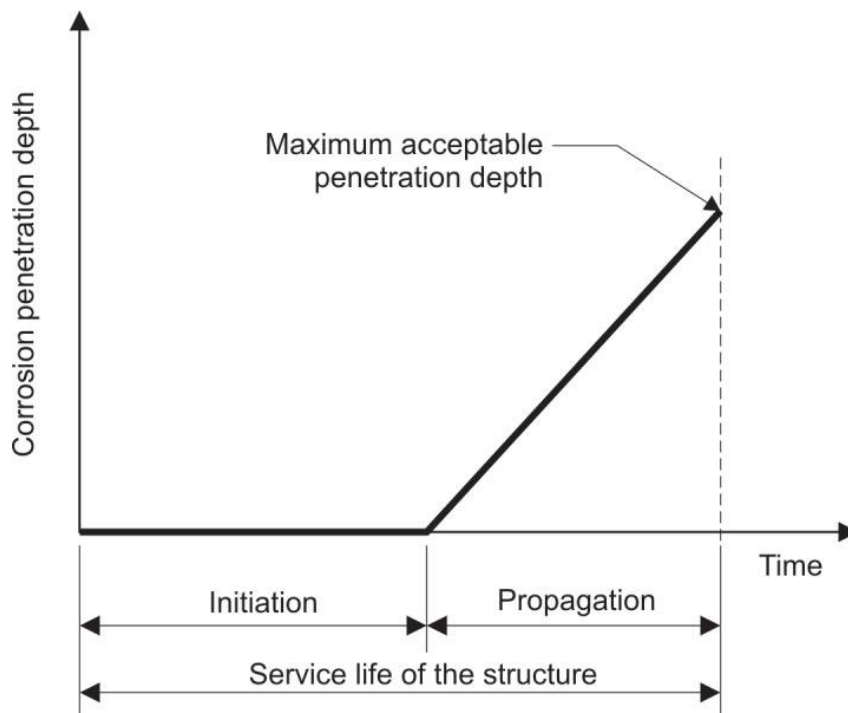


Figure 2. 10: A graph of corrosion penetration depth versus service life time [3]

The second phase, propagation of corrosion, is defined as a period of time from initiation of

corrosion to a serviceability limit state (maximum acceptable penetration depth), that can be defined for example as cracking of cover concrete.

In other approaches also a third phase is considered, deterioration, describes the time to reach a damage level of a per cent which is deemed as the time to rehabilitation. During this phase, from the cracking of the concrete cover at 2.5% cover depth to the time for rehabilitation, it has been shown empirically that the deck will continue to deteriorate at a relatively uniform rate [15].

### **2.5.2.1 Carbonation** [17, 18, 19]

Carbonation, i.e. the reaction of the alkalis in concrete with the carbon dioxide in air, does not cause deterioration of concrete but it has important effects on the durability of reinforced concrete structures. It gradually reduces the alkalinity of concrete to a pH value of about 9 and once the pH of the concrete surrounding the steel drops to below 10, the steel will become de-passivated and if water and oxygen are available the steel will start to corrode.

Carbonation takes place even at small CO<sub>2</sub> concentrations such as are present in rural air, where the CO<sub>2</sub> content is about 0.03%. In an unventilated room, the content may rise to above 0.1%. In large cities it is on average 0.3% and exceptionally up to 1%. The highest concentration of CO<sub>2</sub> is probably encountered by the lining of vehicle tunnels. Carbonation occurs progressively from the outside of concrete exposed to CO<sub>2</sub> but does so at a decreasing rate because CO<sub>2</sub> has to diffuse through the pore system, including the already carbonated surface zone of concrete. Such diffusion is a slow process if the pores in hydrated cement paste are filled with water because diffusion of CO<sub>2</sub> in water is 4 orders of magnitude slower than in air. On the other hand, if there is insufficient water in the pores, CO<sub>2</sub> remains in gaseous form and does not react with the hydrated cement. It follows that the rate of carbonation depends on the moisture content of the concrete.

The highest rate of carbonation occurs at a relative humidity of around 70% (Figure 2.11). Under steady conditions, the depth of carbonation increases in proportion to the square root of time, as depicted by the following equation:

$$d_c = C\sqrt{t} \quad (16)$$

$d_c$  = depth of carbonation,

$C$  = carbonation coefficient and

$t$  = time of exposure.

Apart from the environmental conditions, the carbonation coefficient is dependent mainly on the quality, particularly the diffusivity, of concrete. Broadly speaking, in concrete with a W/C ratio of 0.6, a depth of carbonation of 15 mm would be reached after 15 years, but in concrete with a W/C ratio of 0.45, the same depth of carbonation would not be reached until after 100 years. It has been shown that the depth of carbonation can be described by the following equation:

$$y = \sqrt{2.D \frac{C_1}{C_2} .t} \quad (17)$$

Where;

$y$ = depth of carbonation [mm]

$D$  = diffusion coefficient [ $\text{mm}^2/\text{a}$ ] (a=year)

$C_1$ = concentration of  $\text{CO}_2$  in the air (approx. 0.6-0.8g/m<sup>3</sup>)

$C_2$ = amount of  $\text{CO}_2$  to carbonate concrete (Approx. 10,000-50,000 g/m<sup>3</sup>)

$t$  = time [years]

Since the diffusivity is a function of the pore system of the hardened cement paste, the type of cement, the W/C ratio and the degree of hydration are the relevant factors influencing carbonation. As these factors influence also the strength of concrete, it is often said that the rate of carbonation

may be simply taken as a function of the strength grade of concrete. Whilst this postulation applies quite satisfactorily to laboratory cured concrete, in field cast concrete, which is usually provided with less than ideal curing, the curing conditions also have great effects on the rate of carbonation, as illustrated in Figure 2.11

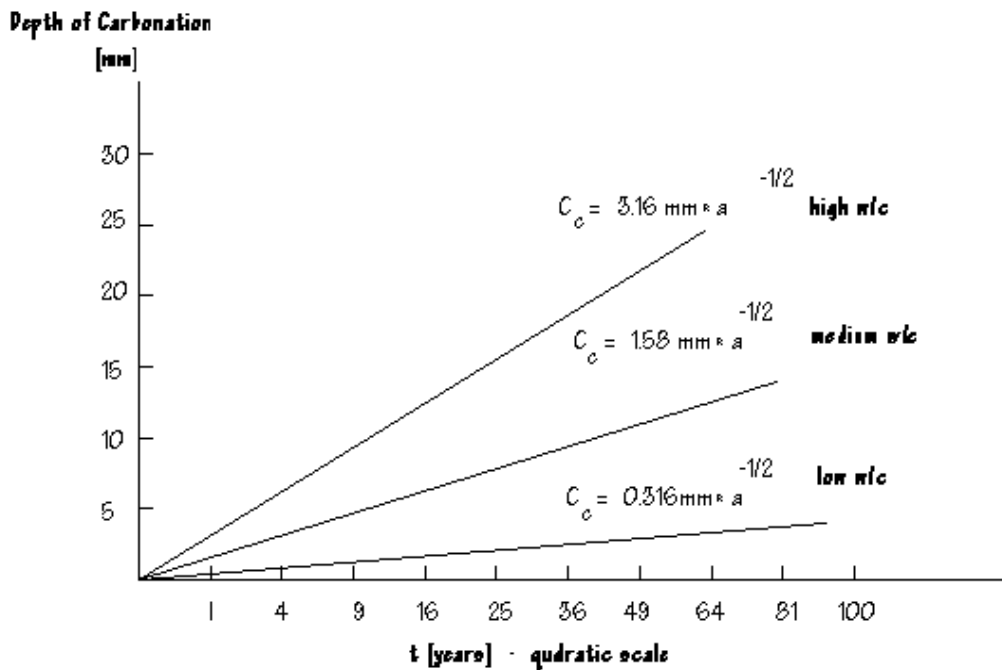


Figure 2. 11: Schematic representation of the depth of carbonation of concrete as a function of the time [17].

### 2.5.2.2 Chlorides

Chloride contamination of concrete is a frequent cause of corrosion of reinforcing steel [20]. Modern design codes for reinforced and prestressed concrete structures impose restrictions on the amount of chloride that may be introduced from raw materials containing significant amounts of chlorides. According to the European standard EN 206, the maximum allowed chloride contents are 0.2–0.4% chloride ions by mass of binder for reinforced and 0.1–0.2% for prestressed concrete. These restrictions are thought to eliminate corrosion due to chloride in the fresh concrete mix. In some structures built in the past, chlorides have been added in the concrete mix, unknowingly or deliberately, through contaminated mixing water, aggregates (for instance by using sea-dredged sand and gravel without washing them with chloride-free water) or admixtures (calcium chloride,

which is now forbidden, in the past was the most common accelerating admixture).

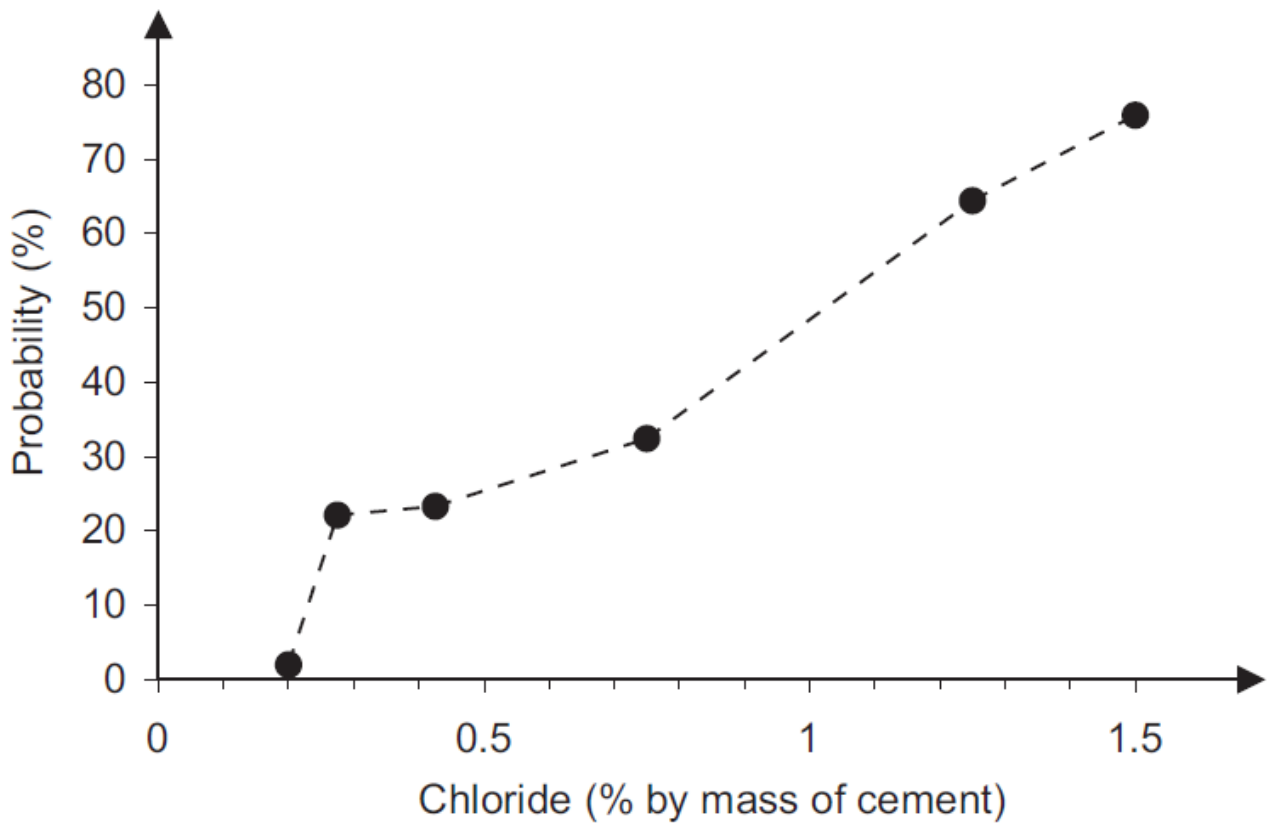


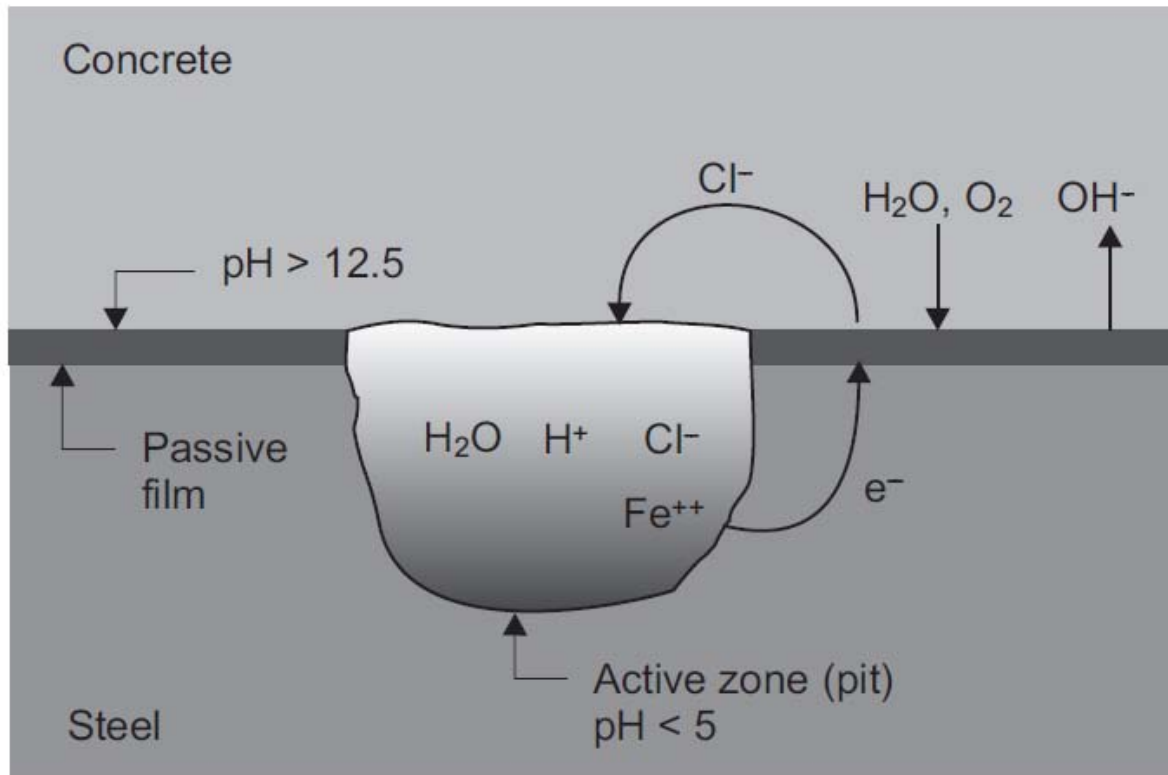
Figure 2.12: Relationship between chloride content found in bridge decks and percentage of reinforcement showing corrosion [21].

Figure 2.12 [21] shows statistical relationships established expressing the percentage of structures showing corrosion as a function of chloride content.

Chlorides lead to a local breakdown of the protective oxide film on the reinforcement in alkaline concrete, so that a subsequent localized corrosion attack takes place. Areas no longer protected by the passive film act as anodes (active zones) with respect to the surrounding still passive areas where the cathodic reaction of oxygen reduction takes place. The morphology of the attack is that typical of pitting shown in Figure 2.13. If very high levels of chlorides reach the surface of the reinforcement, the attack may involve larger areas, so that the morphology of pitting will be less evident. The mechanism, however, is the same. As shown in Figure 2.13, once corrosion has initiated, a very aggressive environment will be produced inside pits. In fact, current flowing from anodic areas to surrounding cathodic areas both increases the chloride content (chlorides, being



negatively charged ions, migrate to the anodic region) and lowers the alkalinity (acidity is produced by hydrolysis of corrosion products inside pits).



.Figure 2. 13: Schematic representation of pitting corrosion of steel in concrete [3]

The chloride threshold for the initiation of pitting corrosion for a given structure depends on numerous factors [20, 22, 23]. Major factors have been identified in the pH of concrete, i. e. the concentration of hydroxyl ions in the pore solution, the potential of the steel and the presence of voids at the steel/concrete interface. The hydroxyl ion concentration in the pore solution mainly depends on the type of cement and additions.

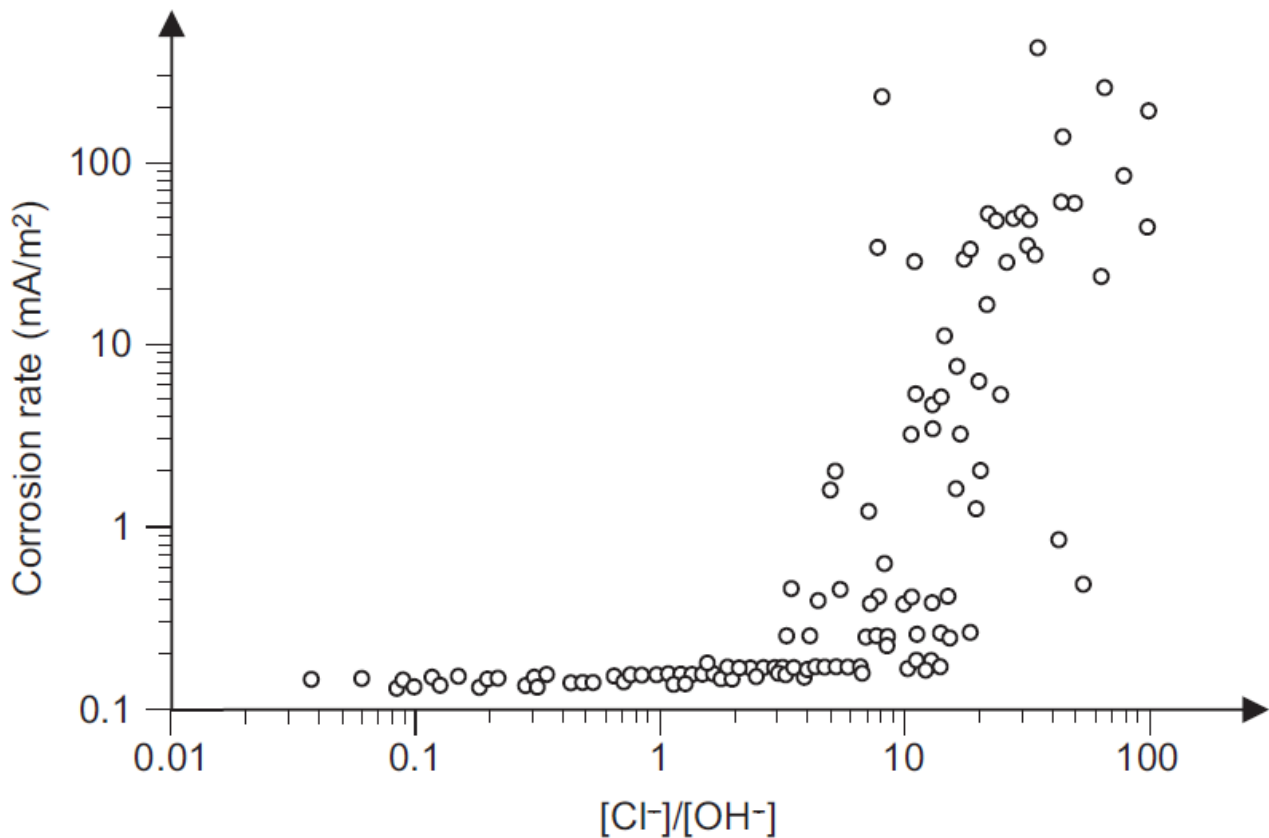


Figure 2. 14: Example of relationship between the molar ratio of  $Cl^-$  and  $OH^-$  in the pore solution and the corrosion rate of steel [24, 25]

#### 2.5.2.4 Electrochemical behaviour [3, 5]

From the cathodic and anodic polarization curves, the conditions of corrosion of reinforcement in various situations can be determined. If the ohmic drop due to the current passing from the anodic to the cathodic areas is negligible, the corrosion rate ( $i_{corr}$ ) and corrosion potential ( $E_{corr}$ ) are determined by the intersection of anodic and cathodic curves. Figure 2.15 shows the intersections of these curves in concrete that is exposed to the atmosphere. In this condition the reinforcement generally has a corrosion potential between  $\square 100$  and 200 mV SCE.

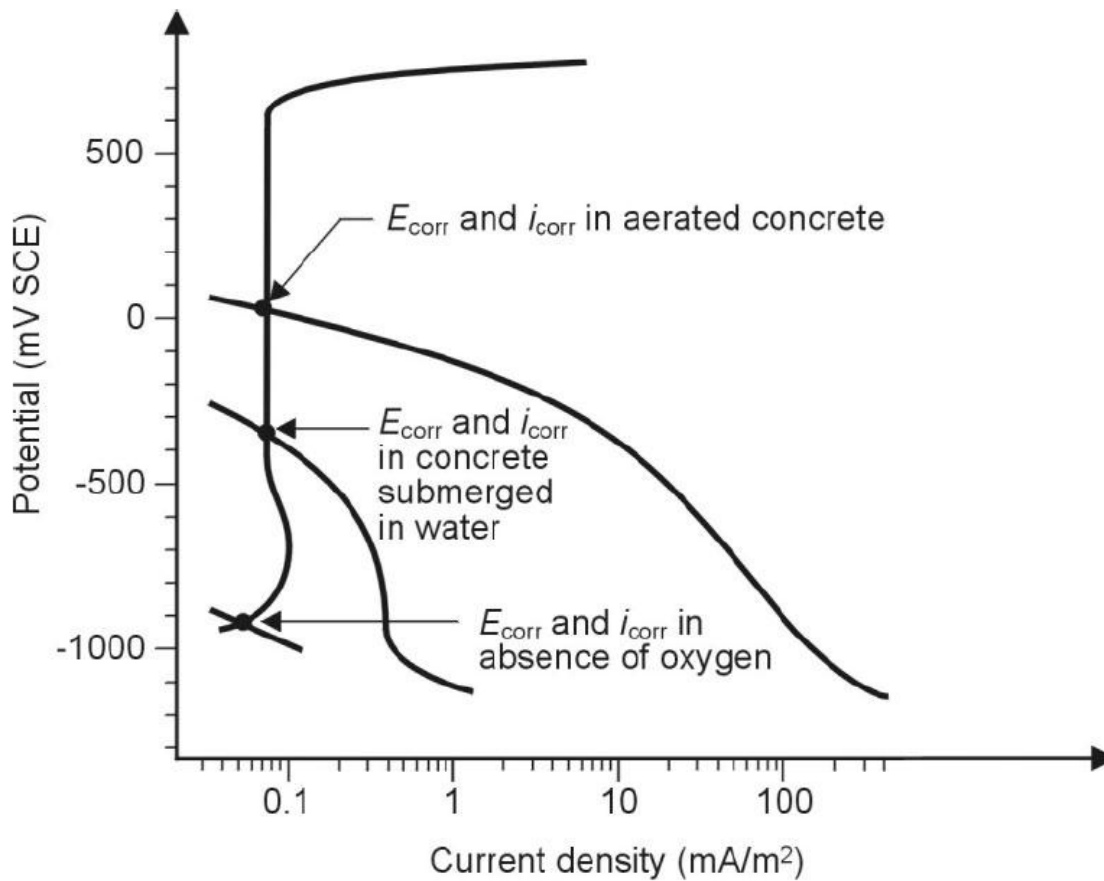


Figure 2.15: Schematic representation of the corrosion conditions of passive steel in concrete, under different conditions of moisture content.

For concrete immersed in water, or in any way saturated with water, the diminished supply of oxygen to the surface of the steel can bring the potential down to values below - 400 mV SCE. Finally, when oxygen is totally lacking (a very difficult condition to achieve, even in the laboratory) the potential may even drop to values below - 900 mV SCE and the cathodic process will lead to hydrogen evolution. Under all of these conditions, embedded steel is subjected to a corrosion rate that is practically zero. Consequently, the cathodic current density is also very small. The corrosion potential of passive reinforcement ( $E_{\text{corr}}$ ) is determined by the availability of oxygen at the surface of the rebar. The maximum and minimum values of potential taken on by passive reinforcement under different environmental conditions are, respectively,  $\approx 100$  mV in aerated concrete and - 1 V in the total absence of oxygen. This means that in concrete the reinforcement does not reach conditions of immunity nor of transpassivity, unless it is polarized by imposing an external current.

The presence of chloride ions in concrete leads to variations in the anodic behavior of steel, modifying the anodic polarization curve as shown in Figure 16.

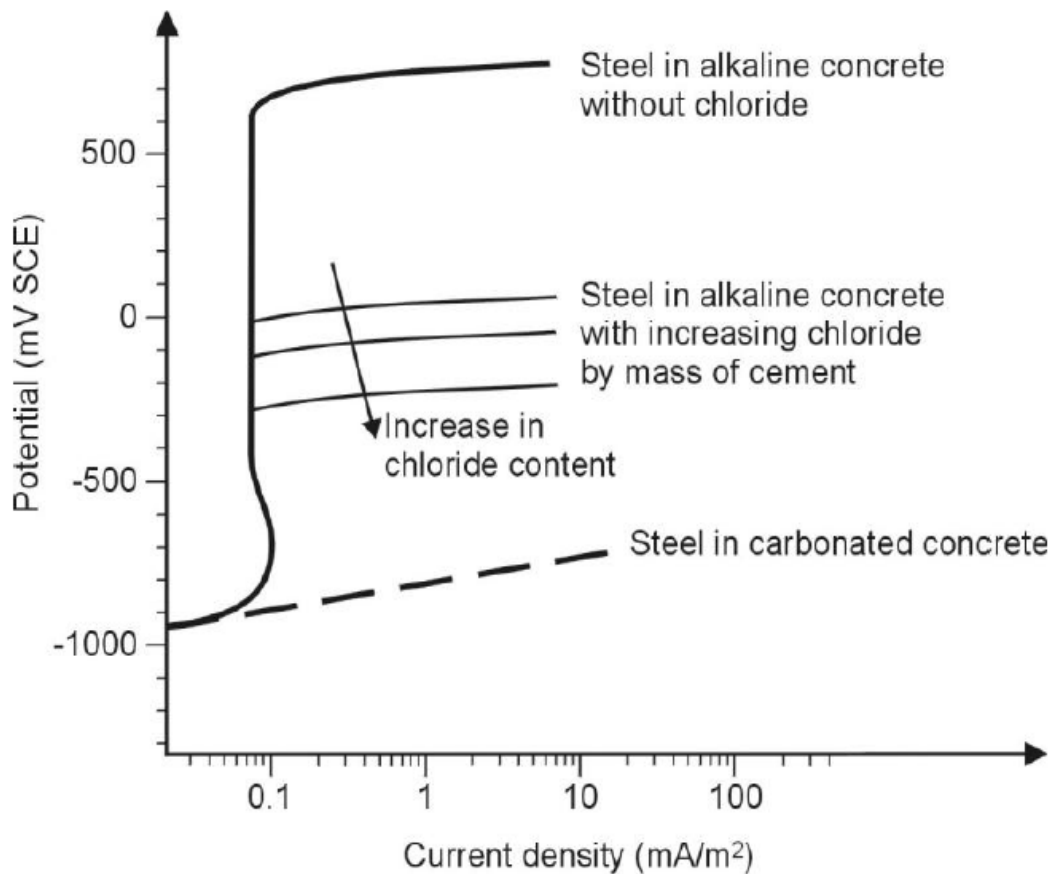


Figure 2.16: Schematic representation of the anodic polarization curve of steel in concrete with different chloride content [3].

The passivity range is reduced because its upper limit,  $E_{pit}$ , known as the breakdown potential or pitting potential decreases as the chloride content increases [5]: it passes from values of about +600 mV SCE in uncontaminated concrete to values below -500 mV in concrete with a high content of chloride.

The presence of chloride ions produces, at more positive potentials than  $E_{pit}$ , localized breakdown of the passive film and thus allows attack on the underlying metal. For potentials below  $E_{pit}$ , the action of chloride is, to a first approximation, negligible. The chloride content being equal,  $E_{pit}$  decreases as the pH of the pore solution in concrete decreases and as temperature and porosity

increase.  $E_{\text{pit}}$  is difficult to measure with laboratory measurements since during the measurement significant variations of pH and chloride level in the concrete near the surface of the steel can be introduced, altering the result.

For a given potential of the steel, the highest content of chlorides compatible with conditions of passivity is the critical chloride content (or chloride threshold) at that potential. For structures exposed to the atmosphere (whose reinforcement operates at a potential around 0 V SCE) the critical level is usually considered to be in the range of 0.4% to 1% of the cement content. For structures immersed in water (whose reinforcement operates instead at a much lower potential, around -400 to -500 mV SCE) or for reinforcement that is cathodically polarized for any reason, the chloride threshold is much higher [3].

### **3.0 Surface coating of reinforced concrete**

While concrete is often considered as a durable material it may in certain circumstances require protection. Following deterioration and repairs, or in the absence of sufficient cover to protect reinforcement, there is often a requirement to provide protection against penetration by aggressive environment (CO<sub>2</sub>, chlorides, water and oxygen).

Additionally, there is an increasing need for decorative or colouring treatments to improve the quality of the surroundings where these contain large areas of concrete, or even for colourless waterproofing treatments to prevent accumulation of dirt and biological growths.

#### **3.1 Classification of surface protection [26, 5, 6]**

Three generic types of surface treatment are available for the decoration and protection of concrete surfaces, designed to control chemical ingress as well as moisture movement. They are described as follows:

1. Pore-liners – these are hydrophobic impregnation treatments such as silicone impregnates, which line the pores of concrete. They repel water and therefore prevent it from entering the concrete, but continue to allow water vapour to escape.
2. Pore blockers: these are materials that partially or completely block the pores in concrete. They may accomplish this by either reacting with the concrete to produce Pore-blocking products or by physically blocking the pores.
3. Film-forms: these are coating systems based on either organic resins such as styrene butadiene and acrylic copolymers or inorganic resins such as potassium silicate, which form a protective/decorative film on the surface of the concrete. Coatings may be endowed with special properties, such as the ability to bridge moving cracks whilst maintaining film integrity.
4. Polymer modified cementitious coatings: they are based on two component mortar based on cementitious binders, fine-grained aggregates, special additives and synthetic polymers in water dispersion. When the two components are mixed, a blend with a plastic consistency is obtained.

The application of this coating can be done by brush, roller or spraying with a worm screw rendering machine on both horizontal and vertical surfaces at a thickness of approximately 2mm. Under all environmental conditions, the coating remains flexible because of the content and high quality of the synthetic resin.

Film-forming coatings for concrete are decorative protective elastomeric products. They are formulated to form a barrier against the ingress of carbon dioxide, and other deleterious substances. They should exhibit a proven resistance to weathering, and maintain their elastomeric and barrier properties in service, which will often be a maintenance free life in excess of 10 years. Test certificates should be sought to demonstrate these properties. Figure 3.1 illustrates these three groups of protection.

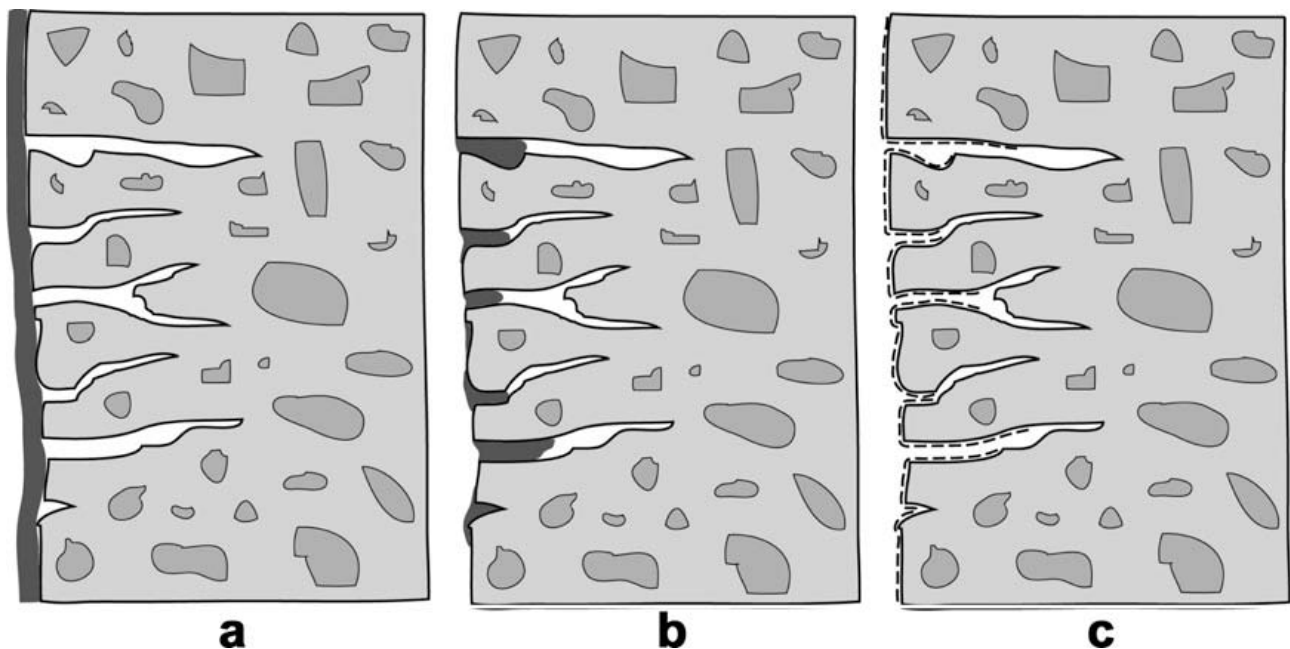


Figure 3. 1: Groups of surface treatments: (a) coating and sealers (b) pore blocker (c) pore liner (adapted from [30])

In general, the mechanism of protection afforded by the coating is related to the chemical-physical characteristics of the material of which it is composed, in particular, to the size of its molecules. If these have larger dimensions of the capillary pores of the concrete, the security mechanism is the film formation; if they are smaller, the penetration will be high and the protection will be achieved according to other mechanisms: making the surface water-repellent (hydrophobic treatment), or to

means of reaction of the constituents of the coating with those of the cement matrix (treatments that block the pores).

### **3.2 Requirements of a Surface Coating**

There are many requirements for the surface treatments, so according to some studies, the most important requirements for the surface treatments are to:

- Prevent or slow down the penetration of aggressive agents
- Prevent the service life of the concrete structure [28]: it is generally acknowledged that the

service life of a structure essentially depends on the optimization of four principal factors as follows:

- materials durability,
- structural and mix design,
- construction process,
- maintenance.

To ensure an effective protection, coating must:

- be impermeable to water and aggressive agents
- have a good ability to breathe (vapour permeability)
- survive in alkaline environments and aging
- have engineering requirements of strength, elasticity et economy.

These coatings must have the potential as a barrier to chlorides and breathability combined with the requirements of compatibility with the concrete and the environment where they will operate. Obviously, their use must also be economically sustainable.[27]

### **3.4 Water Absorption**

The main purpose of coating is to reduce the water absorption during immersion and aggressive agents (oxygen, carbon dioxide, chloride, sulphate...). Creating a water-repellent zone at the surface



of the concrete considerably reduces the uptake of water and aggressive agents. The important property is the water-repellent.

For example, As reported in the paper [29] , the application of two commercial polymer (acrylic) modified cementitious mortars were considered, with 0.35 and 0.55 polymer/cement ratio respectively, highly reduce water absorption during immersion.

The coating highly reduces water absorption during immersion. The effect is more pronounced as the polymer content (p/c) increases. They also reduce water vapour permeability (g), but do not impede it. The equivalent air thickness of one centimetre thickness of concrete covered by 1-1.6 mm coating remains about 2.3-2.9 m. For comparisons, the equivalent air thickness without coating is 1.4-1.7 m for the concrete with 0.5 w/c and 1.1-1.2 m for the concrete with 0.65 w/c.

Owing to the low water absorption and sufficient water vapour permeability, the coating can reduce the water content into concrete. They are able to reduce liquid water ingress during raining periods but they allow the vapour to come out from the concrete. Figure 3.2 shows the weight of plain concrete specimens exposed outdoor in Milan. The weight of coated specimens progressively decreases due to the reduction of water content whereas the weight of specimens without any coating remains high and shows wide oscillations during rain and dry periods. These data are confirmed by Relative Humidity measurements conducted by probe mounted inside specimens.

After three years of exposures, at the end of a long period under dry environmental conditions, the pore saturation degree of uncoated concrete was about 55-60%, much higher than the values found in coated specimens. The water content in these specimens was lower than 30% of water saturation content of the concrete. Values about 20% were measured on specimens covered by the coating with high polymer content. Such low water content can significantly reduce the corrosion rate of reinforcements in carbonated concrete.

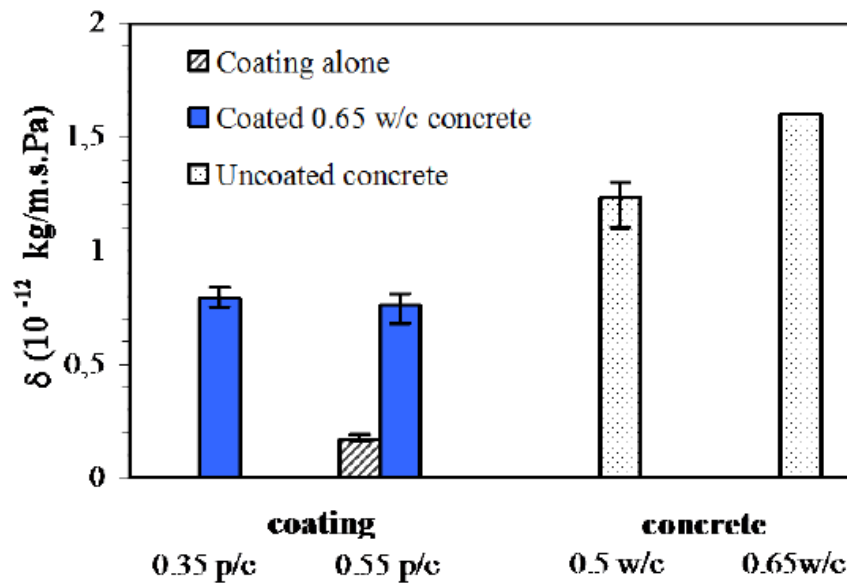


Figure 3. 2: Water vapour permeability according to ASTM E96-80 standard. (10 mm thickness concrete covered on a side by 1,1-1,6 mm coating; 2,6-3 mm thick sheet of coating without any support) [29]

Another example of the effect of water absorption is reported in the paper [4]; Figure 3.3 shows the capillary water absorption test results. It is possible to verify that all the protection systems tested in this work are highly efficient in inhibiting the water absorption by capillary forces. However, the results indicated that the double systems (Double A + C and B + C) and the polyurethane coating (Single D) are more effective in inhibiting water penetration in concrete than the other products studied. This is important because penetrating water can be a vehicle for chloride penetration as it influences the kinetics of the corrosion process in case the steel reinforcements are already depassivated. Where single A-Silane/siloxane dispersed in water (A), single B-Silane/siloxane dispersed in solvent (B), single C-Acrylic dispersed in solvent (C) single D-Polyurethane coating (D) .

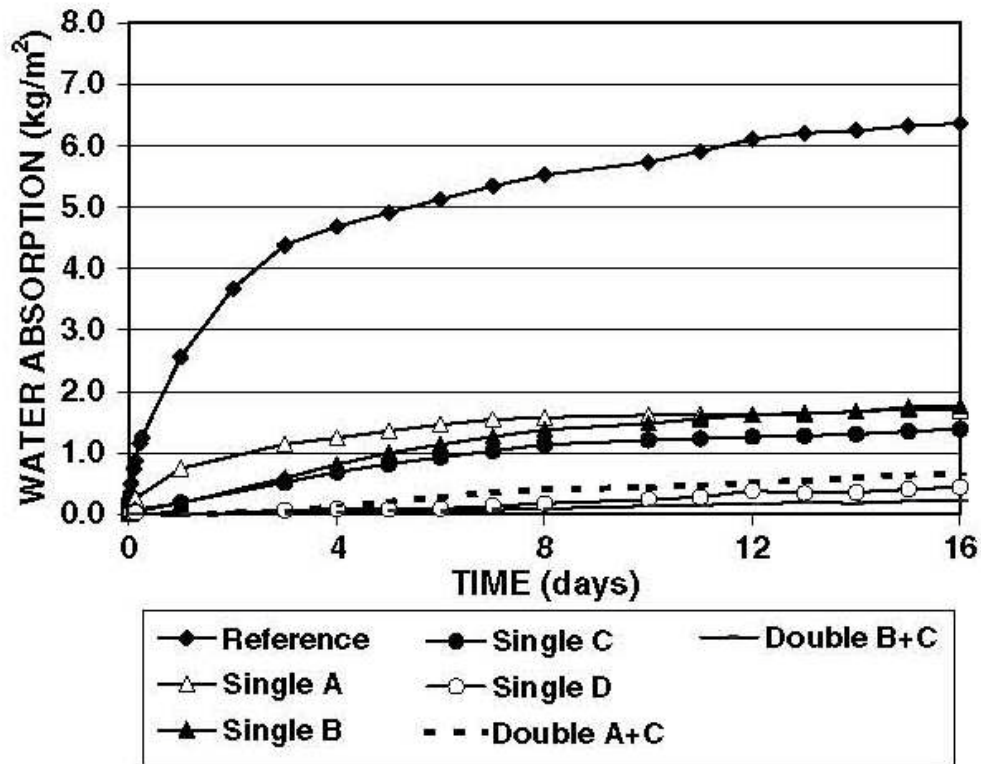


Figure 3. 3: capillary water absorption of treated and untreated concrete surfaces [30]

Further evidence of the efficiency of the protection systems is shown in Fig. 3.4. This figure presents results of sorptivity, which is the volume of water that penetrates per unit of area and time. The sorptivity reduction rates of each protection system are also shown in Figure 3.4. The results clearly show that all the protection systems highly reduced the sorptivity (more than 70%), indicating high efficiency in inhibiting water penetration in concrete [31].

In the case of the double systems (Double A + C and B + C), i.e. Silane/siloxane dispersed in water (A) + Silane/siloxane and Silane/siloxane dispersed in solvent (B) + Acrylic dispersed in solvent (C) when one of the materials of the double system fails, the other continues to protect the concrete. On the other hand, the polyurethane coating (Single D) is more efficient than the other single systems because this type of polymer results in a more closed molecular chain in comparison to the other materials included in this work.

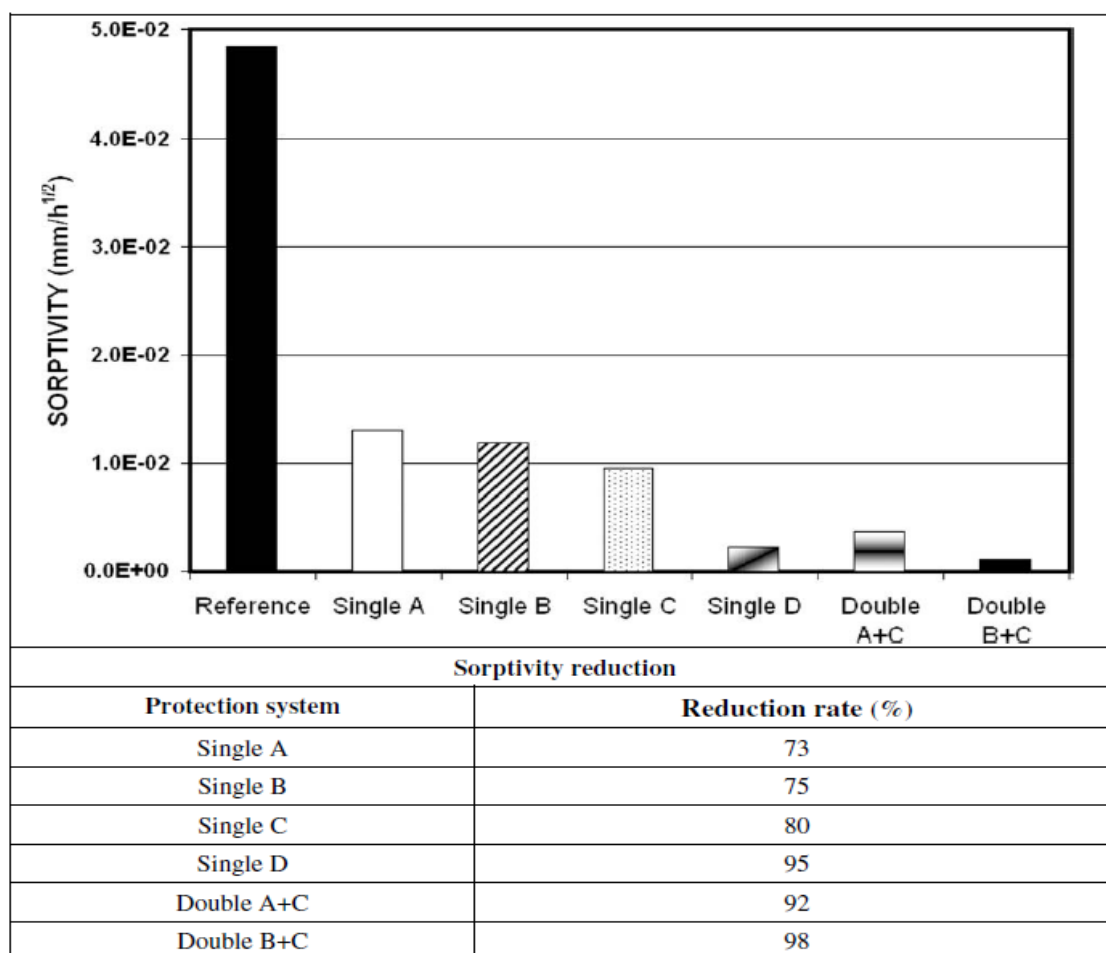


Figure 3. 4: Sorptivity of treated and untreated concrete specimens [30]

### 3.5 Diffusion coefficient

Figure 3.5 presents the result of chloride diffusion coefficient determined by the method proposed by Luping and Nilsson [32]. In this experiment the concrete is saturated; therefore the ion movement caused by absorption and permeability does not exist. Thus the values of chloride diffusion coefficient presented in fig. 5 are for staturated concrete.

It is important to emphasize that, except for the polyurethane coating (Single D), the double systems (water repellent + acrylic coating) are far more advantageous as compared to the single systems due to the double barrier formed in this category of protection. When the chloride ion passes the acrylic topcoat layer, there is still the silane/siloxane treatment, which has some capacity to inhibit the chloride ion penetration inside the concrete. This is illustrated by the fact that the sum of the reduction rate of the chloride diffusion coefficients of the single systems is almost equal to

the reduction rate of the double systems (Single A + Single C = 29% approximately to 33%; Single B + Single C = 37%, approximately to 41%). It should be stressed that this does not lead to the conclusion that the reduction rate of the double systems is equal to the addition of the reduction rate of each single system that forms the double system. A specific experiment should be conducted to prove this. However, it is important to report this fact to stimulate future works on this subject.

The double systems (Double A + C and B + C) reduced the chloride diffusion coefficient by more than 33%. The polyurethane coating (Single D) was the most efficient protection, reducing the chloride diffusion coefficient by 86%. On the other hand, the silane/siloxane dispersed in water (Single A) reduced the chloride diffusion coefficient by 9%, indicating that this material does not greatly influence chloride penetration. The silane/siloxane dispersed in solvent (Single B) and the acrylic coating dispersed in solvent (Single C) presented 17% and 20% chloride reduction rate, respectively.

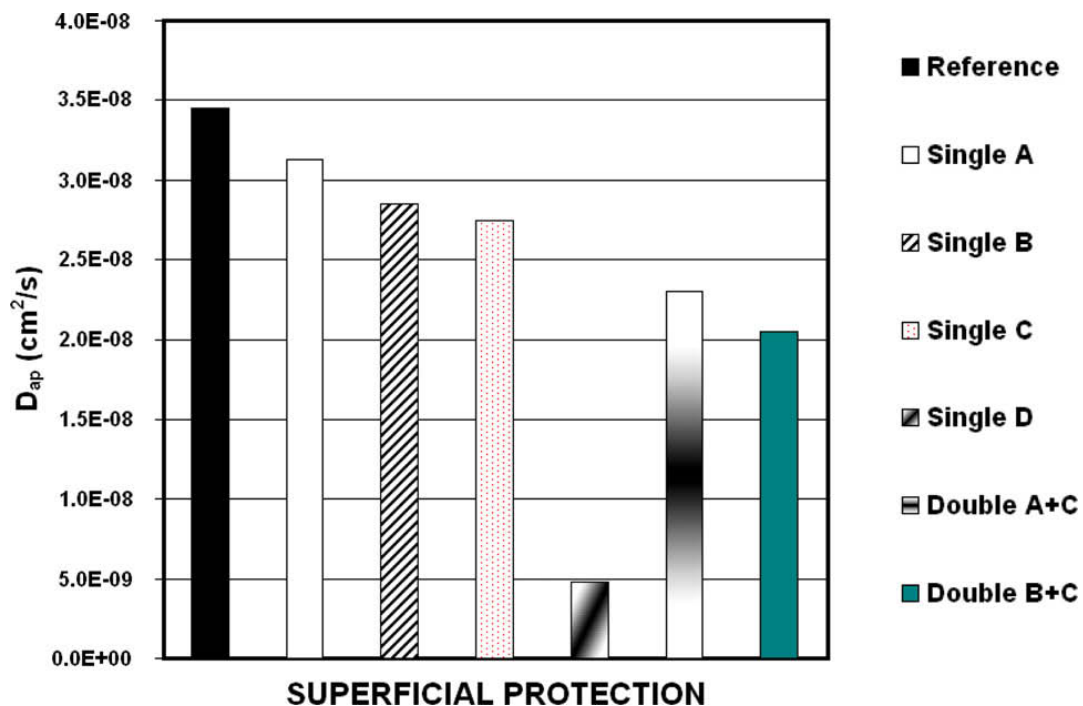


Figure 3. 5: Chloride diffusion coefficients in treated and untreated concrete systems [30]

### 3.8 Physical and mechanical resistance of coatings [6]

#### Mechanical resistance

Figures 3.6 and 3.7 show the results obtained, after 28 days of curing, the compressive strength and flexural specimens of cementitious with addition of acrylic polymers and epoxy. The resistance of the reference specimen, without added and cured for 28 days in a humid environment, is about 40 MPa. It is observed that the resistance of the specimen's cement-polymer increases as the polymer-cement ratio (w/c). For values of p/c of more than 30% there is a resistance higher than the reference specimen despite the seasoning into the atmosphere. These results, reported in the literature [34], confirm the good mechanical resistance of the protective coatings.

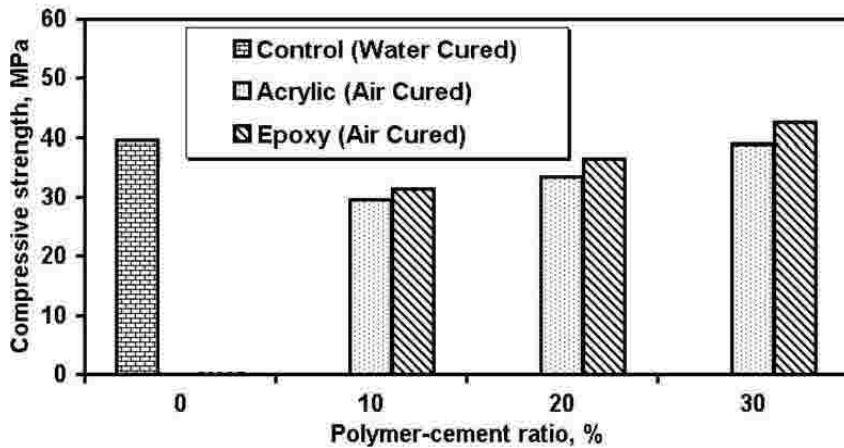


Figure 3. 6: Compressive strength (28 days of curing) as a function of different ratios p/c [6]

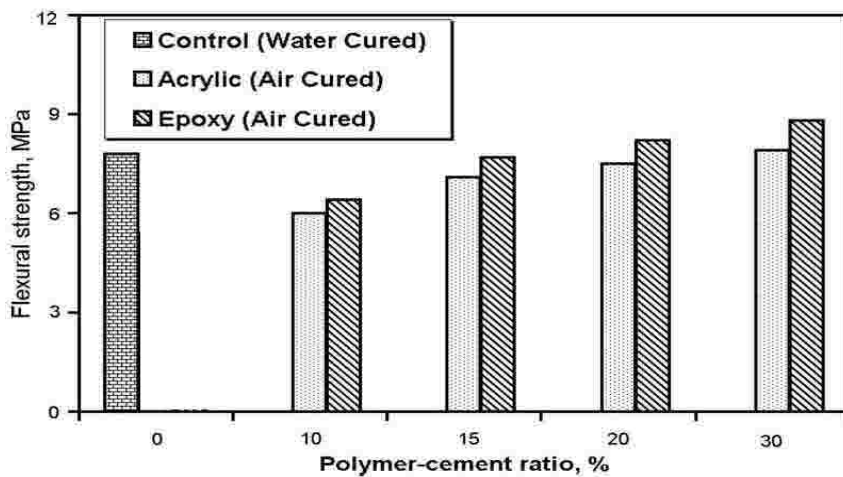


Figure 3. 7: Flexural strength (28 days of curing) as a function of different ratios p/c [6]

### Flexibility and crack-bridging

Due to the high deformability, the polymer modified cementitious coatings are particularly suitable in the case where the concrete is cracked, in fact allow to close the cracks, and then are able to retain their protective properties in the presence of significant cracking in the concrete below were . Have advantages compared to other coatings when, in addition to the action of a particularly aggressive environment, the concrete is subjected to significant mechanical stress, especially if time-varying. Experimental tests conducted on specimens made with concrete modified with acrylic resins and epoxies have shown that the addition of polymers is able to decrease the elastic modulus of concrete and to significantly increase the deformation and the effort bearable [6]. With an increase in flexibility, polymer modified concrete minimize cracking of the concrete in the presence of static and cyclic loads (Figure 3.8).

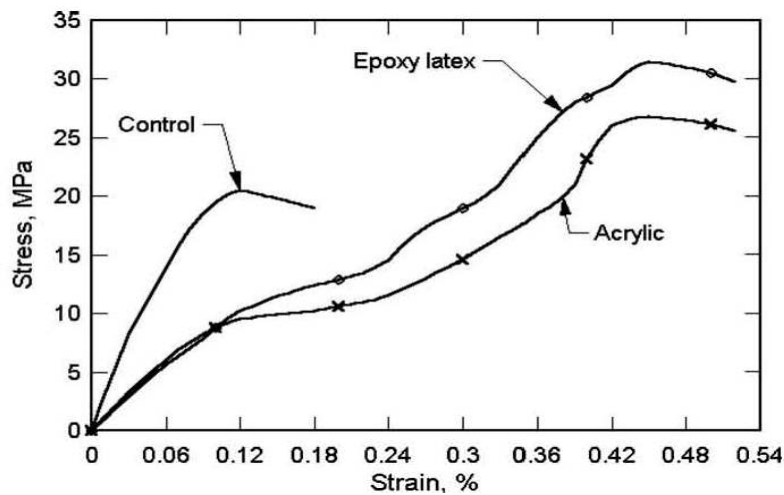


Figure 3. 8: Influence of polymers in the stress-strain curves of the coatings [6]

## 4.0 Methodology

The work is part of a research on the effectiveness of protective coatings (commercial) applied to the concrete for the prevention of corrosion of the reinforced concrete.

The experimental aims to reproduce the typical conditions experienced by reinforced concrete structures operating in the marine environment or deicing salts.

The research, begun in 2005, continues today and is based on:

- Corrosion monitoring by measuring the corrosion potential (E) and polarization resistance ( $R_p$ ) on reinforced specimens subjected to cycles of accelerated penetration of chlorides (ponding)

- Determination of chloride penetration profiles after exposure to cycles of wetting and drying

Monitoring of the potential and corrosion rate of specimens after long term exposure (about 7 months) are reported

During the outlining of this work it was realized that dividing the work in three distinct stages would promote the oversight and execution of the thesis objectives.

Stage 1: Take potential and resistance after one week wet and two weeks dry

Stage 2: Extraction of the core

Stage 3: Determination of chloride profile

The following coatings types from MAPEI spa were studied:

- Polymer modified cementitious coatings (RIV 1-1)
- Polymer modified cementitious coatings “improved” (RIV 1-2)

These coatings must have the potential as a barrier to chlorides and breathability combined with the requirements of compatibility with the concrete and the environment where they will operate. Obviously, their use must also be economically sustainable.



## 4.1 Concrete Specimens

### 4.1.1 Geometry

There are three types of specimens:

1. Reinforced specimens with prismatic shape (340 x 250 x 50 mm), subjected to measurements of corrosion (E, Rp) through cycles of ponding;
2. Reinforced specimens with a prismatic shape (250 x 160 x 70 mm), subjected to measures of corrosion (E, Rp) through cycles of ponding;
3. Unreinforced cubic specimens (of side 150 mm), for measurements of chloride penetration through cycles of ponding

The reinforced specimens of type 1 (Figures 4.1 and 4.2) are made up of 5 rebar of carbon steel (FeB44k that corresponds to B450C in the EN standard) with improved adherence having a length of 290 mm and a nominal diameter of 10 mm. All the rebar in the specimens have holes to allow the connection of an electrical cable; after being sanded the plates were coated at both ends with a heat shrink tube for a length of 40 mm.

A reference electrode of activated titanium was added in the vicinity of each rebar and two electrodes of stainless steel of type AISI 304 with a diameter of 2 mm were also placed such that the rebar is between the two stainless steel. The presence of these electrodes is to perform the measurements of the corrosion rate through the technique of polarization resistance (Rp), and to eventually distribute the current on the reinforced specimens. The internal reference electrode is a wire of activated titanium (MMO-Mixed Metal Oxide) of the length of about 20 cm, electrically connected with a copper wire to allow the connection with the measuring instruments. In order to isolate the connections and secure seal against the alkalinity of concrete, all electrical connections were coated with Teflon and heat shrinkable tubing.

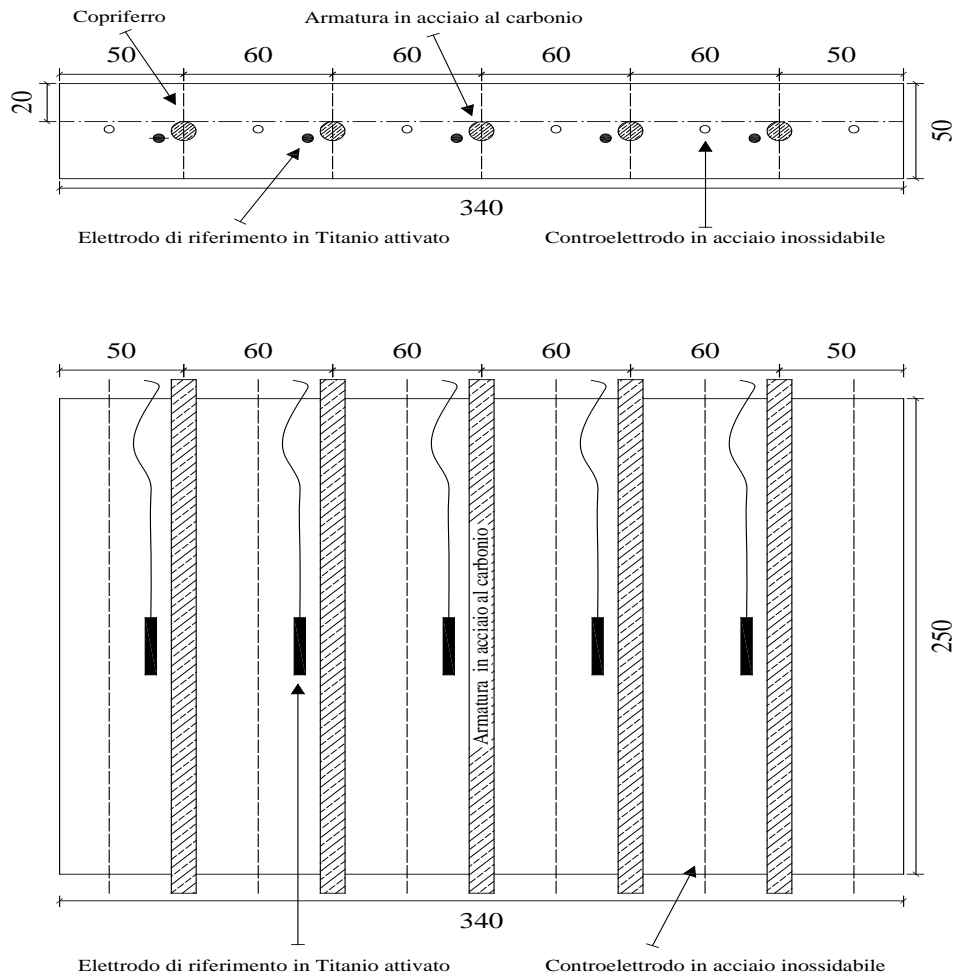


Figure 4. 1: Cross section and top view of a concrete specimen type 1.

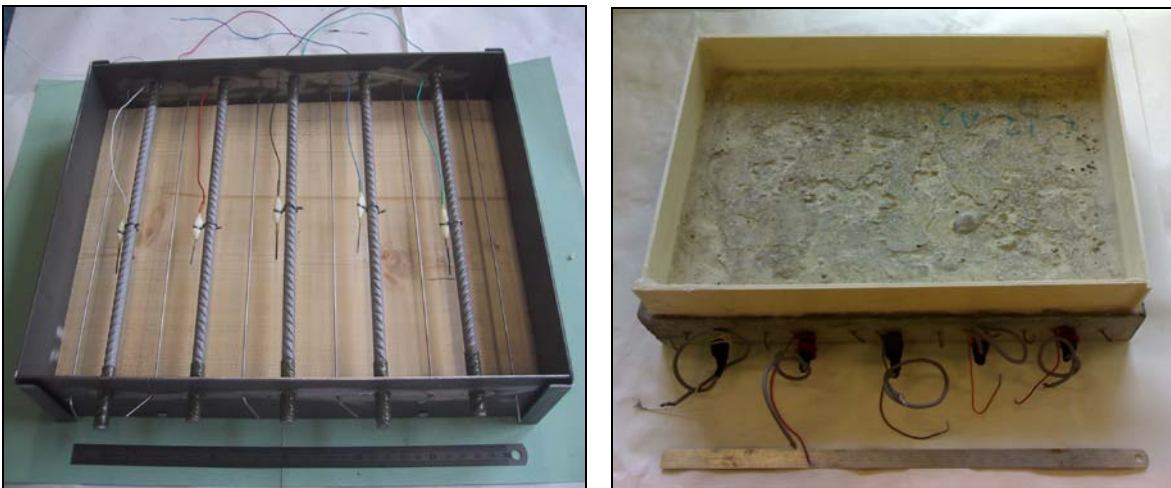


Figure 4. 2: Filmstrip reinforced type 1: a) particular of the reinforcement, reference electrode and b) provided with sample tray fro containing the test solution.

The reinforced specimens of type 2 (Figures 4.3 and 4.4) consist of three (3) smooth rebar of length 270 mm and 10 mm in diameter. The outer rebar is of stainless steel of type AISI 304 (for measurement of corrosion rate), the central rebar is of carbon steel (Fe370). The bars were drilled to allow electrical contact and subsequently coated at the ends with shrink wrap. In the vicinity carbon steel rebar is placed a reference electrode of activated titanium.

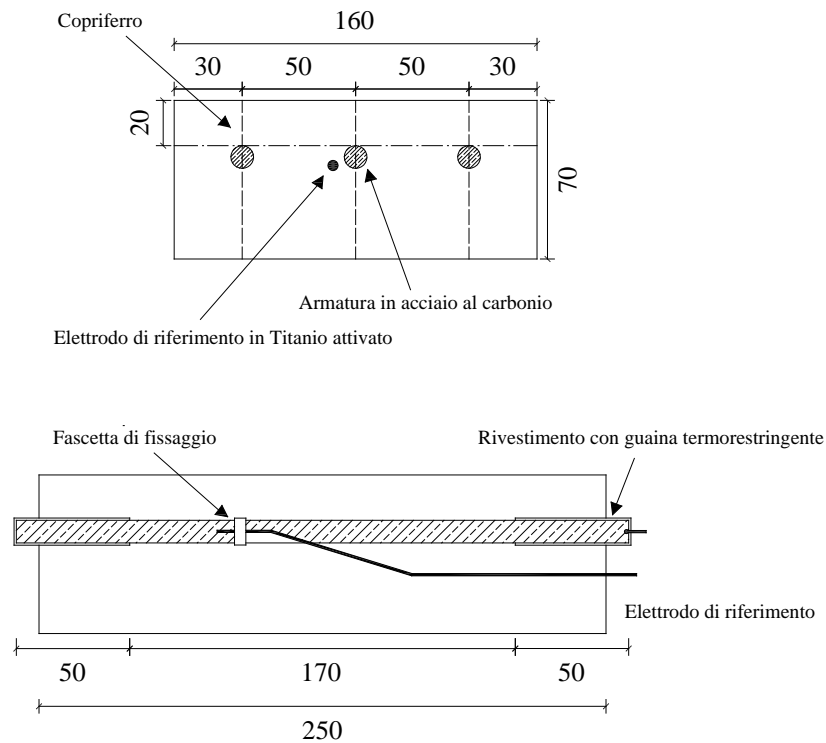


Figure 4. 3: cross section and top view of concrete specimen type 2



Figure 4. 4: Reinforced specimen of type 2

The reinforced specimens of type 2 for testing corrosion caused by chlorides were coated with protective products on five of the six faces; while for specimens of type 1 only one face was coated (upper face). All specimens were subsequently equipped with a tray of plastic material to contain the test solution (Figure 4.2b and 4.4b).

The specimens of type 3 have been cast without rebar in order to allow the extraction of the cores of concrete for the determination of the concentration profiles of the chlorides. Also, on the specimen of type 3 were tanks made for the containment of the NaCl solution for the cycles of ponding (Figure 4.5a and 4.5b).

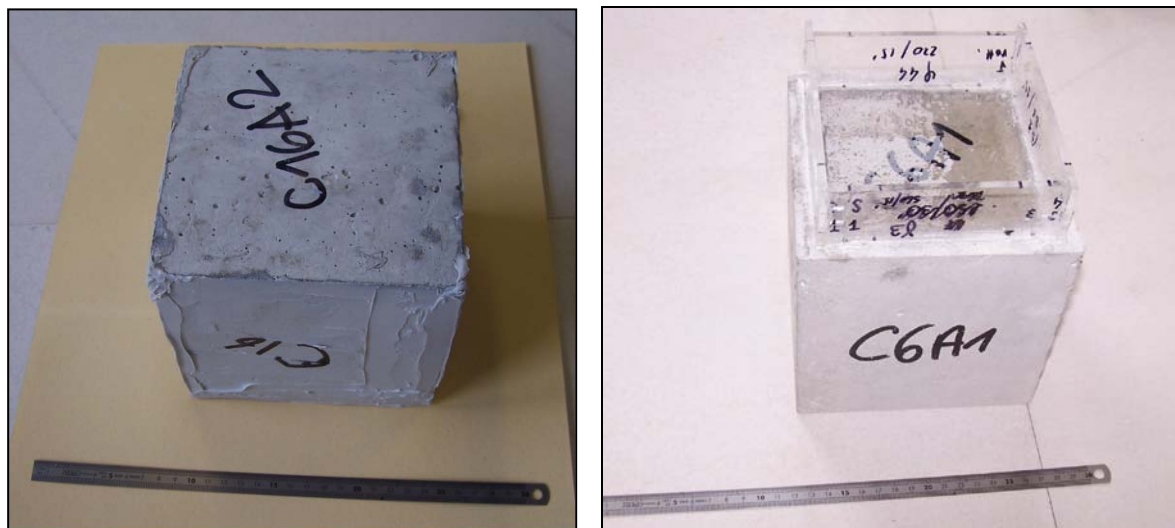


Figure 4.5: Specimen of type 3 without rebar a) specimen for immersion and b) specimen for ponding.

#### 4.1.2 Mix Design

The reinforced specimens of type 1 and all those unreinforced of type 3 were made with cement CEM II A / L 42.5 R (according to standard CEN ENV 197/1 [4]), i.e. a mixture of Portland cement to rapid hardening, with maximum content of 20% limestone and characteristic resistance at 28 days normalized cube of greater than 42.5 MPa (standard mortar). With the aim of evaluating the influence of the coatings in concretes of different porosity, there were two different types of w/c ratios: 0.55 and 0.65.

	<b>TYPE</b>		<b>PROPORTIONS</b>	
<b>W/c</b>			0,55	0,65
<b>CEMENT</b> (kg/m <sup>3</sup> )	CEM II A/L 42,5R		320	310
<b>WATER</b> (L/m <sup>3</sup> )	Of aqueduct		180	200
<b>AGGREGATES</b> (kg/m <sup>3</sup> )	Gravel 10-20 mm	35%	651	630
	Gravel 8-10 mm	10%	187	181
	Gravel up to 8 mm	44%	819	790
	Sand 0.25 mm	5%	99	96
	Carbonate 0.075 mm	6%	119	115
	Total	100%	1876	1812
<b>FLUIDIZING</b>	Dyn SX-HB		0,64% (vs cem.)	0,14% (vs cem.)

Table 4. 1: Mix – design of specimen type 1

The aggregates used were calcareous; of rounded shape and a diameter up to 16 mm. Aggregates are divided into 5 classes based on size (Table 4.1).

The super plasticizer additive used is a product based on acrylic (Super-fluid Dyn SX-HB 21/3/5), added in an amount of 0.64% and 0.14% by weight with respect to the cement, according to the w/c used. The specimens of type 2 have been made with the same cement of specimens 1 and 3, cement CEM II A / L 42.5 R with characteristic resistance at 28 days of normalized cube > 42.5 MPa. As reported in Table 4.2, two w/c ratios were used and two different distribution curves of aggregates. For all specimens the class of S5 is guaranteed workability (slump > 210 mm), according to the

requirements of UNI EN 206/1. The curing of the samples was conducted in a curing chamber for 28 days at a constant temperature of 20 ° C and with relative humidity of 95%.

	<b>TYPE</b>	<b>PROPORTIONS</b>
<b>w/c</b>		0,50
<b>CEMENT</b> (kg/m <sup>3</sup> )	CEM II A/L 42,5R	300
<b>WATER</b> (L/m <sup>3</sup> )	Of aqueduct	150
<b>AGGREGATES</b> (kg/m <sup>3</sup> )	Powder up to a 2 mm	700
	Limestone (1) 2-3 mm	240
	Limestone (2) 3-5 mm	200
	Limestone (3) 5-10 mm	260
	Limestone (4) 5-15 mm	600
	Total	2000
<b>FLUIDIZING</b>		4,5 kg/m <sup>3</sup>

Table 4. 2: Mix design of the specimens of type 2

For the type 2 only W/C 0.55 has been used for reinforced specimens, 0.65 has been used for other specimens not used in this work.

## 4.2 Properties and application of the coatings

After a curing period of 28 days, protective layers of commercial polymer modified cementitious mortars, developed by MAPEI SpA, were applied to all specimens (type 1). The coatings are described in the following sub-headings.

The different coatings have been developed in different time, so it can be said that the coatings are RIV 1-2 is an updated or “modified” version of the coatings RIV 1-1.

They are based on two component mortar based on cementitious binders, fine-grained aggregates, special additives and synthetic polymers in water dispersion. When the two components are mixed, a blend with a plastic consistency is obtained. The application of this coating can be done by brush, roller or spraying with a worm srew rendering machine on both horizontal and vertical surfaces at a thickness of approximately 2mm. Under all environmental conditions, the coating remains flexible because of the content and high quality of the synthetic resin.

These coatings are completely waterproof up to a pressure of 1.5 bars and resistant to the penetration of aggressive substances in the atmosphere such as carbon dioxide, sulphur dioxide and sulphuric anhydride and soluble salts like chlorides and sulphates which are present in seawater or in the ground. It has excellent bonding properties on all cementitious, ceramic and marble surfaces as long as they are sufficiently clean. Together with all these properties is a special property of resistance to the deteriorating effect of UV rays which ensure that structures protected with these coatings has long service life even in particularly rigid climatic conditions, coastal areas with a saline-rich atmosphere or industrials areas where the air is very polluted.

Table 4.3 shows the main properties and characteristics of the products used. The Table 4.4 shows the different coatings applied to each specimen of type 1 and 3, alone. Twelve (12) specimens were made with rebar having identification as C23 to C26 (A1 and A2), all samples were subjected to cycles of ponding. The C23 and C25 samples were prepared with a w/c ratio of 0.55, all others with w/c 0.65. Another twelve (12) cubic samples without rebar were made and were given the same identification as the samples with rebar. The samples C1 and C2, devoid of protective coating, represent the reference against which the efficiency of the coatings will be evaluated.

<b>COATING</b>	<i>RIV 1-1, 1-2</i>
<b>Texture</b>	Plastic spatula
<b>Color</b>	Gray
<b>Density (g/cm<sup>3</sup>)</b>	1,7
<b>Dry matter (%)</b>	87

Table 4. 3: coating properties

The specimens of type 2 (covering H and K) were coated with two different commercial product (from two producers), similar to the type RIV 1-1. The difference between the two coatings is in the polymer-cement ratio ( $p/c$ ): H = 0.35, K = 0.55.

<b>Specimens</b>		<b>COATING</b>	
<b>Abb.</b>	<b>w/c</b>	<i>RIV 1-1</i>	<i>RIV 1-2</i>
<b>C1</b>	0,55	-	-
<b>C2</b>	0,65	-	-
<b>C23</b>	0,55	X	-
<b>C24</b>	0,65	-	X
<b>C25</b>	0,55	-	X
<b>C26</b>	0,65	X	-
<b>H</b>	0,35		-
<b>H</b>	0,35		-
<b>K</b>	0,55		-
<b>K</b>	0,55		-

Table 4. 4: Coatings used

### 4.3 Preparation of support

A key issue for the application of any type of coating is the preparation and cleaning of the support. The surface must be perfectly clean of solids; it is necessary to remove particles and any traces of dust, grease and oils by sandblasting or washing with water under pressure. The choice of the



cleaning system, in the case of old surfaces depends on the type of dirt. In general, it may be sufficient to wash with cold water. Washing with hot water or steam is particularly beneficial if there are the presences of oils or fats, sandblasting can also be used. In the absence of dirt, simple thorough brushing and de-dusting with compressed air is enough.

#### 4.5 Exposure

To simulate the conditions that occur on roadways where salt is spread frost and the marine environment, we chose to use an aqueous solution of sodium chloride 5%. The solution was prepared with tap water and commercial salt.

- PONDING: the solution was poured in the PVC bowl mounted on to all the reinforced specimens and unreinforced specimens of non-cubic; the penetration of chlorides occurs with a diffusion mechanism and capillary absorption (Figures 4.6);



Figure 4. 6: Condition of exposure of the samples (ponding)

The specimens were subjected to cycles of ponding with two weeks of wetting followed by one week of drying. The measurements of corrosion potential and polarization resistance were carried out after two weeks of wetting

## 4.6 Experimental Measures

Two types of experimental measurements were carried out namely: monitoring of corrosion potential and corrosion rate and concentration profile as showed in Table 4.5.

- Electrochemical measurements of corrosion potential and polarization resistance is to monitor the state of corrosion of reinforcement in reinforced specimens;
- Measures for determining the concentration profiles of chloride in the reinforced specimens and unreinforced specimens.

Specimens	Experimental Measurement on reinforced specimen		
	Potential	Polarization resistance	Chloride concentration
C23 (A1-A2)	X	X	X
C24 (A1-A2)	X	X	X
C25 (A1-A2)	X	X	X
C26 (A1-A2)	X	X	X
H	X	X	-
K	X	X	-

Table 4. 5: Experimental measurements

## 4.7 Corrosion Monitoring

The conditions of corrosion of the reinforcement were monitored by measuring the corrosion potential and the polarization resistance

### 4.7.1 Measuring the potential of steel

The potential of the reinforcement carbon steel was measured by a high impedance voltmeter using a saturated calomel reference electrode (SCE,  $E = +244$  mV vs. SHE) placed in the aqueous solution contained in the PVC tank (Figure 4.7)



Figure 4. 7: Tools for measuring the corrosion potential

The corrosion potential is the most widely used technique to identify the areas where the plates corrode without requiring the removal of the concrete cover. This technique relies on the fact that the potential of the reinforcement depends on their corrosion conditions.

The measure of corrosion potential indicates, therefore, the likelihood of corrosion as a function of potential intervals. The ASTM C876-91 [34] proposes an empirical criterion for predicting the conditions of corrosion of reinforcement (Table 4.6).

MEASURE POTENTIAL (vs SCE)	CORROSION PROBABILITY
$E > -100 \text{ mV}$	$P < 10\%$
$-100 \text{ mV} < E < -270 \text{ mV}$	$10\% < P < 90\%$
$E < -270 \text{ mV}$	$P > 90\%$

Table 4. 6: Criteria for corrosion as stated by ASTM C876-91 [34]

When the corrosion of the reinforcement is started, the corrosion potential undergoes a significant decrease of about 100 to 200 mV. The rebar are considered corroded if the lowering of potential is maintained for at least 5 consecutive cycles (approximately 4 months of testing). This is because, in some special cases (for attacks affecting small areas of rebar), it is possible a repassivation of the

same with a consequent increase in the value of potential. The interpretation of these measures must however, be performed with caution, as the same potential value may correspond to different conditions of corrosion, depending on the moisture content (and thus oxygenation) and of chlorides in the concrete [1]. The data were collected in a spreadsheet and graphed

#### 4.7.2 Measurement of the polarization resistance

When a weak current density circulates in the outer of a metal, its potential (E) undergoes a variation (the metal is subjected to a slight polarization); the ratio  $dE/di$  is said to be the polarization resistance ( $R_p$ ) and is inversely proportional to the corrosion rate. This technique also called linear polarization (LPR-Linear Polarization Resistance), was applied via a Potentiostat/galvanostat (EG & G Princeton Applied Research), using the stainless steel wires (or rebar in the test specimens of type 2) as counter-electrode and as a reference electrode the activated titanium in the vicinity of the reinforcement of carbon steel in the concrete (Figure 4.8).



Figure 4. 8: Measurement of polarization resists

The measurements of the current density and potential difference between rebar and reference electrode were carried out with the program 352 SoftCorr III. The two counter-electrodes were used to distribute the current over the entire surface of the concrete. A potentiodynamic technique, operating between -10 mV and +10 mV with respect to the free corrosion potential and with a scanning rate equal to 10 mV / min was used.

The polarization resistance  $R_p = dE/di$  [ $\Omega$ ], was calculated as the slope of the straight section of the final potential-current density curve. Recalling that the iron has an anodic current density of 1 mA/m<sup>2</sup> corresponds to a corrosion rate of 1.17  $\mu\text{m}/\text{year}$ , the average corrosion rate ( $\mu\text{m}/\text{year}$ ) was calculated with the formula of Stern-Geary:

$$i_{corr} = 1,17 \cdot \frac{B}{R_p} \quad (18)$$

Where; the parameter  $B$  is 26 mV and 52 mV for active and passive rebar respectively. As corrosion rate is considered negligible for a corrosion rate less than 1 to 2  $\mu\text{m}/\text{year}$ , a resistance value of polarization higher than 10  $\Omega \cdot \text{m}^2$  is an indication of the absence of corrosion.

Despite the limitation of this technique to the application to localized corrosion, corrosion initiation causes the lowering of at least an order of magnitude of  $R_p$ ; the technique is still reliable and the margin of error reduced.

### **4.7.3 Determination of the concentration profiles of chloride**

The concentration profiles of chlorides in the samples with rebar subjected to ponding, were determined from 97 to 101 exposure cycle for the specimens coated with RIV 1-1 and 1-2.

From each sample, using a core drill column (Figure 4.9a), a carrot was taken with a diameter of 15 mm, which was then cut into 4 or 6 slices with a thickness of about 15 mm with a water cooled diamond blade (Figure 4.9b).

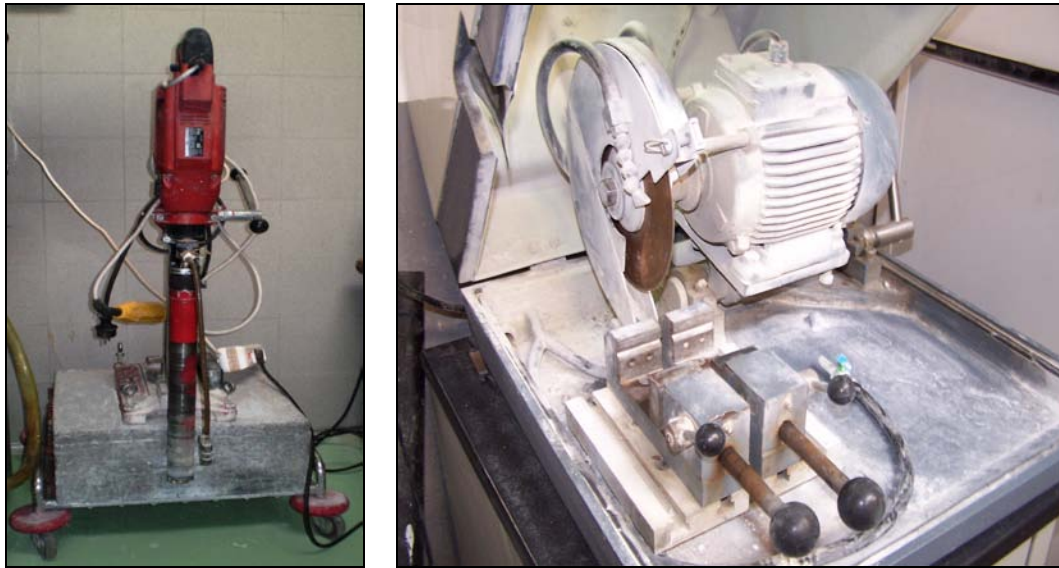


Figure 4. 9: Tools used for the determination of chloride concentration profiles: a) coring in column b) fitted with a circular saw cutting (diameter 25 mm, thickness 1 mm)

With the aid of a stereoscope Leica DFC290, the thickness of coating applied to the specimens was measured (Figure 4.11).

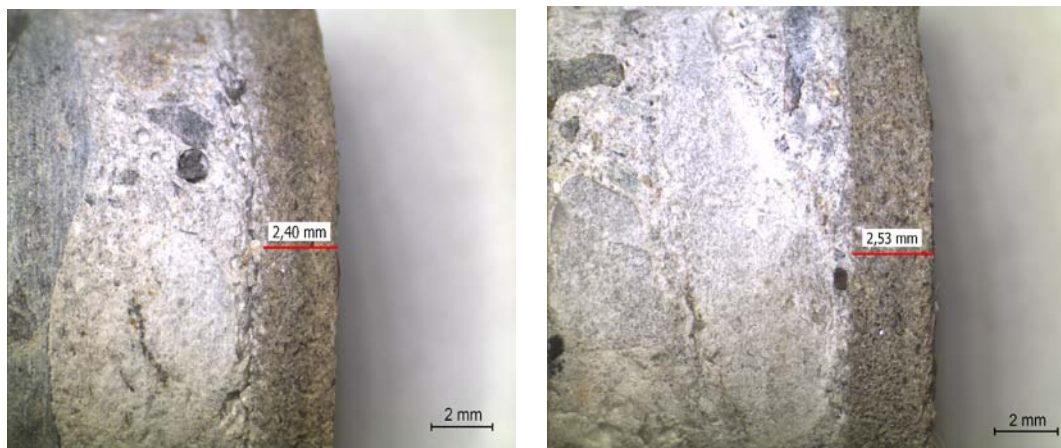


Figure 4. 10: Examples of measurement of coating thickness using stereoscope

The thickness of individual slices of concrete was measured with a micrometer screw gauge; the slices were then milled through a mill jaws (Figure 4.11a). About 3 g of each ground sample were put in a beaker and dried in an oven at a temperature of 105 ° C for 24 hours in order to remove the

moisture present (Figure 4.11b). In order to obtain the net weight of the beaker containing the powder were weighed before and after drying in an oven using a precision balance ( $\pm 0.1$  mg).



Figure 4. 11: Instruments used for the determination of the concentration profiles of the chlorides:  
a) mill jaws for crushing the concrete, b) oven for drying of the powders

The powder was subsequently dissolved: to each sample were added 50 mL of distilled water and 25 mL nitric acid ( $\text{HNO}_3$ ) to 32%. The solution was brought to boiling for 1 minute and subsequently poured into a flask, where, once cooled, the volume was brought to 100 mL with the addition of distilled water. Potentiometric titrations were performed with automatic titrator Metro-Ohm Titrino 751 (Figure 4.12) by addition of a solution of 0.01 M silver nitrate, using an ion-selective electrode and detecting the end point (point of inflection on the curve) on the graph-potential volume of  $\text{AgNO}_3$  added. The release of the reagent has been carried out keeping the solution in motion with a magnetic stirrer.

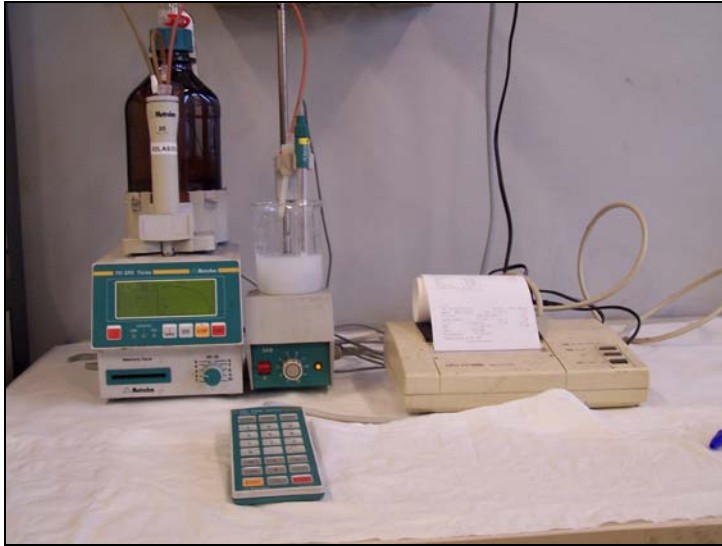


Figure 4.12: Automatic titrator to determine the profile of chlorides

By the volume of titrant added, it was possible to calculate the chloride content in solution (g/L) via the relation:

$$[Cl^-] = \frac{Vol_{AgNO_3} \cdot N_{AgNO_3} \cdot PM_{Cl^-}}{Vol_{sol}} \quad (19)$$

Where  $Vol_{AgNO_3}$  is the volume of reagent added at the end point (mL),  $N_{AgNO_3}$  is the normality of the reagent (mol / L),  $PM_{Cl^-}$  is the atomic weight of chlorine (g / mol) and  $Vol_{sol}$  is the volume of titrant.

Chloride content vs. concrete weight has been evaluated by taking into account the quantity of concrete dissolved in 100 ml of solution.

The chloride content expressed as weight percent respect to cement has been evaluated by multiplying the weight percent respect to concrete by density of the concrete ( $7200 \text{ Kg/m}^3$ ) and divide by the cement content ( 310 for w/c = 0.65 and 320 for w/c = 0.55).



## 5.0 Experimental Results

The experimental results reported in this chapter have been obtained in the department of Chemistry, Chemical Engineering, and laboratory of Corrosion. The thesis work was aimed at:

- Corrosion monitoring by measuring the corrosion potential (E) and polarization resistance ( $R_p$ ) on reinforced specimens subjected to cycles of accelerated penetration of chlorides (ponding).
- Determination of chloride profile
- Measurement of the coating thickness

### 5.1 Corrosion Monitoring

The experience of this work was carried out from 2484 days to 2569 days. According to the data of the past experimental results, we noticed that there is a decrease in corrosion potential E and the corrosion resistance  $R_p$ .

#### 5.1.1 Uncoated specimens

The specimens without coating are the reference specimens that have been measured in the previous work, and the results are reported here in the order to compare with the specimens coated with the two polymers modified cementitious coatings (RIV 1-2 and RIV 1-1).

The reference specimen C1 ( $w/c = 0.55$ ), Figure 5.1, without coating showed that all the rebar have been affected by corrosion and the rate of corrosion is high. For the potential, the initiation of corrosion is indicated by the decrease from the initial value -100 mV SCE to values between -300 and -400 mV SCE of few cycles and decreased gradually until the potential reached -500 to -600 mV SCE. For the polarization resistance (figure 5.2), the initiation of corrosion is indicated by the

decrease of the shape that passes from the initial value  $100 \Omega m^2$  to value  $10 \Omega m^2$ , this means the corrosion rate of steel increases, after remain nearly constant for the following exposure.

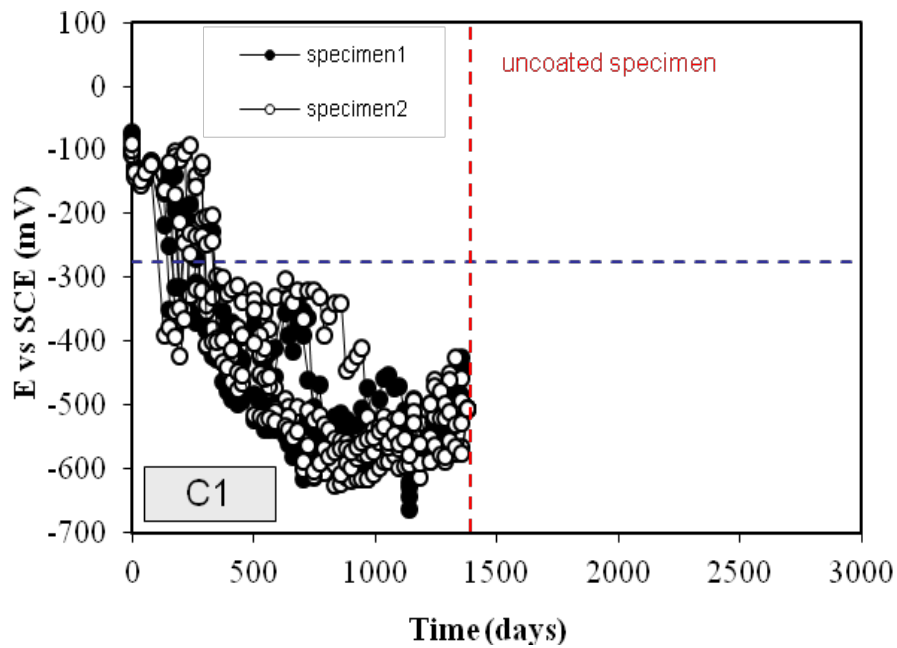


Figure 5. 1: A graph of corrosion potential vs. time in days for the uncoated specimen

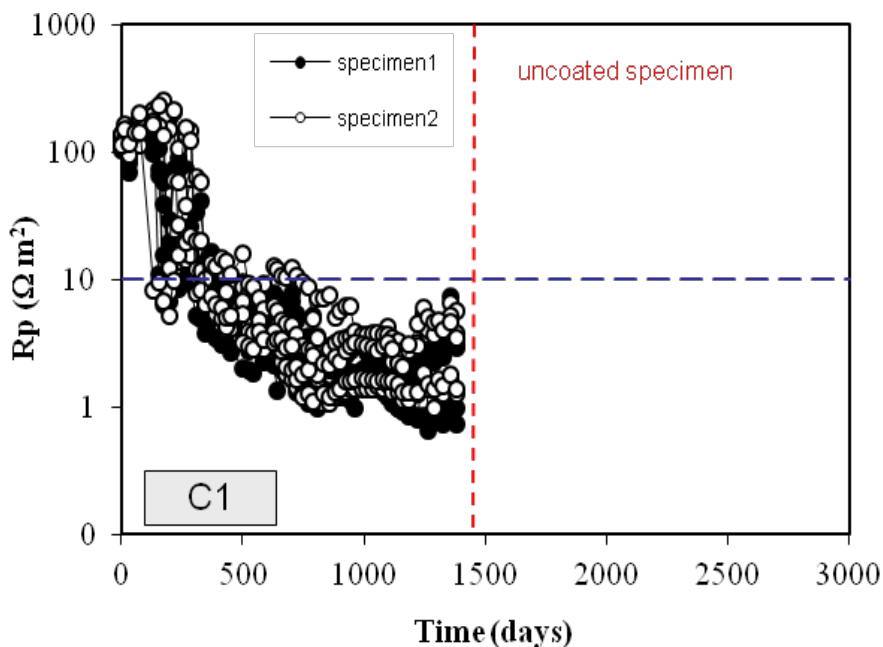


Figure 5. 2: Polarization resistance of the reinforced concrete of uncoated samples.

The same trend is noticed for the reference specimen C2 ( $w/c = 0.65$ ), Figure 5.3 and 5.4, but due to

higher porosity of the concrete corrosion initiation occurred before.

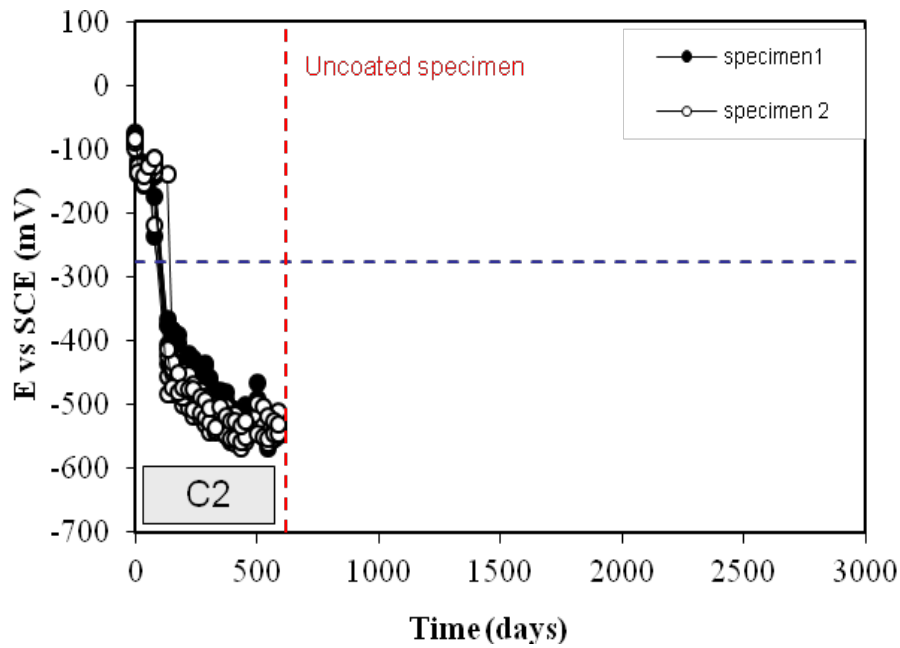


Figure 5. 3: A graph of potential vs. time for uncoated specimen C2

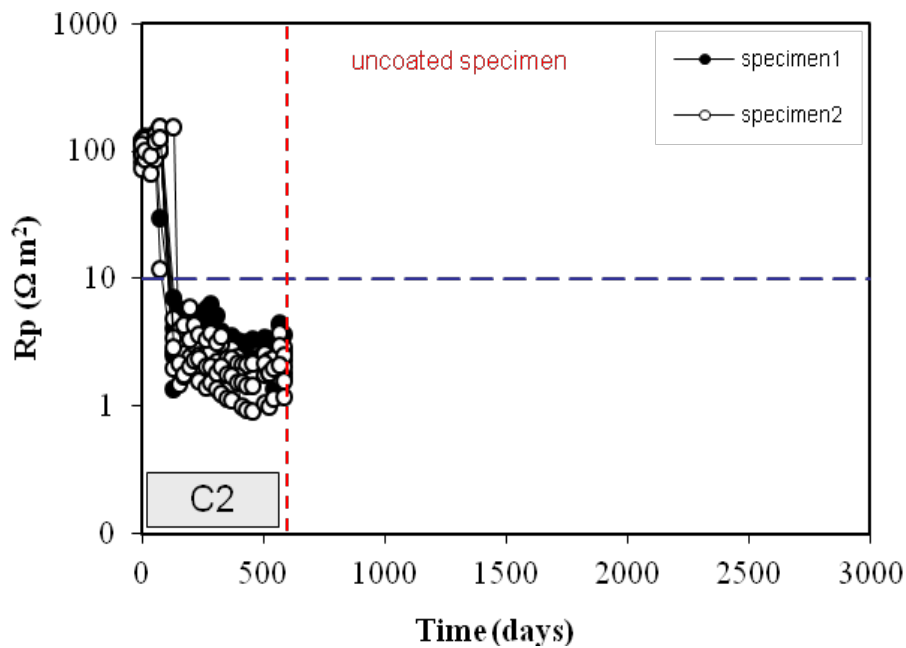


Figure 5. 4: Polarization resistance of the reinforced concrete of uncoated samples.

### 5.1.2 Specimens coated with Polymer modified cementitious RIV 1-2

Figures (5, 6, 7 and 8) show the corrosion potential  $E_p$  and polarization resistance  $R_p$  of the polymer

modified cementitious coated specimens RIV 1-2 (C24 and C25) with the ratio  $w/c = 0.65$  and  $w/c = 0.55$

The two specimens of C24 (RIV 1-2) with  $w/c = 0.65$  behave in different way.

Specimen C24 A1 is not yet corroded, the value of potential is high, figure 5.5a. The trend of the polarization resistance is in agreement of that of corrosion potential: the value of polarization resistance is higher than  $10 \Omega m^2$ , so the corrosion rate is negligible.

Specimen C24 A2 is in active condition, that means is corroded. The potential values are very low, close to  $-550 \text{ mV SCE}$ . Also the polarization resistance is less than  $1 \Omega m^2$  which is in agreement with the corrosion potential.

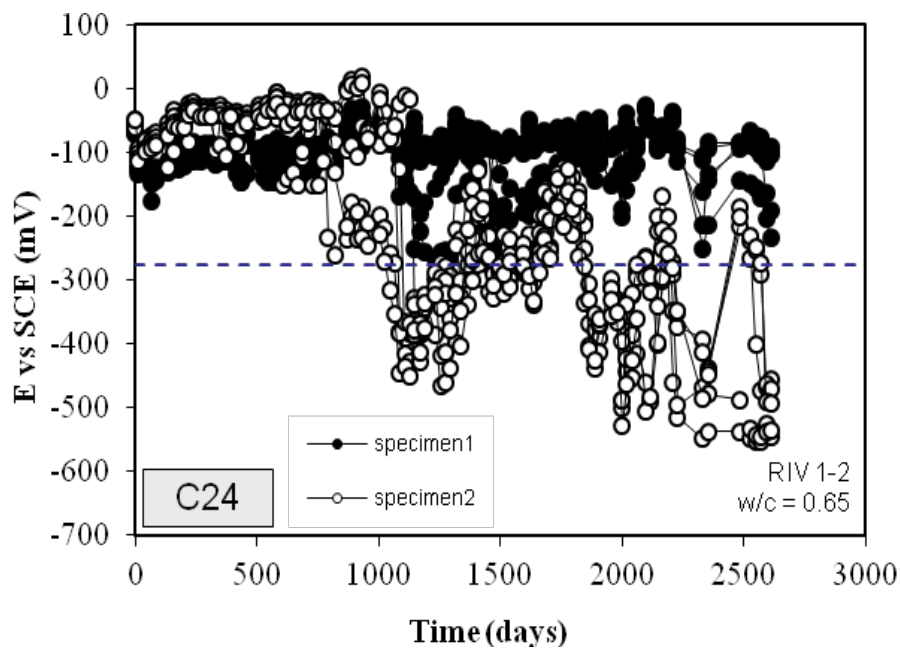


Figure 5. 5: A graph of potential vs. time for RIV 1-2

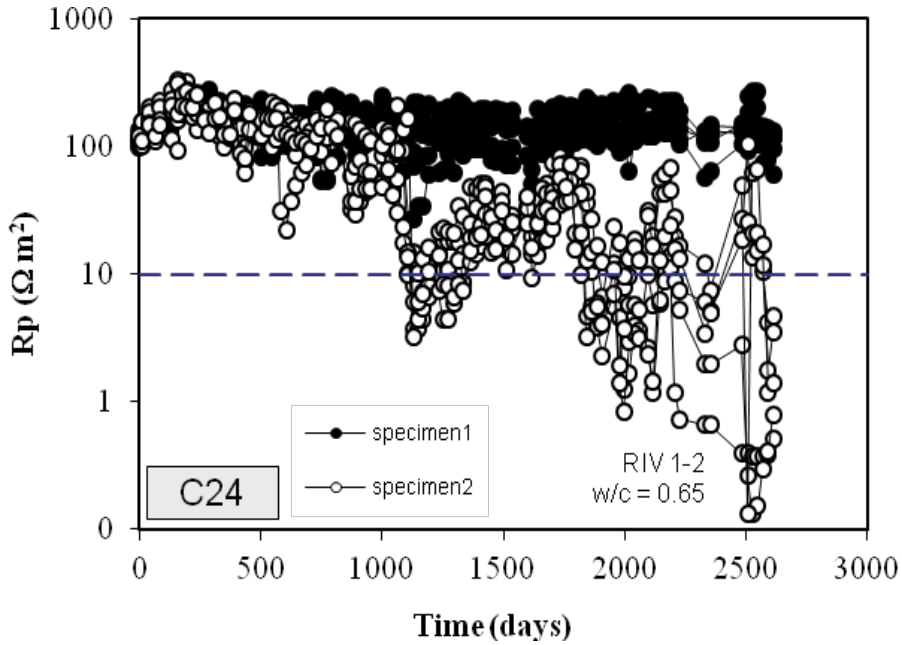


Figure 5. 6: Potential and polarization resistance of the rebar specimens C24 A1 and C24 A2 coated with RIV 1-2 (Measurement taken from 97 cycles to 101 cycles)

The two coated specimens of C25 (RIV 1-2) with ratio  $w/c = 0.55$  show a similar behavior of polarization resistance (high) and corrosion potential (high). The two specimens are in passive condition that means C25 is not yet corroded as shown in figure 5.6a and figure 5.6b

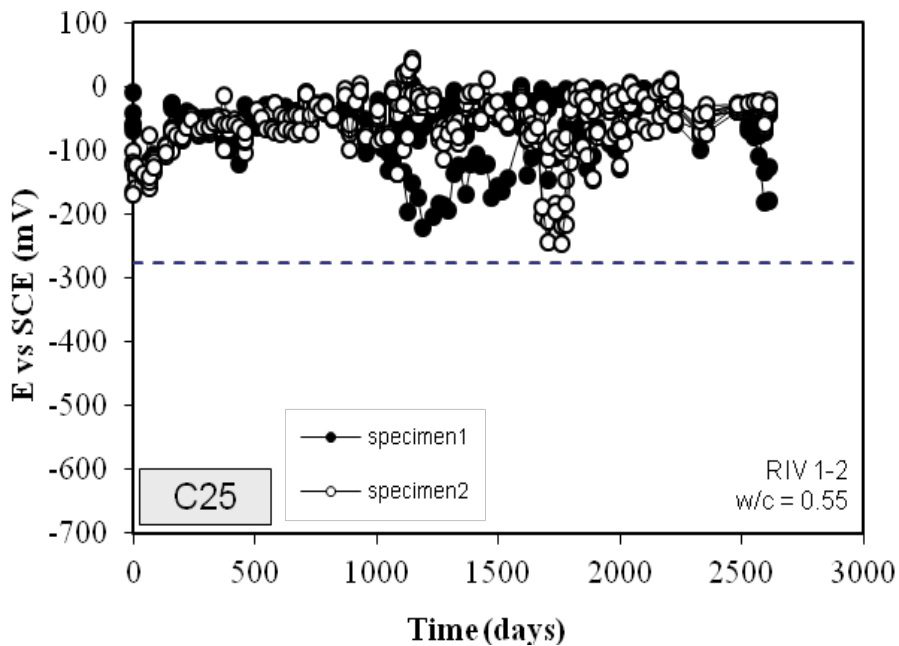


Figure 5. 7: Potentials vs. time for RIV 1-2 C25  $w/c = 0.55$

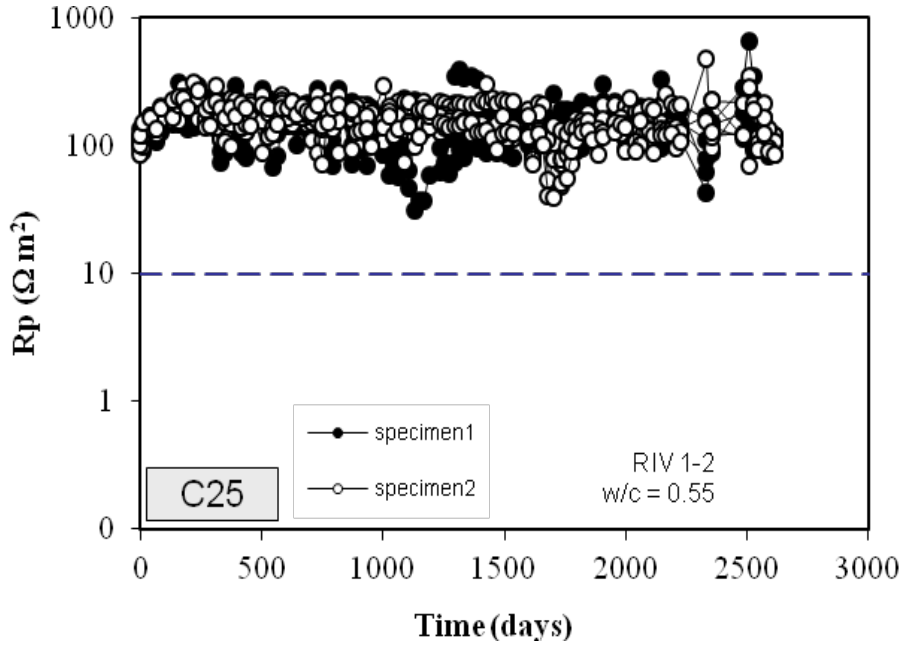


Figure 5. 8: Polarization resistance of the rebar specimens C25 A1 and C25 A2 coated with RIV 1-2 (Measurement taken from 97 cycles to 101 cycles)

### 5.1.3 Specimens coated with Polymer modified cementitious “improved”

Figures (9, 10, 11 and 12) show the graphs for corrosion potential  $E_p$  and corrosion resistance  $R_p$  of the polymer modified cementitious coated specimens RIV 1-1 “improved” (C23 and C26) with the ratio  $w/c = 0.55$  and  $w/c = 0.65$  respectively.

Specimen C23 A1 (RIV 1-2) with ratio  $w/c = 0.55$  is in active condition (low potential), that means is corroded. The trend of the polarization resistance is in agreement of that of corrosion potential: the value of this parameter is lower than  $10 \Omega m^2$ , and the corrosion rate is  $i_{corr} > 2 \mu m/year$ . So the corrosion rate is not negligible.

Specimen C23 A2 (RIV 1-2) with ratio  $w/c = 0.55$  is in passive condition, that means is not yet corroded. The trend of the polarization resistance is in agreement of that of corrosion potential: the value of polarization resistance is higher than  $20 \Omega m^2$ , so the corrosion rate is negligible and its value is  $i_{corr} < 1 \mu m/year$ .

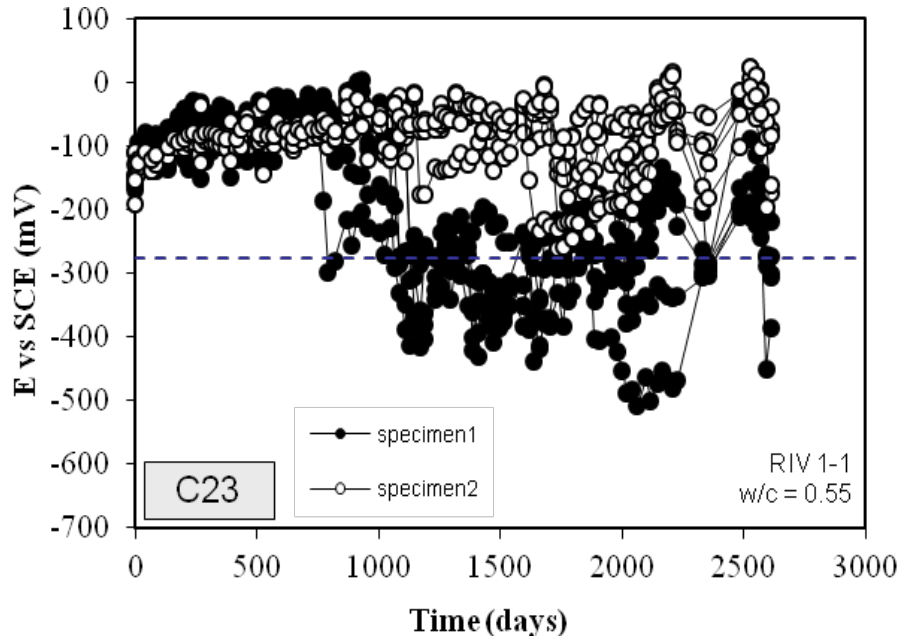


Figure 5. 9: Potential resistance of the rebar specimens C23 A1 and C23 A2 coated with Map elastic smart (Measurement taken from 97 cycles to 101 cycles)

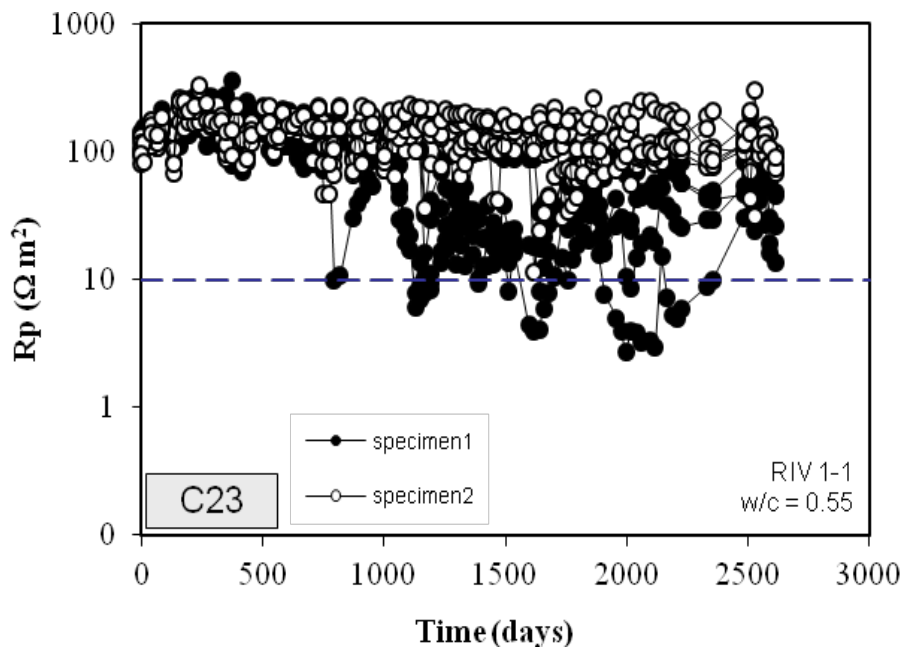


Figure 5. 10: polarization resistance of the rebar specimens C23 A1 and C23 A2 coated with polymer modified cementitious (Measurement taken from 97 cycles to 101 cycles)

Specimen C26 A1 (RIV 1-2) with ratio  $w/c = 0.65$  is in passive condition, that means C26 A1 is not

yet corroded. The trend of the polarization resistance is in agreement of that of corrosion potential: the value of corrosion is higher than  $100 \Omega\text{m}^2$ , so the corrosion rate is negligible and its value is  $i_{\text{corr}} < 1 \mu\text{m}/\text{year}$ .

Specimen C26 A2 (RIV 1-2) with the ratio  $a/c = 0.65$  is in active condition, that means C26 A2 is corroded. The potential values are low, close to  $-500 \text{ mV SCE}$ . Also the polarization resistance is less than  $10 \Omega\text{m}^2$  which is in agreement with the corrosion potential. The corrosion rate is  $i_{\text{corr}} \approx 2 \mu\text{m}/\text{year}$

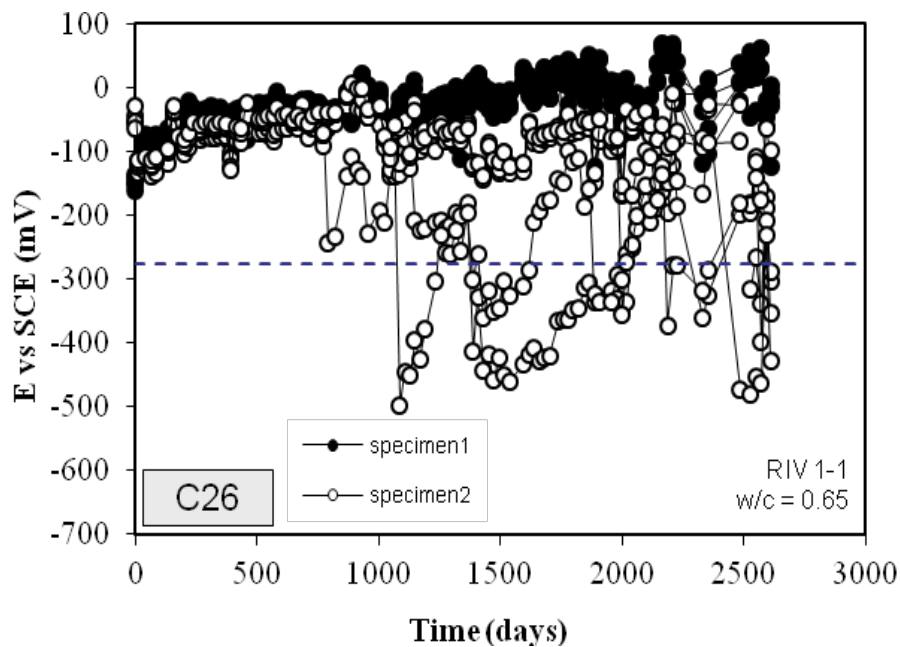


Figure 5. 11: Potential resistance of the rebar specimens C26 A1 and C26 A2 coated with polymer modified cementitious (Measurement taken from 97 cycles to 101 cycles)



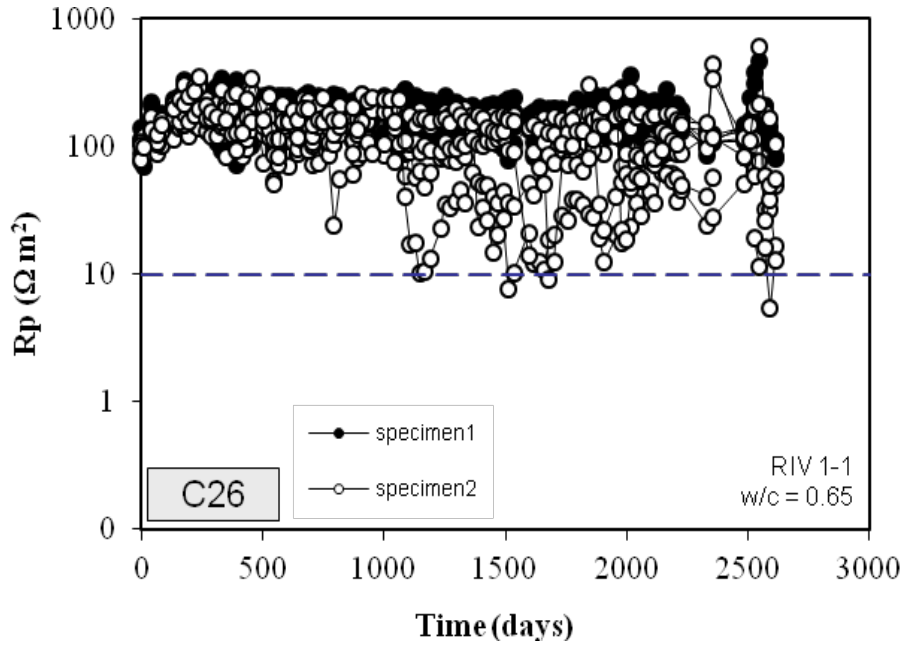


Figure 5. 12: Potential and polarization resistance of the rebar specimens C26 A1 and C26 A2 coated with polymer modified cementitious (Measurement taken from 97 cycles to 101 cycles)

### 5.1.4 Coatings with different p/c ratios

We reported also the measurements of corrosion potential (Figure 5.13) and polarization resistance (Figure 5.14) of five specimens on which the measurements were made in the six months of experimentation. These specimens are coated with products similar to RIV 1-2 and RIV 1-1 (K is of the same producer and H not) and have the characteristic to be exposed to ponding for more than 10 years. The polymer/cement (p/c) ratio in specimen H is 0.35 and that of specimen K is 0.55.

The measurements taken in this work are between 14 and 15 years.

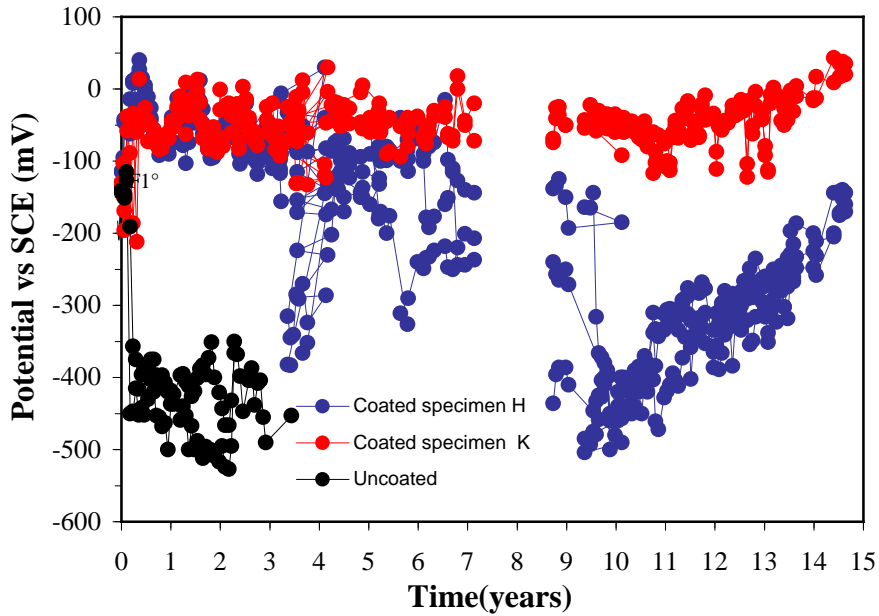


Figure 5. 13: Potential of reinforcement of reinforced specimen subjected to ponding

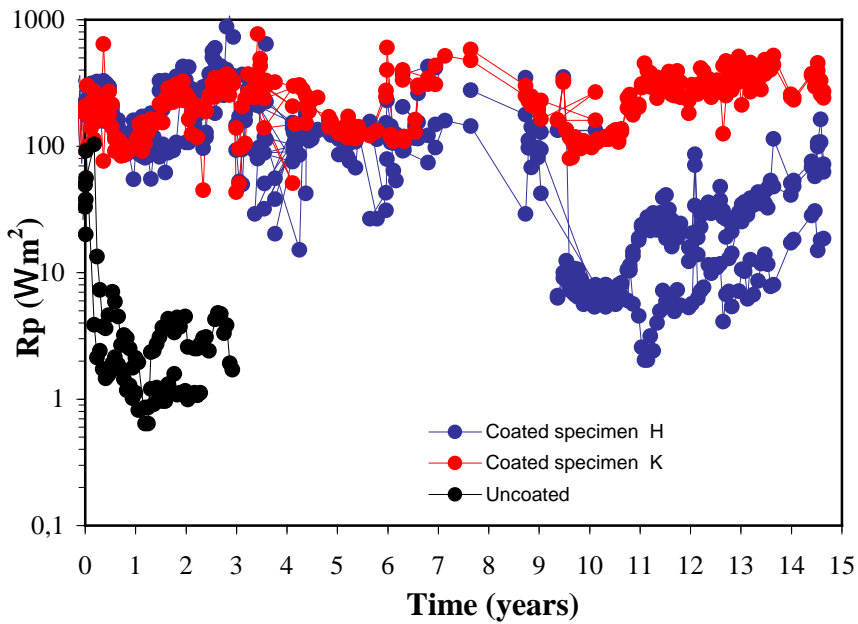


Figure 5. 14: Polarization resistance of reinforcement in concrete specimen subjected to ponding

We noticed that the specimen H in which the ratio  $p/c = 0.35$  is more affected by the corrosion because the corrosion potential is about  $-500$  mV vs SCE. Also the polarization resistance of the coating is less than  $3 \Omega m^2$  i.e. corrosion rate is  $> 1 \mu m/year$  which is in agreement with the

corrosion potential.

In contrast the specimen K in which the ratio  $p/c = 0.35$  is not affected by corrosion. The corrosion potential is about  $-200$  mV SCE. The trend of the polarization resistance is in agreement with that of corrosion potential: the value of polarization resistance is about  $45\Omega m^2$ , so the corrosion rate is negligible.

## 5.2 Measure of Chloride concentration

The measurement of chloride concentration was made by extracting the core from all the specimens. The core samples were crushed in a machine in order to get the powder. The powder has been titrated. The measures of concentration were represented in weight percent with respect to concrete (% vs. concrete). There is a relationship between the weight percent respect to concrete and the weight percent respect to cement. The chloride content expressed as weight percent respect to cement has been evaluated by multiplying the weight percent respect to concrete by density of the concrete ( $7200 \text{ Kg/m}^3$ ) and divide by the cement content ( 310 for  $w/c = 0.65$  and 320 for  $w/c = 0.55$ ).

The titrations were realized on all the reinforced specimens subjected to cycles of ponding: at  $101^\circ$  cycle for the coated specimens with polymer modified cementitious RIV 1-2 and polymer modified cementitious RIV 1-1. This titration was carried out for a comparison with the uncoated specimens and to evaluate the concentration of chlorides at the level of the reinforcement.

The experimental data of concentration for each slice of concrete titrated were interpolated using the analytical solution of Fick's 2<sup>nd</sup> Law, which describes the nonstationary diffusion phenomena. This makes it possible to estimate the values of the diffusion coefficient and the content of chlorides surface that minimize the standard deviation between experimental and theoretical values.

In the presence of the coating one can still use non-linear regression and estimate the values of

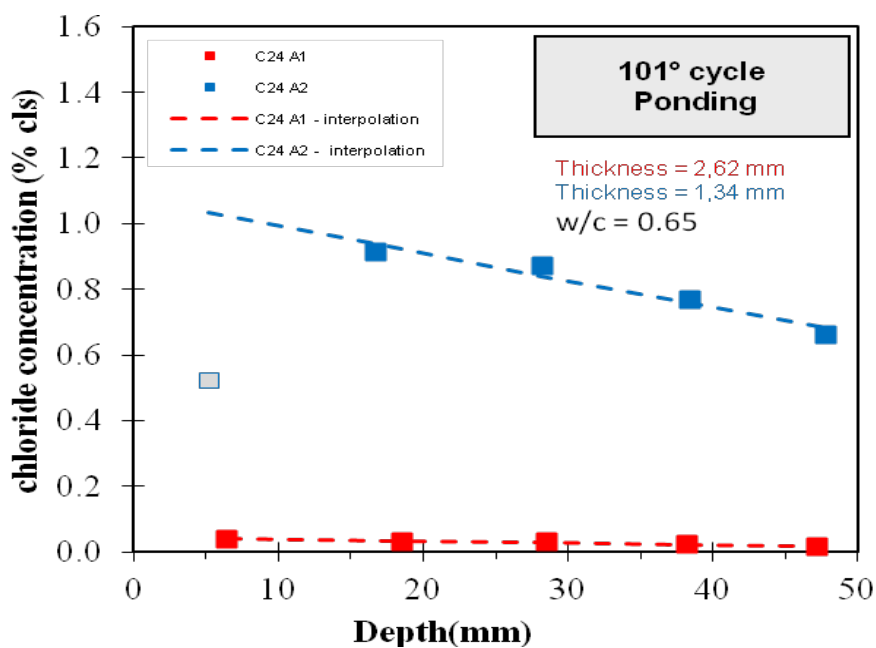
Chloride concentration and coefficient of diffusion by considering the coating and concrete as a single conglomerate, or use a more complex analytical solution. Knowing the cover thickness (20 mm), and once the diffusion coefficient and the content chloride surface has been calculated, it is possible to obtain the chloride concentration in the vicinity of the reinforcement

### 5.2.1 Specimens Coated with RIV 1-2

Figure 5.15 shows the profiles of chloride penetration of the coated specimens of reinforced concrete with RIV 1-2 coating exposed to ponding (C24 and C25).

In one of the coated specimens C24 with a w/c =0.65 (specimen A2) has a higher concentration profile, and these data are in agreement with the fact that corrosion has already started in this specimen. In the other specimen of the same concrete and coating (specimen A1) chloride concentration is low and corrosion has not yet started because the chloride content is lower than critical chloride concentration for corrosion, between 0.4 to 1% vs. cement weight (Fig. 5.15).

In the case of w/c = 0.55 (C25), both specimens show very little chloride content. This is in agreement with the fact that in both these specimens corrosion has not yet started.



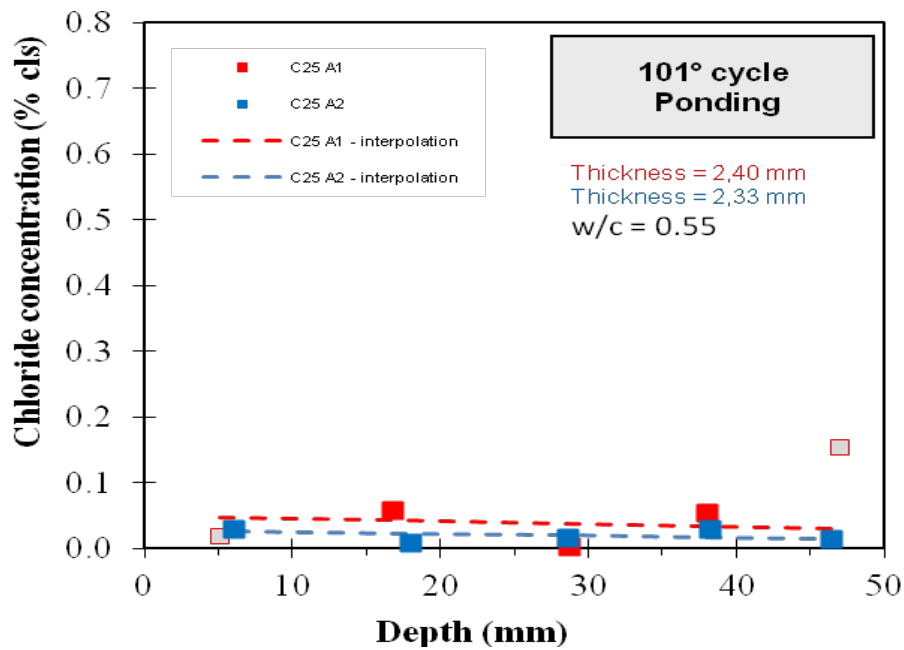


Figure 5. 15: shows the profiles of chloride penetration of the coated specimens of reinforced concrete with RIV 1-2 coating exposed to ponding.

The values of the chloride concentration near the surface are different for the two specimens C24: in one case (A1) 0.04% vs. concrete (about 0.34% vs cement weight), in the other (A2) 1.08% vs. concrete (about 6.07% by weight respect to cement).

In the specimens C25 with the ratio  $w/c = 0.55$  the values near the surface are of the order of 0.03 to 0.05% vs. concrete (less than 0.4% by cement weight). The values at a depth of about 20 mm, equivalent to the thickness of the concrete cover, are very similar (about 0.17% to 0.31% by weight relative to cement).

### 5.2.2 Specimens Coated with polymer modified cementitious improved RIV 1-1

Figure 5.16 shows the profiles of chloride penetration of the coated specimens of reinforced concrete with RIV 1-1 coating exposed to ponding (C23 and C26).

The values of the chloride concentration are different for the two specimens C23, with  $w/c = 0.55$  (Fig. 5.16); in one case (specimen A2), surface concentration is low (0.04% vs concrete, about 0.2% by cement weight), in the specimen A1 the concentration is much higher (0.5% vs concrete). The

same trend can be observed at a depth of about 20 mm, equivalent to the thickness of the concrete cover, the chloride concentrations is about 0.18% for A2 and 1.5% for A1 (weight respect to cement).

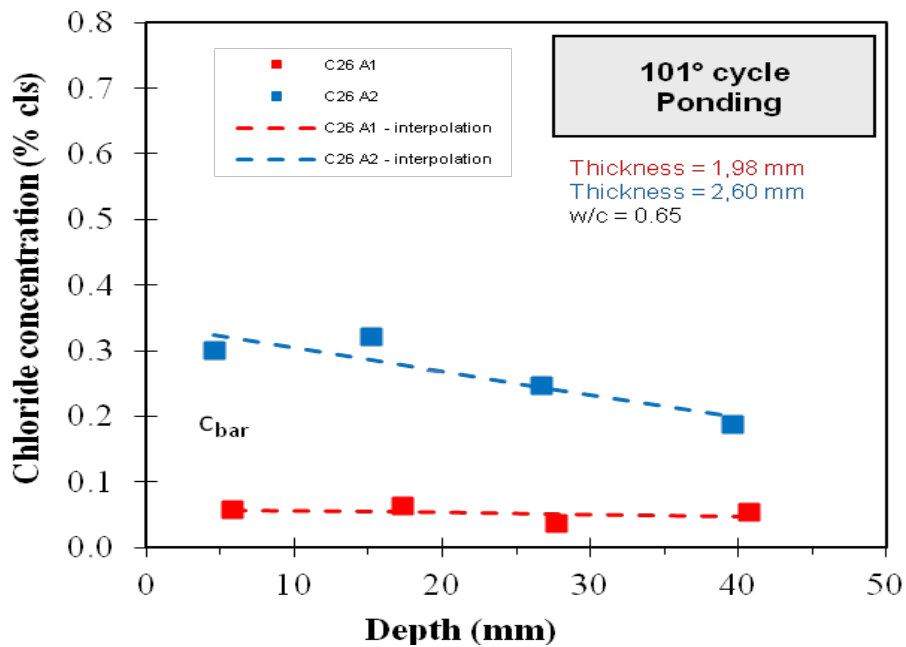
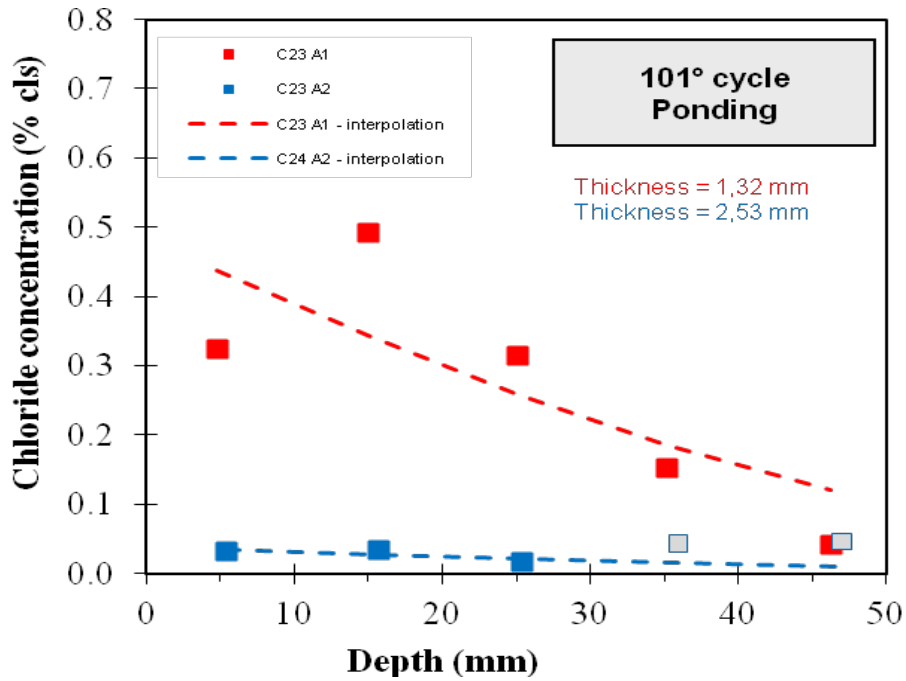


Figure 5. 16: Profiles of chloride penetration of the coated specimens of reinforced concrete with RIV 1-1 coating exposed to ponding.

The specimens C26 with the ratio  $w/c = 0.65$  also show two different behavior: the values near the surface are of the order of 0.06% (A1) and 0.34% (A2) vs. concrete, corresponding to about 0.4% (A1) and 2.5% (A2) by cement weight. At a depth of about 20 mm, equivalent to the thickness of the concrete cover, the chloride concentrations is about 0.40% (A1) to 1.7% (A2) by weight relative to cement.

### 5.3 Measurement of Coating Thickness

In order to compare the penetration of chloride of each coated specimens, we made the measurement of thickness of the coating. The measurements of the thickness of coating of each individual sample were performed with a stereoscope Leica DFC290. These data are useful for comparing the concentration profiles of chloride and determining the barrier effect

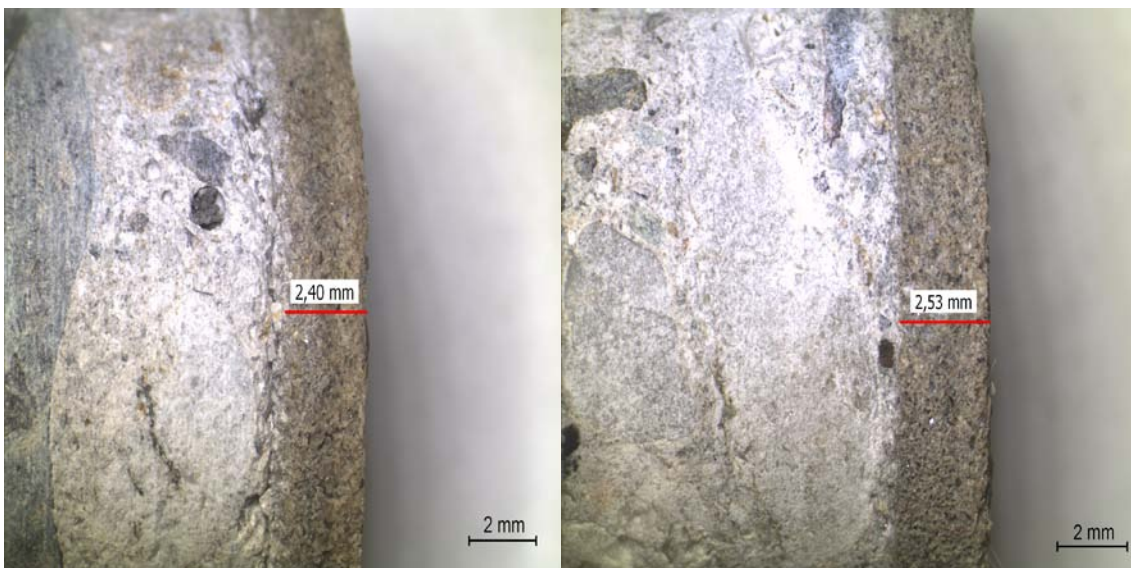


Figure 5. 17: Examples of measurement of the coating thickness made with the stereoscope

The measurement is not general but it still represents a significant parameter for the analysis and discussion of results. We measured the thickness of the coated specimens (Table 5.1).

<b>COATING THICKNESS</b>			
<b>Specimens</b>	<b>w/c</b>	<b>Coatings</b>	<b>Thickness of coatings [mm]</b>
<b>C23 A1</b>	0,65	<i>RIV 1-1</i>	<b>1.32</b>
<b>C23 A2</b>	0,65	<i>RIV 1-1</i>	<b>2.53</b>
<b>C24 A1</b>	0,65	<i>RIV 1-2</i>	<b>2.62</b>
<b>C24 A2</b>	0,65	<i>RIV 1-2</i>	<b>1,34</b>
<b>C25 A1</b>	0,55	<i>RIV 1-2</i>	<b>2.40</b>
<b>C25 A2</b>	0,55	<i>RIV 1-2</i>	<b>2.33</b>
<b>C26 A1</b>	0,55	<i>RIV 1-1</i>	<b>1.98</b>
<b>C26 A2</b>	0,55	<i>RIV 1-1</i>	<b>2.60</b>

Table 5. 1: Coating thickness of reinforced specimen



## 6.0 Discussion

In this chapter, we are going to analyze and discuss the results that we have obtained from the chapter 5. In discussing the corrosion of rebar in concrete, it is important to know that the overall lifespan of a concrete structure ( $t_T$ ) is divided into the initiation time ( $t_i$ ) and propagation time ( $t_p$ ) which is shown in the equation below (chapter 2). It is also important that the coating applied should be able to prevent, delay or slow the corrosion rate after the initiation.

$$t_T = t_i + t_p \quad (20)$$

The thickness and the permeability of the coating are the main barrier to chloride penetration in the concrete.

The barrier ability of the coatings was defined through the use of some parameters derived from analysis of the concentration profiles.

- Diffusion coefficient of chlorides:

Diffusion coefficient of concrete ( $D_{cls}$ ) and diffusion coefficient of the concrete + coating

- Concentration of chlorides:

Surface concentration in contact with the external environment ( $C_s$ );

Concentration at the interface concrete-coating ( $C_{s, cls}$ );

Concentration at the level of rebars ( $C_{bar}$ );

- Resistance of the coating  $R_{riv}$ ;

Analyzing these parameters it can be explained the effect of coating on initiation time of corrosion

The diffusion coefficient and the surface concentration are two very important parameters and are discussed extensively in this chapter. The diffusion coefficient  $D_{cls}$  and the surface concentration  $C_s$  were obtained by extrapolation of the concentration profile. The determination of the concentration

profile, the subsequent extrapolation of the parameters of diffusion coefficient of concrete and coating system ( $D_{cls+rev}$ ) and Concentration at the interface of concrete-coating ( $C_{s,cls}$ ) was performed without dividing the contributions of the concrete and the coating. This is a simplified approach since the penetration of chloride has two (2) stages to reach the rebar.

- The diffusion of chloride through the coating  $D_{riv}$
- The diffusion of chloride through the concrete  $D_{cls}$

The parameter  $C_{s,cls}$  represents the concentration measured at the interface concrete-coating or in the first layer of the concrete, while  $C_s$  represents the concentration of chlorides on the surface of the coating in contact with the external environment. This parameter cannot be measured in the coating, but it is assumed equal to the surface concentration  $C_s$  in the concrete specimens not coated

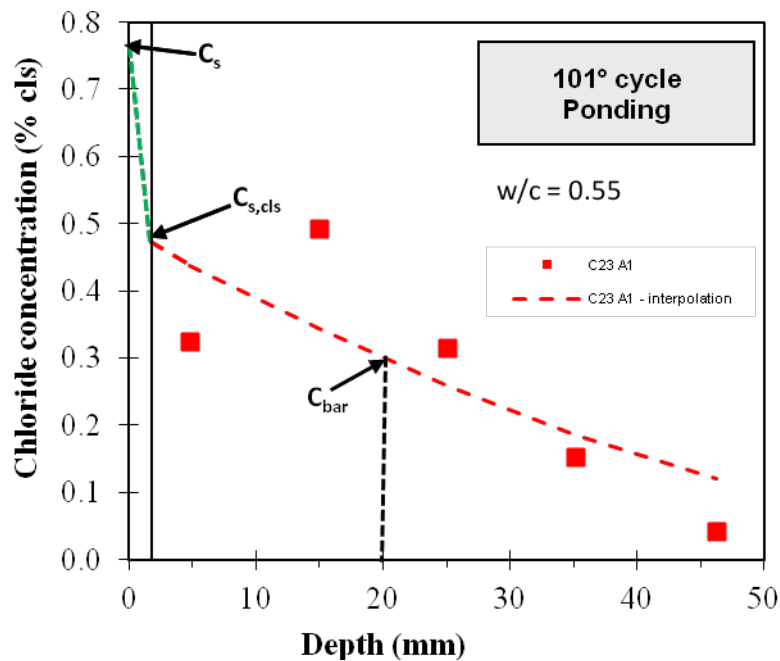


Figure 6. 1: Example of Chloride concentration profile of coated specimen

The chloride concentration profile as well as the surface chloride concentration for the uncoated specimens at 40 cycles has been showed in figure 6.2. The two profiles with  $w/c = 0.5$  for C1 and  $w/c = 0.65$  for C2 show high amount of chloride at 40 cycles which is almost half cycles of the specimen coated with polymer modified cementitious. The chloride profile content in the uncoated

specimen C1 with  $w/c = 0.55$  presents lower values respect to the uncoated specimen C2 with  $w/c = 0.65$  at the same number of cycles (40). This is because the porosity of the concrete depends also on water-cement which is high in the uncoated specimen C2.

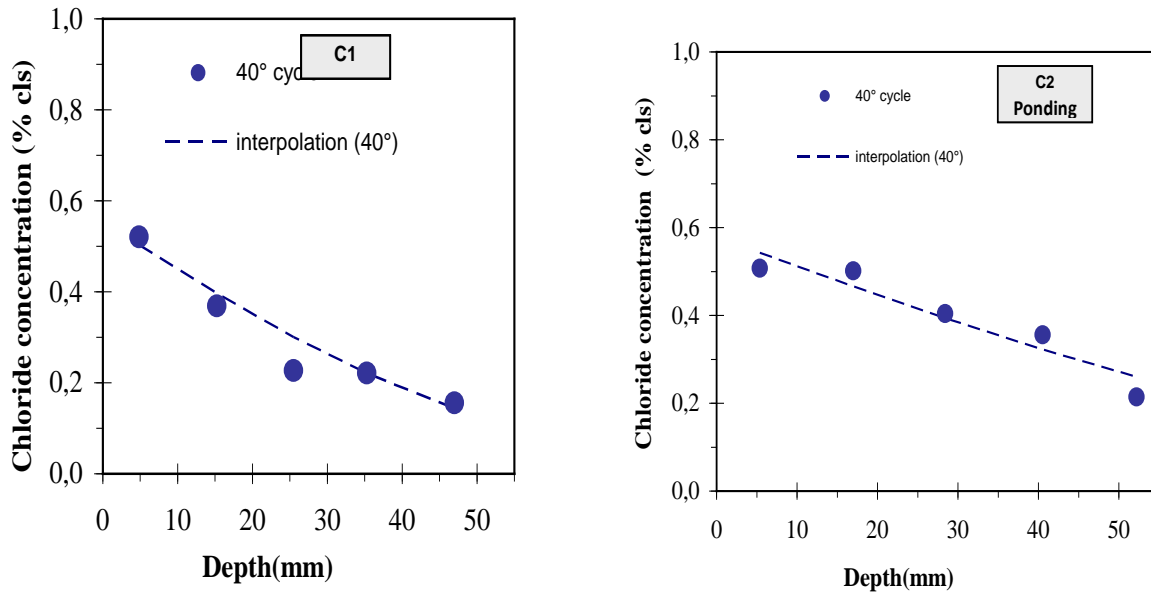


Figure 6. 2: Chloride surface concentration for uncoated specimens at 40 cycles

## 6.1 Specimens coated with Polymer Modified Cementitious RIV1-2

Let us examine the diffusion coefficient of chlorides  $D_{cls+riv}$  and the chloride concentration parameters in the case of polymer modified cementitious RIV1-2:

### 6.1.1 Chloride profile and surface concentration RIV 1-2

Figure 5.15 (see chapter 5) shows the profile and the surface concentration of chloride at 101 cycles for specimens coated with polymer modified cementitious. The coated specimen C24 with  $w/c = 0.65$  shows two different profiles between C24 A1 and C24 A2 with the same coating.

The difference in the behaviour of the two specimens ( C24 A1 and C24 A2) can be attributed to the thickness of the coatings which is lower in C24 A2 and therefore higher chloride concentration.

These measurements are in agreement with corrosion monitoring, in fact, rebars in the specimen A2 show initiation after about 40 – 50 cycles (see chapter 5).

For the coated specimen C25 with  $w/c = 0.55$  shows similar behaviour of chloride concentration for the two specimens having the same coatings and here, the thickness is almost the same.

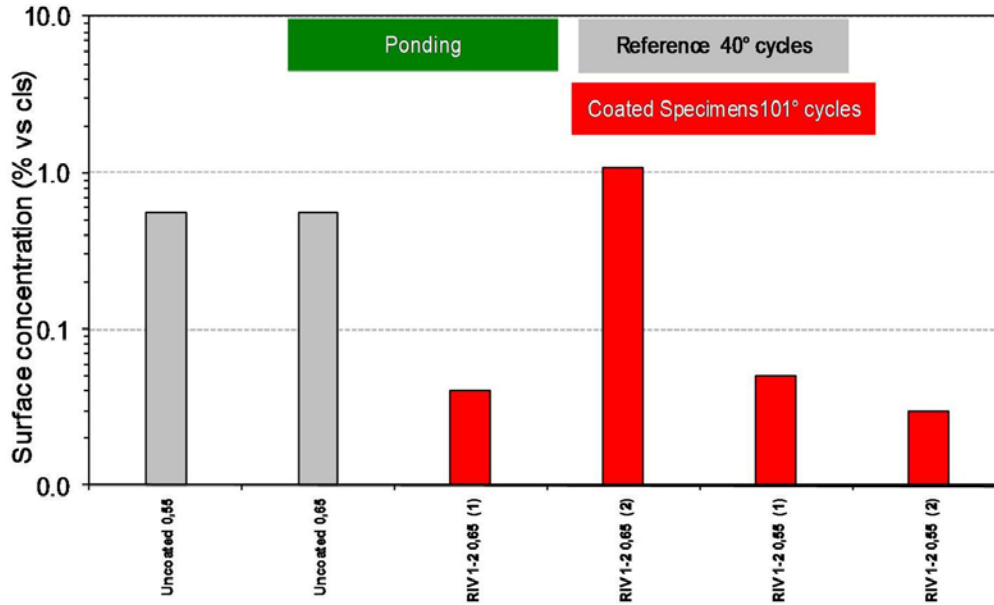


Figure 6. 3: Surface Chloride concentration of RIV 1-2 coated specimens

Figure 6.3 shows the values of chloride concentration obtained by extrapolating the experimental profiles using the non-stationary diffusion of the 2nd Fick's law. The uncoated specimens underwent ponding for  $40^\circ$  cycles and the coated for  $101^\circ$  cycles. For the uncoated specimens, irrespective of the  $w/c$  ratio, the surface chloride concentrations have the same value of 0.6% vs. cls which is about 4.6% vs. cement. With respect to the coated specimens, specimen with a  $w/c = 0.55$  shows a lower surface chloride concentration than those without coating indicating that the coating is playing very important role in reducing the concentration of chloride at the surface between the coating and the concrete. For a  $w/c = 0.65$ , the behavior of the two specimens C24 A1 and C24 A2 is not the same as previous. C24 A1 which has a higher thickness show surface concentration lower than the uncoated while C24 A2 having a lower thickness shows high surface chloride concentration, comparable with uncoated concrete.

The chloride concentration in contact with the reinforcement  $C_{\text{bar}}$  is a fundamental parameter to verify the conditions of corrosion of the reinforcement. At the level of the reinforcement, a critical chloride concentration value of about 0.4 to 1% by weight with respect to the cement will mean there will be corrosion of the rebar.

In general, comparing the coated to the uncoated specimens, it shows that the coated have lower chloride concentration throughout the thickness of the concrete after 101° cycles. These concentrations are lower than the critical chloride concentration for corrosion. The exception is the C24 A2 which we have attributed its behaviour to low thickness of coatings, in which chloride concentration at the rebar level is as high as  $\approx 0.9\%$  to concrete weight about 6.8% vs. cement weight.

### **6.1.2 Diffusion coefficient of Chloride $D_{\text{cls+riv}}$**

Figure 6.4 shows the values of diffusion coefficients obtained by extrapolating the experimental data, only for the specimens with significant amount of chlorides. The Riv 1-2 covers C24 and C25 with the water-cement ratio of  $w/c=0.65$  and  $w/c=0.55$  respectively. The diffusion coefficient for coated specimen has been measured after 101 cycles while the diffusion coefficient of the uncoated has been measured at 40 cycles.

Also, in figure 6.4, it is observed that the diffusion coefficient for the uncoated specimen with a lower  $w/c$  ratio is lower than the one with higher  $w/c$  as expected. This is because the higher the  $w/c$  ratio the higher the porosity and therefore the permeability. For the coated specimen C24 A2 ( $w/c$  0.65), the estimate value for the diffusion coefficient are similar to the uncoated specimen with the same  $w/c$  ratio.

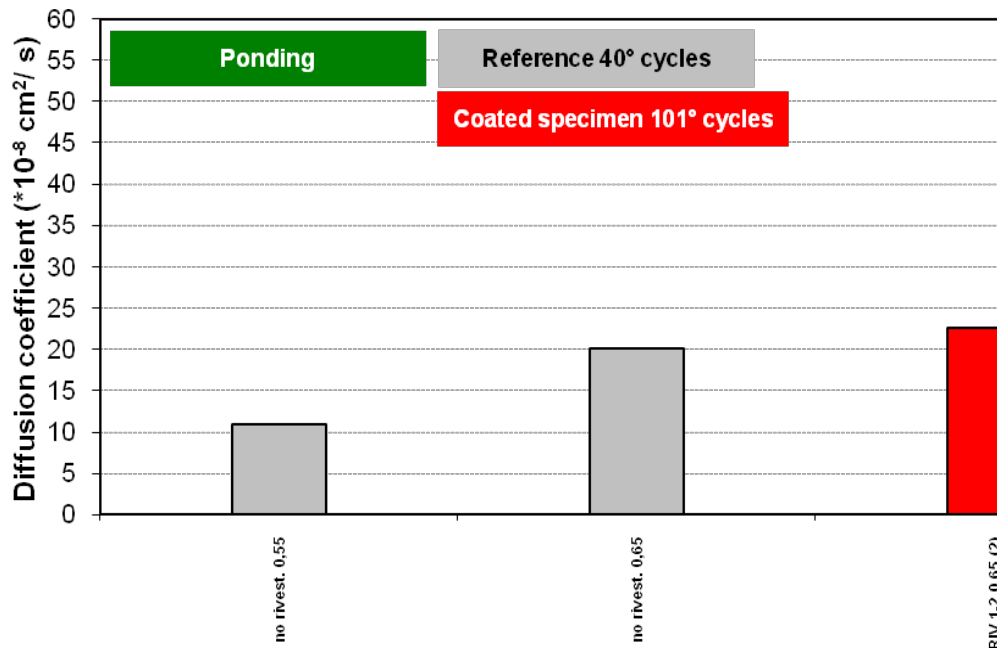


Figure 6. 4: Diffusion coefficients of RIV 1-2 coated specimens

## 6.2 Specimens coated with Polymer Modified Cementitious “improved” RIV1-1

The diffusion coefficient and the surface chloride concentration for the specimens coated with polymer modified “improved” are also discussed.

### 6.2.1 Chloride profile and surface concentration RIV 1-1

In figure 5.16 (see chapter 5) the chloride concentration profile for coated as well as the uncoated specimens are showed with different w/c.

The coated specimens C23 A1 and C26 A2 show high amount of the surface concentration as 0.5% and 0.4% vs. cls weight. In the case of C23 A1 this can be attributed to lower thickness of the coating. The exception to this is C26 A2 which shows higher values of thickness with higher chloride concentration. So it is possible that there is some damage in the coating specimen although it was not revealed by visual inspection.

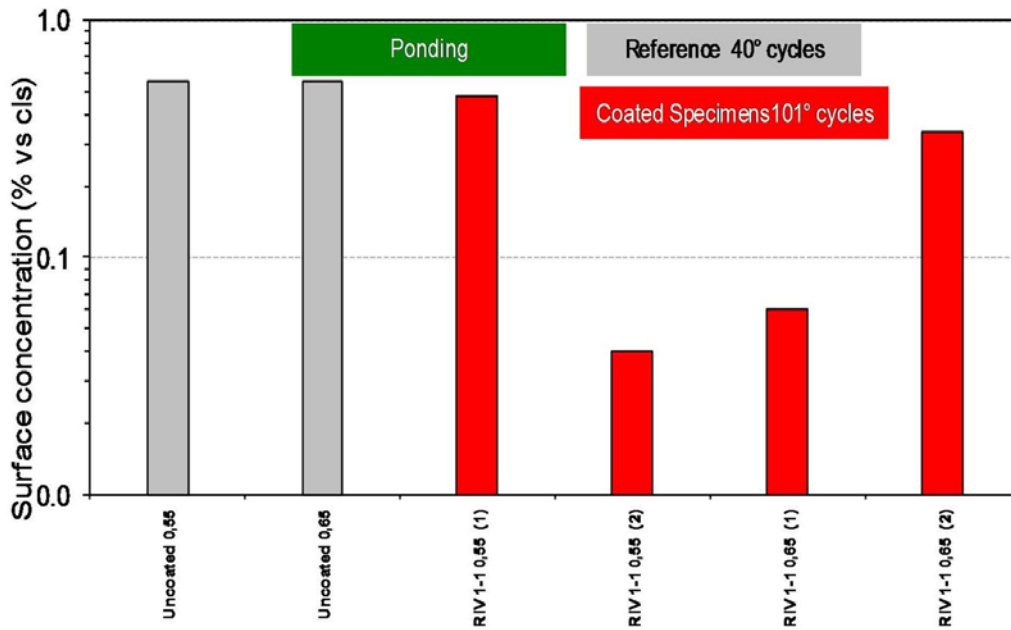


Figure 6. 5: Surface concentration RIV 1-1 coated and uncoated specimens with different w/c ratios.

For the uncoated specimens, after 40 cycles irrespective of the w/c ratio the chloride concentration at the concrete surface is the same. In the case of specimens coated with RIV 1-1, it took a longer cycles to have the chloride concentration at the surface to be close to the value for the uncoated specimen. Therefore, this delay can be attributed to the presence of the coating thereby increasing concrete lifetime. The results of the chloride concentration are in agreement with the monitoring of corrosion (see Chapter 5).

## 6.2.2 Diffusion coefficient

Figure 6.6 shows the diffusion coefficient of both the coated and uncoated specimens.

For a w/c = 0.55, the coated specimen C23 A1 shows lower diffusion compared to not coated one with the same w/c ratio. For the w/c = 0.65, the coated specimen C26 A2 show diffusion coefficient lower than the uncoated with the same w/c ratio. The measurement have been taken at 40 cycles for the uncoated and 101 for the coated

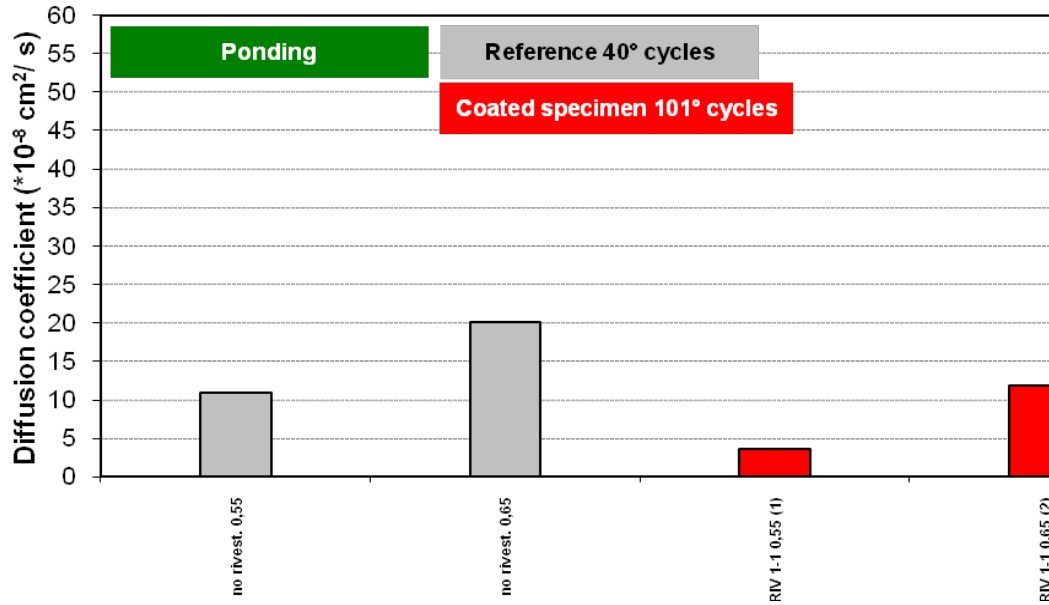


Figure 6. 6: Diffusion coefficient for RIV1-1 coated specimens.

### 6.3.1 Resistance of the coating and diffusion coefficient of the coating

Since the direct estimation of the diffusion coefficient of the coating only has not been performed in this work, it has been tried to find a parameter, called “resistance of the coating”, related to the diffusion in the coating.

The effectiveness of protective coatings used in the experimentation was evaluated in relation to the ability to prevent the penetration of chlorides towards the concrete. The resistance of the coating ( $R_{riv}$ ) is the gradient of concentration of chlorides in the coating and was calculated using the following equation:

$$R_{riv} = \frac{C_s - C_{s,cls}}{s} \quad (21)$$

Where  $C_s$  is the surface concentration of chlorides external taken equal to the concentration measured for uncoated concrete about 0.6% vs. concrete weight,  $C_{s,cls}$  is the concentration at the interface between the concrete and the coating and  $s$  is the thickness of coating.



The barrier effect is quite similar for both coatings and w/c ratio of the coating, with only two exceptions as shown in figure 6.7; the coating resistances of all specimens show the very similar values (1.5 to 2.2) except one specimen (RIV 1-1) showing a value of 1 and the specimen C24 A2 (RIV 1-2) that we were not able to measure the parameter because the chloride concentration in the concrete is nearly the same of the uncoated specimen.

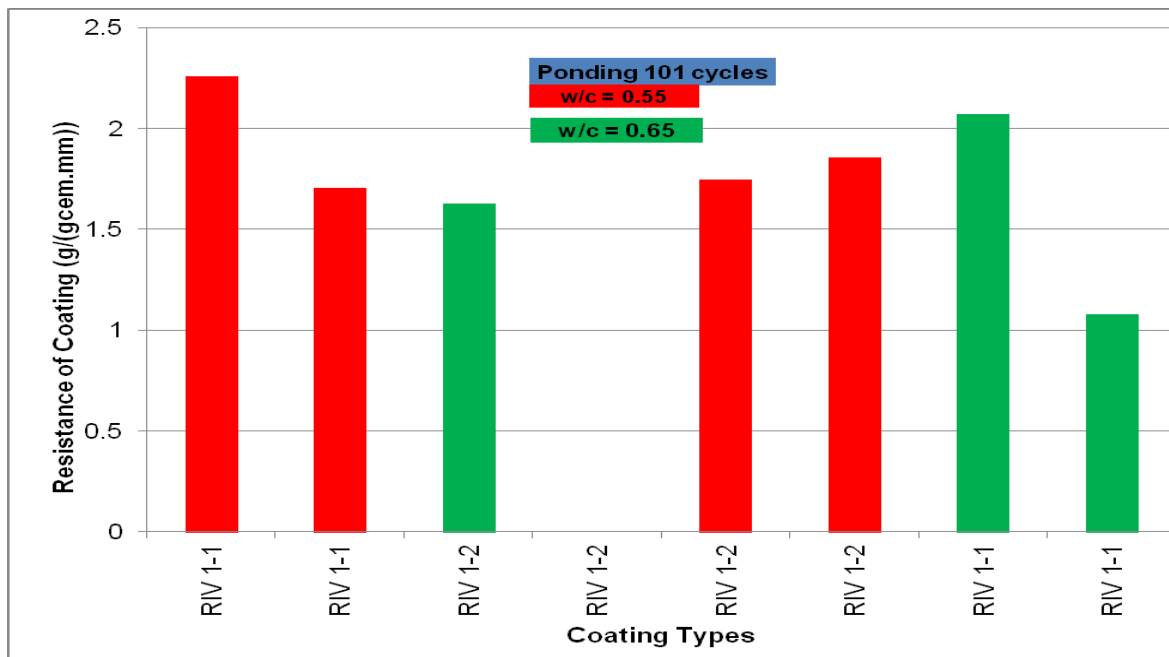


Figure 6. 7: Coating resistances of all specimens

### 6.3.2 Initiation of corrosion of the rebar

Figure 6.8 show the initiation of corrosion of the uncoated specimens and coated specimen with the water-cement  $w/c = 0.55$ . The graph shows after approximately 12° cycles, all the rebar in the uncoated specimens have been affected by corrosion. In general, the presence of the coating increases the lifetime of the reinforced specimen. On the other hand the specimens coated with RIV 1-1 show corrosion of five (5) rebar after 50° cycles while the specimens coated with RIV 1-2 show

no corrosion of rebar even at 101° cycles. This indicates that for w/c = 0.55 RIV 1-2 proves to be better at preventing corrosion of rebar than RIV 1-1.

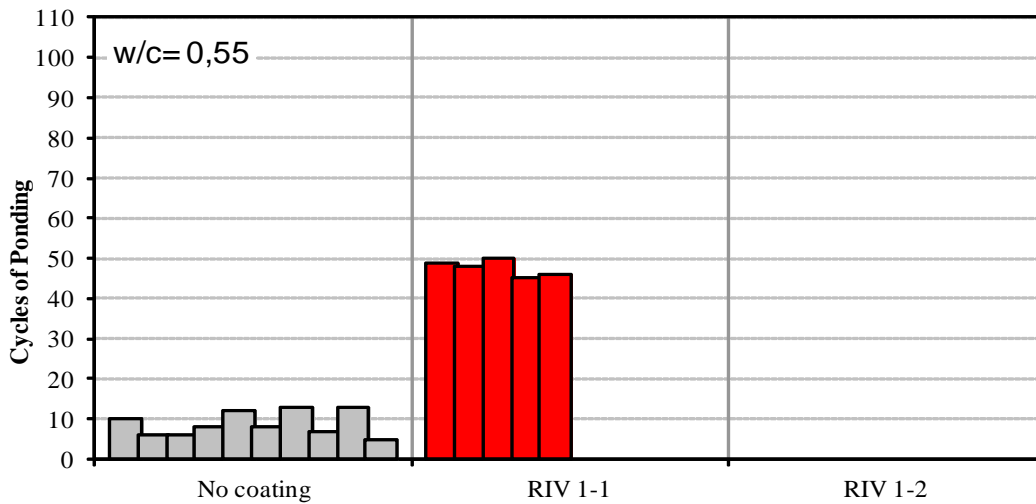


Figure 6. 8: Number of rebar corroding after various cycles for coated and uncoated specimens with w/c = 0.55

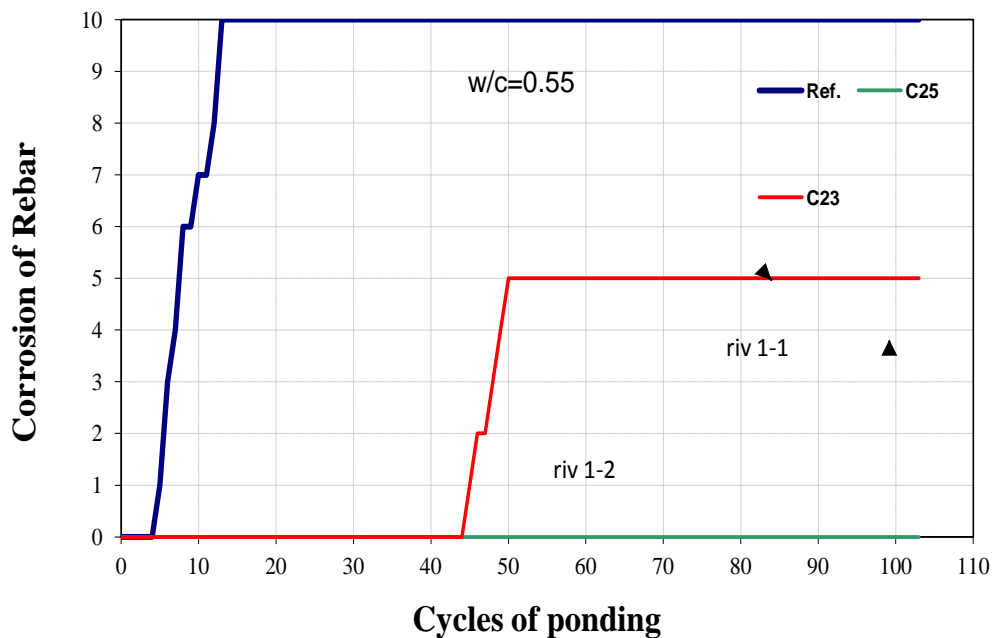


Figure 6. 9: Cumulative corrosion of rebar for w/c = 0.55 specimens

The results for the initiation of corrosion of rebar in specimens with a w/c ratio of 0.65 is showed in figure 6.9.

In figure 6.10, all the rebar of the uncoated specimen shows corrosion of the rebar after 5 cycles which is lower than for the specimens with w/c = 0.65. This is a results of the porosity of the concrete with high w/c ratio. For the specimens coated with RIV 1-1, four of the rebars are showing corrosion initiation with two of them corroding after 50 cycles and the other two after almost 100 cycles. RIV 1-2 shows corrosion of five rebars after about 40 cycles. Here again, the presence of the coating increases the lifespan of the concrete structure and can be used for corrosion prevention. In this case the performance of RIV 1-1 seems slightly better than RIV 1-2.

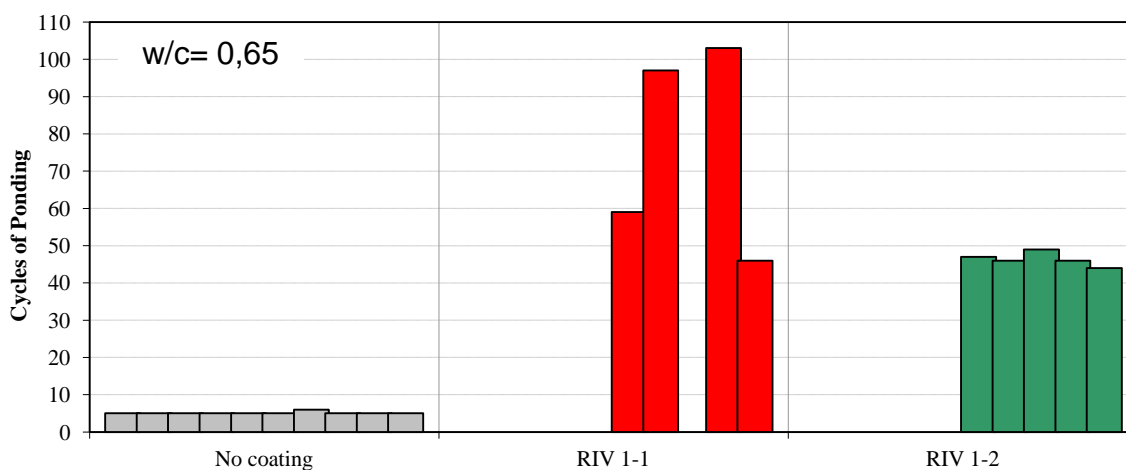


Figure 6. 10: Number of rebars corroding after various cycles for coated and uncoated specimens with w/c = 0.65

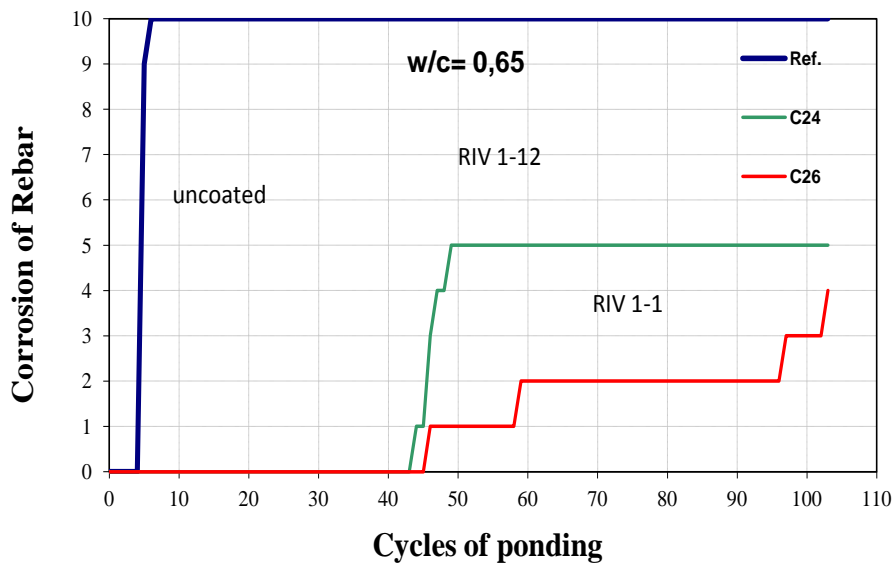


Figure 6. 11: Cumulative corrosion of rebar for w/c = 0.65 specimens

In general the corrosion initiation depends on many parameters; here are some of the parameters discussed in this work.

#### 6. 4 Comparison between RIV 1-1 and RIV 1-2

From the graph (6.3 and 6.5), it can be observed that, the two coatings are both able to reduce the surface concentration with respect the uncoated concrete (with only 1 exception) and there is not a very big difference between both polymer modified cementitious coatings.

The resistance of coating in the case of polymer modified cementitious “improved” (RIV 1-1) is quite similar to the resistance of coating in the case of polymer modified cementitious (RIV 1-2), (see figure 6.7).

#### 6.5 Different Cycling: 101 and 52

We now look at the exposure time, so we compare two different exposure times of 52 and 101 cycles. Figure 6.12 and Figure 6.13 show graphs of the diffusion coefficients and surface chloride concentration of all the samples used in this project.

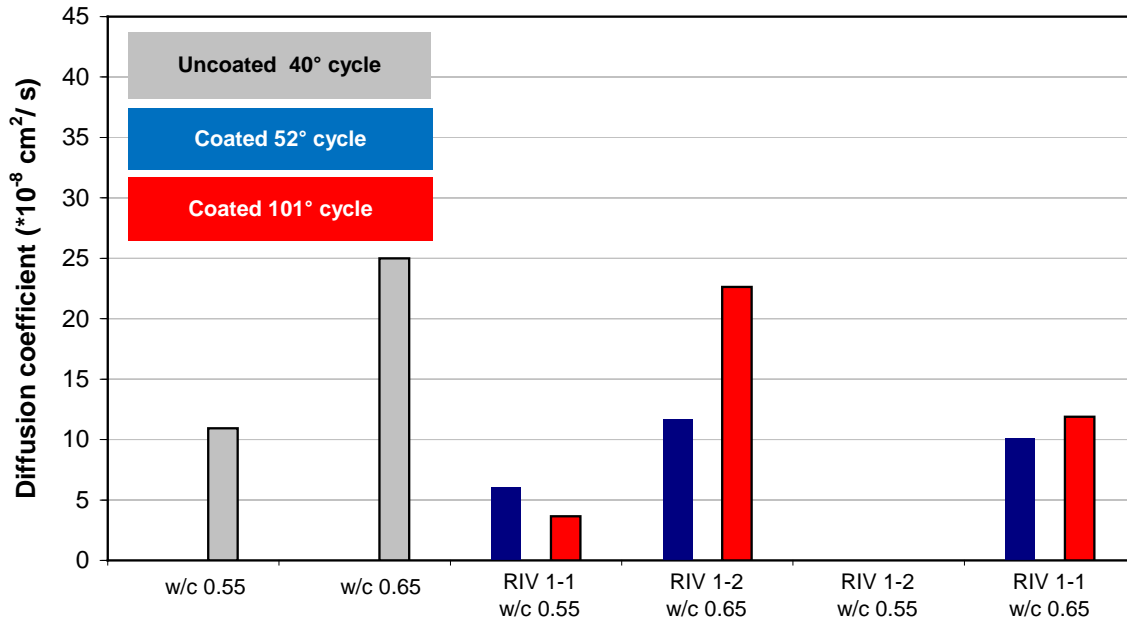


Figure 6. 12: Diffusion coefficient for all specimens at different cycling times (52 and 101)

It can be observed that for the specimens coated with RIV 1-1, the trend in the effect of the exposure time depends on the w/c ratio. For a w/c of 0.55, increasing the number of cycles from 52 to 101 shows a slightly lower diffusion coefficient. On the other hand, for the w/c = 0.65, doubling the number of cycling increases the diffusion coefficient, especially in the case of one specimen (RIV 1-2).

For the surface concentration, in some specimens the surface concentration remain low for both cycles, 0.1% vs concrete weight or lower. Only in some cases significant values of chloride surface concentration ( $C_s$ ) have been measured: for RIV 1-1 w/c 0.55 (1<sup>st</sup> specimen), RIV 1-2 w/c 0.65 2<sup>nd</sup> specimen and RIV 1-1 w/C 0.65 (2<sup>nd</sup> specimen)  $C_s$  is increased with time, that is coherent with the mechanism of diffusion, an anomalous behaviour was observed at the reverse for RIV 1-1 w/C 0.65 (1<sup>st</sup> specimen), with  $C_s$  decreased with time.

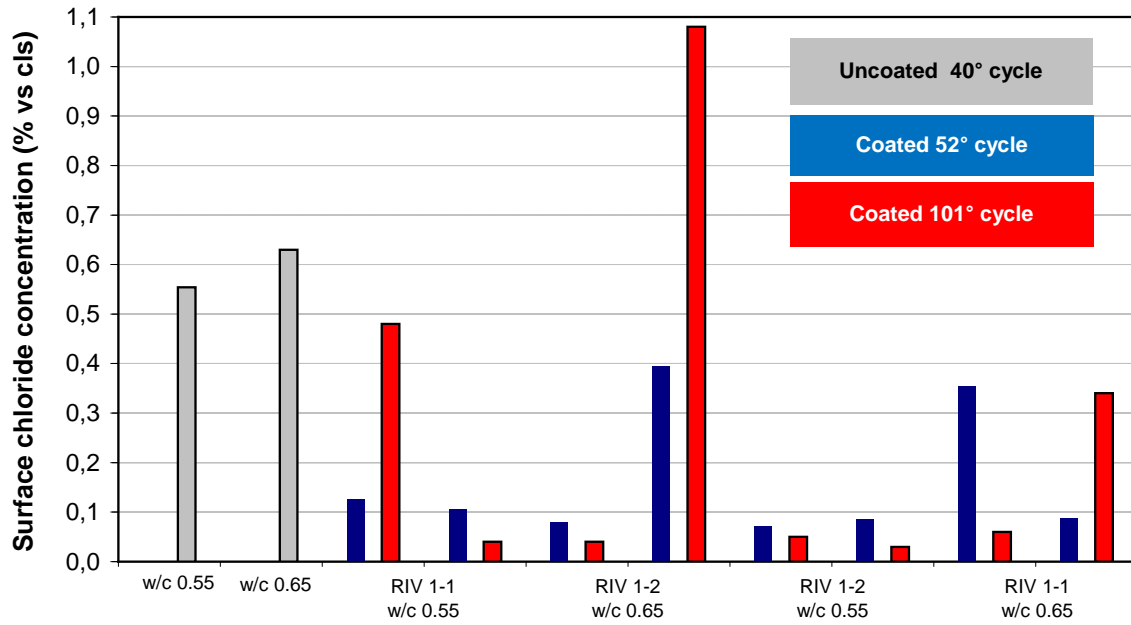


Figure 6. 13: Surface concentration for all specimens at different cycling times (52 and 101)

## 7.0 Conclusion

In this project it has been confirmed that the w/c has a marked effect on the corrosion of steel concrete: an increase in w/c ratio increases the porosity of the concrete and therefore increases the chloride transport in concrete. So the critical chloride threshold is reached in shorter time, and corrosion started earlier.

The application of polymer modified cementitious coatings on concrete structures increase the lifespan of concrete structure by decreasing the transport of chloride in the concrete. This therefore reduces in most cases the concentration in concrete and namely at the rebar level below the critical chloride concentration for corrosion initiation. In the few cases where corrosion has started, the initiation time for corrosion is greatly increased compared to uncoated concrete.

The type of coating also plays important role in preventing corrosion of the rebar or concrete. In this work, the difference between the two polymer modified cementitious coatings used was not significant. In fact, concerning the barrier effect to chlorides (estimated as the concentration gradient across the coating), the “improved” (or updated) coating RIV 1-1 showed similar behaviour with respect to coating RIV 1-2.

Just as the coating is important, the morphology and the thickness of the coating is also important. This work shows that the thickness is important as coating having thickness lower than 2mm showed lower resistance to chloride diffusion and increased the probability of corrosion initiation of reinforcing steel.

## 8.0 References

- [1] - Edward G Nawy, "Reinforced concrete: A Fundamental Approach" (6<sup>th</sup> Edition) (2004)
- [2] – Ali Falakian, Seyed Yaser Mousavi, "A survey study on durability of high-performance concrete" International Research Journal of Applied and Basic Sciences. Vol., 3 (5), 902-910, 2012
- [3] – Luca Bertolini, Bernhard Elsener, Pietro Pedferri, Rob P. Polder "Corrosion of Steel in Concrete" Wiley-VCH Verlag GmbH & Co. KGaA, Weinheim (2004)
- [4] - Cahn, R.W. (ed.) /Haasen, P. (ed.) / Kramer, E. J. (ed.) "Corrosion and Environmental Degradation": A Two Volume Set of the Materials Science and Technology Series (2000)
- [5] - C. L. Page, K. W. J. Treadaway, "Aspects of the electrochemistry of steel in concrete", Nature, **297** (13), 109–114, 1982
- [6] - L.K. Aggarwal, P.C. Thapliyal, S.R. Karade - Properties of polymer-modified mortars using epoxy and acrylic emulsions - Construction and Building Materials 21 - pp. 379-383 - 2005)
- [7] Colleparidi M., Marcialis, A., Turriziani, R., 'Penetration of Chloride Ions into Cement Pastes and Concretes', Journal of the American Ceramic Society, 55(10), 1972; pp.534-535
- [8] - Crank J., The Mathematics of Diffusion, Oxford, Clarendon Press, (1954).
- [9] Bamforth P., "The Derivation of Input Data for Modelling Chloride Ingress from Eight-Year UK Coastal Exposure Trials", Magazine of Concrete Research, 51, No.2, 1999, pp.87-96
- [10] - P. B. Bamforth, J. Chapman-Andrews, "Long term performance of RC elements under UK coastal conditions", Proc. Int. Conf. On Corrosion and Corrosion Protection of Steel in Concrete, R. N. Swamy (Ed.), Sheffield Academic Press, 24–29 July 1994, 139–156.
- [11] - Susan Macdonald "The Investigation and Repair of Historic Concrete" Parramatta N.S.W. : NSW Heritage Office, 2003.
- [12] – Townsend, H. E., Cleary H. J., Allegra L. (1981). "Breakdown of Oxide films in Steel Exposure to Chloride Solutions," Corrosion - NACE, vol. 37, pp. 384-391
- [13] – Nielsen A., "Durability" in Beton Bogen, Aalborg Cement Company, Aalborg, Portland, pp.



200-243 (1985).

[14] - Crank, J. (1956). *The Mathematics of Diffusion*, The Clarendon Press, Oxford.

[15] - Cady, P.D., and Weyers R.E. (1984). "Deterioration Rates of Concrete Bridge

[16] - L.K. Aggarwal, P.C. Thapliyal, S.R. Karade - Properties of polymer-modified mortars using epoxy and acrylic emulsions - *Construction and Building Materials* 21 - pp. 379-383 – 2005

[17] - John A. Bickley and Associates, *Determine Potential of Carbonation of Concrete in Canada-State-of- the- Art, Literature Review*, CMHC, 1987,

[18] - *Extent of Carbonation in Buildings in Toronto*, CMHC, 1990, John A. Bickley and Associates

[19] - *Anti-Carbonation Coatings for Use on Canadian Buildings*, CMHC, 1992, Halsall and Associates

[20] - H. Arup, "The mechanisms of the protection of steel by concrete, in *Corrosion of Reinforcement in Concrete Construction*", Ellis Horwood Ltd., Chichester, 151–157, 1983.

[21] - P. R. Vassie, "Reinforcement corrosion and the durability of concrete bridges", *Proceedings of the Institution of Civil Engineers, Part 1, Vol. 76*, paper 8798, 713, 1984.

[22] – COST 521, "Determination of chloride threshold in concrete", C. Andrade, in *Corrosion of Steel in Reinforced Concrete Structures. Final report*, ed. R. Cigna, C. Andrade, U. Nürnberger, R. Polder, R. Weydert, E. Seitz, European Communities EUR 20599, Luxembourg (2003) p. 100–108.

[23] – G. K. Glass, N. R. Buenfeld, "Chloride threshold level for corrosion of steel in concrete", *Corrosion Science*, 1997, 39, 1001–1013.

[24] - C. L. Page, P. Lambert, P. R. W. Vassie, "Investigation of reinforcement corrosion: 1. The pore electrolyte phase in chloride contaminated concrete", *Materials and Structures*, 1991, 24, 243–252.

[25] - P. Lambert, C. L. Page, P. R. W. Vassie, "Investigation of reinforcement corrosion: 2. Electrochemical monitoring of steel in chloride-contaminated concrete", *Materials and Structures*, 1991, 24, 351–358.

[26] - *Residual life Models for Concrete Repair - Assessment of the Concrete Repair Process*

- [27] - A, Diamond S, Berke NS. Corrosion control. In: Steel corrosion in concrete - Fundamentals and civil engineering practice. London: E and FN SPON; 1997. p. 94–145
- [28] – “Durability of concrete and Service life of Structures: Two Solvable problems”,
- [29] - : M. Berra, F. Bolzoni, M. Ormellese, T. Pastore “Reinforcement corrosion control of concrete structures based on modified polymer mortar coatings”
- [30] - M.H.F. Medeiros, P. Helene, Surface treatment of reinforced concrete in marine environment: Influence on chloride diffusion coefficient and capillary water absorption,
- [31] – Uemoto KL, Agopyan V, Vittorino F. Concrete protection using acrylic latex paint: effect of the pigment volume content on water permeability. Mater Struct 2001;34:172–7.
- [32] - Medeiros MHF, Helene P. Efficacy of surface hydrophobic agents in reducing water and chloride ion penetration in concrete. Mater Struct 2008;41(1):59–71.
- [33] - F.P. Incropera, D.P. DeWitt, - Fundamentals of heat and mass transfer - JOHN WILEY & SONS - Southampton UK - Giugno 1992
- [34] - Linee guida sul calcestruzzo strutturale - Consiglio Superiore dei Lavori Pubblici - 19 novembre 1996.

